

JYX



JYVÄSKYLÄN YLIOPISTO
UNIVERSITY OF JYVÄSKYLÄ

This is a self-archived version of an original article. This version may differ from the original in pagination and typographic details.

Author(s): Cougoulic, Florian; Kovchegov, Yuri V.; Tarasov, Andrey; Tawabutr, Yossathorn

Title: Quark and gluon helicity evolution at small x : revised and updated

Year: 2022

Version: Published version

Copyright: © The Authors. Article funded by SCOAP3

Rights: CC BY 4.0

Rights url: <https://creativecommons.org/licenses/by/4.0/>

Please cite the original version:

Cougoulic, F., Kovchegov, Y. V., Tarasov, A., & Tawabutr, Y. (2022). Quark and gluon helicity evolution at small x : revised and updated. *Journal of High Energy Physics*, 2022(7), Article 95. [https://doi.org/10.1007/jhep07\(2022\)095](https://doi.org/10.1007/jhep07(2022)095)

Quark and gluon helicity evolution at small x : revised and updated

Florian Cougoulic,^a Yuri V. Kovchegov,^b Andrey Tarasov^{b,c} and Yossathorn Tawabutr^b

^a*Department of Physics, University of Jyväskylä,
P.O. Box 35, Surfontie 9 C, Jyväskylä 40014, Finland*

^b*Department of Physics, The Ohio State University,
191 W. Woodruff Ave, Columbus, OH 43210, U.S.A.*

^c*Joint BNL-SBU Center for Frontiers in Nuclear Science (CFNS) at Stony Brook University,
100 Nicolls Road, Stony Brook, NY 11794, U.S.A.*

E-mail: florian.f.cougoulic@jyu.fi, kovchegov.1@osu.edu,
tarasov.3@osu.edu, tawabutr.1@osu.edu

ABSTRACT: We revisit the problem of small Bjorken- x evolution of the gluon and flavor-singlet quark helicity distributions in the shock wave (s -channel) formalism. Earlier works on the subject in the same framework [1–3] resulted in an evolution equation for the gluon field-strength F^{12} and quark “axial current” $\bar{\psi}\gamma^+\gamma^5\psi$ operators (sandwiched between the appropriate light-cone Wilson lines) in the double-logarithmic approximation (summing powers of $\alpha_s \ln^2(1/x)$ with α_s the strong coupling constant). In this work, we observe that an important mixing of the above operators with another gluon operator, $\overleftarrow{D}^i D^i$, also sandwiched between the light-cone Wilson lines (with the repeated transverse index $i = 1, 2$ summed over), was missing in the previous works [1–3]. This operator has the physical meaning of the sub-eikonal (covariant) phase: its contribution to helicity evolution is shown to be proportional to another sub-eikonal operator, $D^i - \overleftarrow{D}^i$, which is related to the Jaffe-Manohar polarized gluon distribution [4]. In this work we include this new operator into small- x helicity evolution, and construct novel evolution equations mixing all three operators ($D^i - \overleftarrow{D}^i$, F^{12} , and $\bar{\psi}\gamma^+\gamma^5\psi$), generalizing the results of [1–3]. We also construct closed double-logarithmic evolution equations in the large- N_c and large- $N_c \& N_f$ limits, with N_c and N_f the numbers of quark colors and flavors, respectively. Solving the large- N_c equations numerically we obtain the following small- x asymptotics of the quark and gluon helicity distributions $\Delta\Sigma$ and ΔG , along with the g_1 structure function,

$$\Delta\Sigma(x, Q^2) \sim \Delta G(x, Q^2) \sim g_1(x, Q^2) \sim \left(\frac{1}{x}\right)^{3.66 \sqrt{\frac{\alpha_s N_c}{2\pi}}},$$

in complete agreement with the earlier work by Bartels, Ermolaev and Ryskin [5].

KEYWORDS: Deep Inelastic Scattering or Small-X Physics, Resummation

ARXIV EPRINT: [2204.11898](https://arxiv.org/abs/2204.11898)

Contents

| | | |
|----------|---|-----------|
| 1 | Introduction | 1 |
| 2 | Sub-eikonal quark and gluon S-matrices in the background field | 5 |
| 3 | Quark and gluon helicity distributions and g_1 structure function at small x | 8 |
| 3.1 | Gluon helicity distribution | 8 |
| 3.2 | Quark helicity distribution | 12 |
| 3.3 | g_1 structure function | 17 |
| 4 | Helicity evolution at small x | 21 |
| 4.1 | Evolution equations in the operator form | 21 |
| 4.1.1 | Evolution equations for fundamental and adjoint $Q_{10}(zs)$ | 21 |
| 4.1.2 | Evolution equations for fundamental and adjoint $G_{10}^i(zs)$ | 28 |
| 4.2 | Evolution equations in the large- N_c limit | 31 |
| 4.3 | Evolution equations in the large- N_c & N_f limit | 37 |
| 4.4 | Cross-check against the spin-dependent DGLAP evolution | 44 |
| 5 | Helicity evolution at small x: the background field method | 47 |
| 5.1 | The background field method | 47 |
| 5.2 | Quark and gluon propagators in the shock-wave background | 49 |
| 5.2.1 | Scalar propagator in the shock-wave background | 49 |
| 5.2.2 | Gluon propagator in the shock-wave background | 53 |
| 5.2.3 | Quark propagator in the shock-wave background field | 55 |
| 5.3 | Evolution equation for Q_{10} in the background field method | 60 |
| 5.4 | Evolution equation for G_{10}^i in the background field method | 64 |
| 6 | Small-x asymptotics of the quark and gluon helicity distributions and g_1 structure function in the large-N_c limit | 67 |
| 7 | Conclusions and outlook | 73 |
| A | Schwinger's notation | 75 |

1 Introduction

Understanding the proton spin puzzle [6–14] is one of the main goals of contemporary hadronic physics. Apart from being a question of general scientific interest testing our understanding of the proton internal structure, the proton spin puzzle is one of the central

topics to be addressed by the experimental program at the future Electron-Ion Collider (EIC) [7, 11, 12, 14].

The main question of the proton spin puzzle is how the proton spin ($1/2$) is made up of the contributions of quark and gluon helicities and their orbital angular momenta (OAM) (see [6, 8, 13] and references therein for reviews). It is usually formulated in terms of either Jaffe-Manohar [4] or Ji [15] spin sum rules. The Jaffe-Manohar sum rule [4] reads

$$S_q + L_q + S_G + L_G = \frac{1}{2}, \quad (1.1)$$

where S_q and S_G are the contributions to the spin of the proton carried by the quarks and gluons, respectively, and L_q and L_G are their OAM. All four terms on the left-hand side of eq. (1.1) can be written as integrals over the Bjorken x variable. For the quark and gluon spin contributions, S_q and S_G , the decomposition is (see [16–20] for decompositions for the OAM terms)

$$S_q(Q^2) = \frac{1}{2} \int_0^1 dx \Delta\Sigma(x, Q^2), \quad S_G(Q^2) = \int_0^1 dx \Delta G(x, Q^2), \quad (1.2)$$

where

$$\Delta\Sigma(x, Q^2) = \sum_{f=u,d,s,\dots} \Delta q_f^+(x, Q^2) \quad (1.3)$$

is the flavor-singlet quark helicity distribution function with $\Delta q_f^+ = \Delta q_f + \Delta \bar{q}_f$ [21, 22]. Here Δq_f and $\Delta \bar{q}_f$ are the quark and anti-quark helicity distributions for each quark flavor f , while ΔG is the gluon helicity distribution. As usual, the distributions also depend on the momentum scale Q^2 . The current values of the proton spin carried by the quarks and gluons, as extracted from the experimental data, are $S_q(Q^2 = 10 \text{ GeV}^2) \approx 0.15 \div 0.20$ for $x \in [0.001, 1]$, and $S_G(Q^2 = 10 \text{ GeV}^2) \approx 0.13 \div 0.26$, for $x \in [0.05, 1]$ (see [7–10, 12, 13] for reviews). The fact that the sum of these two numbers comes up short of $1/2$, especially if one takes into account the error bars, is the proton spin puzzle: we do not know where the rest of the proton spin is. The remaining missing spin of the proton may be found in the quark and gluon OAM and/or at smaller values of x .

The latter possibility received a lot of attention in the literature, starting with the groundbreaking work by Bartels, Ermolaev and Ryskin (BER) [5, 23], which studied the small- x asymptotics of the g_1 structure function along with $\Delta\Sigma$ and ΔG employing the infrared evolution equations (IREE) approach pioneered in [24–27]. The phenomenology based on BER work was developed in [28, 29]. The BER approach resummed double logarithms in x , that is, powers of $\alpha_s \ln^2(1/x)$. This is known as the double-logarithmic approximation (DLA). In the pure-gluon case the BER approach resulted in the asymptotics given by

$$\Delta\Sigma(x, Q^2) \sim \Delta G(x, Q^2) \sim g_1(x, Q^2) \sim \left(\frac{1}{x}\right)^{3.66 \sqrt{\frac{\alpha_s N_c}{2\pi}}}. \quad (1.4)$$

More recently, an effort has been under way [1–3, 22, 30–40] to reproduce BER results [5, 23] and, possibly, expand on them using the s -channel/shock wave approach to

small- x evolution from [41–53] (see [54–61] for reviews) modified to work at the sub-eikonal level and beyond [62–65]. (Small- x asymptotics of parton distribution functions (PDFs) and transverse momentum-dependent PDFs (TMDs) can be classified by the leading power of x : our notation is such that, neglecting the quantum-evolution order- α_s or $\sqrt{\alpha_s}$ corrections to the power of x , the eikonal distributions scale as $\sim 1/x$, the sub-eikonal ones scale as $\sim x^0$, the sub-sub-eikonal ones scale as $\sim x$, etc.) The approach to helicity evolution in the s -channel formalism developed in [1–3, 31–33, 36, 37] resulted in the small- x asymptotics of $\Delta\Sigma$ and ΔG different from that found by BER.¹ Despite the cross-check in [2] and an alternative calculation in [39] the origin of the difference remained unknown. In this work we identify the sub-eikonal operator which was not included in the approach of [1–3, 31–33, 36, 37]: after including it, we obtain a new set of small- x evolution equations for helicity, whose solution gives the asymptotics (1.4) consistent with BER.

When going beyond the eikonal approximation, the degrees of freedom are no longer the light-cone Wilson lines: instead one has to modify the Wilson lines by inserting one or more sub-eikonal operators between segments of Wilson lines [3, 33, 62–70]. The sub-eikonal operators entering the helicity evolution of [1–3, 31–33, 36, 37] are the gluon field strength operator F^{12} or the bi-local quark operator $\bar{\psi}(x_2)\gamma^+\gamma^5\psi(x_1)$. When wrapped around by light-cone Wilson lines they lead to the operators in eqs. (2.7a) and (2.7b) (or eqs. (2.12a) and (2.12b)) below. (Our calculations here are carried out in $A^- = 0$ light-cone gauge of the projectile, while the expressions for the operators are valid in any gauge where the gluon field A_μ vanishes at $x^- \rightarrow \pm\infty$.) The operators F^{12} and $\bar{\psi}(x_2)\gamma^+\gamma^5\psi(x_1)$ enter the calculation with the helicity-dependent prefactor, e.g., with $\sigma\delta_{\sigma,\sigma'}$ in the quark helicity basis, as defined in light-cone perturbation theory (LCPT) [71, 72]. This is what makes them natural operators for helicity evolution. The helicity evolution of [1–3, 33] mixes these two operators with each other. However, since F^{12} is a local operator, it cannot be used to construct a PDF: hence the mapping of evolution from [1–3, 33] onto the spin-dependent Dokshitzer-Gribov-Lipatov-Altarelli-Parisi (DGLAP) evolution equation [73–75] in the gluon sector has been problematic [2]. At the same time, F^{12} is not the only gluon operator at the sub-eikonal order: there exists another sub-eikonal operator, $\overleftarrow{D}^i D^i$, as derived in [30, 64, 66, 70]. Here $D_\mu = \partial_\mu - igA_\mu$ is the right-acting covariant derivative, $\overleftarrow{D}_\mu = \overleftarrow{\partial}_\mu + igA_\mu$ is the left-acting covariant derivative, and $i = 1, 2$ is the transverse index. The operator $\overleftarrow{D}^i D^i$, whose contribution is simplified in our helicity-evolution calculations to $D^i - \overleftarrow{D}^i$, is related to the Jaffe-Manohar gluon helicity PDF [4], as we show below. The $\overleftarrow{D}^i D^i$ operator enters the calculations with a helicity-independent prefactor $\delta_{\sigma,\sigma'}$; an expression for this operator, sandwiched between the light-cone Wilson lines, is given below in eq. (2.7c) (or (2.12c)). In the background field method [76, 77] this operator arises naturally due to the canonical momentum squared term, $(P^i)^2$, present even in a scalar particle propagator [66, 67]. In this work we show that small- x helicity evolution mixes the $D^i - \overleftarrow{D}^i$ operator with F^{12} and $\bar{\psi}(x_2)\gamma^+\gamma^5\psi(x_1)$. This mixing was neglected

¹In the flavor non-singlet channel, the two approaches were in complete agreement [2, 23] at large N_c .

in [1–3, 33] due to the apparent helicity-independence of the $\overleftarrow{D} D^i$ term, which gives rise to the $D^i - \overleftarrow{D}$ operator (i.e., due to the fact that it comes in with $\delta_{\sigma,\sigma'}$). The physical origin of the mixing still requires further understanding. Here we note that the mixing probably happens because the quark and gluon polarization indices σ and λ in LCPT are not true helicities: they are projections of the particle’s spin on the fixed z -axis, instead of being spin projections on the direction of the particle’s 3-momentum.

In this paper we derive a new small- x evolution equations for helicity distributions mixing the three operators $D^i - \overleftarrow{D}$, F^{12} , and $\bar{\psi}(x_2)\gamma^+\gamma^5\psi(x_1)$. The equations resum longitudinal logarithms, keeping the accompanying transverse integrals exactly. We, therefore, can and do extract the DLA evolution equations from them, obtaining two closed systems of integral evolution equations in the ’t Hooft’s large- N_c [78] and Veneziano’s large- N_c & N_f [79] limits. Performing a numerical solution of the large- N_c helicity evolution equation we arrive at the asymptotics given in eq. (6.12), thus reproducing BER results.

The paper is structured as follows. In section 2 we summarize the results of the earlier calculation [70] for high-energy S -matrices of massless quarks and gluons scattering on the background quark and gluon fields at the sub-eikonal accuracy. As we mentioned, these results are consistent with the earlier calculation [64]. The relevant sub-eikonal operators are given in eqs. (2.7) and (2.12) for the quarks and gluons, respectively.

To identify which sub-eikonal operators are relevant for helicity distributions and for the g_1 structure function, we re-analyse these quantities at small x in section 3.² In section 3.1 we reconstruct the known result [30, 33] that the gluon helicity TMD and PDF at small x are related to the dipole amplitude G^j from eq. (3.22), dependent on the novel sub-eikonal operator $D^i - \overleftarrow{D}$ entering eq. (3.17). This is summarized in eqs. (3.25) and (3.26) with the amplitude G_2 entering those equations defined in eq. (3.24). Small- x quark helicity distributions are studied in section 3.2 with the result given by eqs. (3.52) and (3.50). The dipole amplitude Q in those equations, defined in eq. (3.48), contains the operators F^{12} and $\bar{\psi}(x_2)\gamma^+\gamma^5\psi(x_1)$: this part of the results for quark helicity distributions was known before [1–3]. The amplitude G_2 in the same expressions contains the new operator $D^i - \overleftarrow{D}$, which, in turn, originated in the sub-eikonal $\overleftarrow{D} D^i$ operator. (Comparing this with eq. (3.26) we conclude that the $\overleftarrow{D} D^i$ operator is related to the Jaffe-Manohar distribution.) This G_2 contribution in eqs. (3.52) and (3.50) is new compared to [1–3, 33]. Finally, in section 3.3 we re-analyse the g_1 structure function at small x , arriving at eqs. (3.61) and (3.62). Again, the contribution of the dipole Q has been known before [1–3, 40], while the contribution of G_2 is new.

The small- x evolution of the sub-eikonal operators $D^i - \overleftarrow{D}$, F^{12} and $\bar{\psi}(x_2)\gamma^+\gamma^5\psi(x_1)$ with the appropriate light-cone Wilson lines is studied in sections 4 and 5. The calculation in section 5 is done using the background field method [44, 77], while in section 4 the calcu-

²Note that there is a possible role of the topological effects in g_1 due to the chiral anomaly, which has been debated in the literature [4, 80–83], see also the recent works [84–87]. This can be inferred from the first moment of the structure function and is related to the $U_A(1)$ problem in QCD. However, we leave the question about the relation of our results to the chiral anomaly for future publications.

lation employs a hybrid formalism developed in [3, 33, 70] which combines the elements of LCPT [71, 72] with the background field method: we refer to it as the light-cone operator treatment (LCOT) method. In section 5.2 we derive the structure of sub-eikonal operators from the analysis of quark and gluon propagators in the background field. At the level of sub-eikonal operators the main evolution equations we obtain are (4.15), (4.19), (4.26), and (4.27) in section 4.1. The same equations are derived again in section 5 using the background field method (see eqs. (5.69) and (5.82) there). These equations contain leading logarithms in the longitudinal integral in their kernels, along with the exact transverse integrations, similar to the unpolarized small- x evolution [41–53, 88, 89]. Using the technique of [1, 3] we take the DLA limit of those equations obtaining closed large- N_c evolution equations (4.53) in section 4.2. Similarly, the large- N_c & N_f evolution equations are studied in section 4.3, resulting in the closed system of equations (4.75). These large- N_c and large- N_c & N_f equations extend and generalize the results of [1, 3]. We cross-check our large- N_c evolution equations (4.53) against the small- x limit of the pure-gluon spin-dependent DGLAP evolution in section 4.4 and find an agreement up to and including three loops [90, 91], the highest-known order for the spin-dependent DGLAP splitting functions.

The large- N_c evolution equations (4.53) are solved numerically in section 6, following the technique of [22, 31, 37]. The resulting numerical solution for the amplitudes G (defined in eq. (4.29) with $Q \approx G$ at large N_c) and G_2 is plotted in figure 6. The extracted intercepts are given in eq. (6.10); within the uncertainty, they are the same for both amplitudes. This leads to the asymptotics of eq. (6.12), in complete agreement with BER, eq. (1.4).

We conclude in section 7 by outlining future directions of this research program.

2 Sub-eikonal quark and gluon \mathcal{S} -matrices in the background field

We define our light-cone coordinates by $x^\pm = (t \pm z)/\sqrt{2}$, while the transverse vectors are denoted by $\underline{x} = (x^1, x^2)$ with $\underline{x}_{ij} = \underline{x}_i - \underline{x}_j$ and $x_{ij} = |\underline{x}_{ij}|$ for $i, j = 0, 1, 2, \dots$ labeling the partons. Our proton is always moving in the light-cone plus direction, while the projectile quarks and gluons are moving in the light-cone minus direction. The gluon field is denoted by A_μ^a , while the quark and anti-quark fields are ψ and $\bar{\psi}$. The calculations for small- x evolution will be carried out in $A^{a-} = 0$ gauge. However, the expressions for the operators in this section are also valid in the Lorenz gauge $\partial_\mu A^{a\mu} = 0$, and in any gauge where the gluon field vanishes at $x^- \rightarrow \pm\infty$ (cf. [64, 70]).

We denote the fundamental light-cone Wilson lines by

$$V_{\underline{x}}[x_f^-, x_i^-] = \mathcal{P} \exp \left[ig \int_{x_i^-}^{x_f^-} dx^- A^+(0^+, x^-, \underline{x}) \right] \tag{2.1}$$

with the abbreviation $V_{\underline{x}} = V_{\underline{x}}[\infty, -\infty]$ for infinite lines. Here \mathcal{P} is the path ordering operator, $A^\mu = \sum_a A^{a\mu} t^a$ is the background gluon field with t^a the fundamental $SU(N_c)$ generators, and g is the strong coupling constant. The adjoint light-cone Wilson line is

defined similarly as

$$U_{\underline{x}}[x_f^-, x_i^-] = \mathcal{P} \exp \left[ig \int_{x_i^-}^{x_f^-} dx^- \mathcal{A}^+(0^+, x^-, \underline{x}) \right] \quad (2.2)$$

with $\mathcal{A}^\mu = \sum_a A^{a\mu} T^a$, where T^a are the adjoint $SU(N_c)$ generators, $(T^a)_{bc} = -if^{abc}$. Again, $U_{\underline{x}} = U_{\underline{x}}[\infty, -\infty]$.

Define an S -matrix for the quark-target scattering in the helicity basis³ by

$$V_{\underline{x}, \underline{y}; \sigma', \sigma} \equiv \int \frac{d^2 p_{\text{in}}}{(2\pi)^2} \frac{d^2 p_{\text{out}}}{(2\pi)^2} e^{i p_{\text{out}} \cdot \underline{x} - i p_{\text{in}} \cdot \underline{y}} \left[\delta_{\sigma, \sigma'} (2\pi)^2 \delta^2(\underline{p}_{\text{out}} - \underline{p}_{\text{in}}) + i A_{\sigma', \sigma}^q(\underline{p}_{\text{out}}, \underline{p}_{\text{in}}) \right], \quad (2.3)$$

where $A^q(\underline{p}_{\text{out}}, \underline{p}_{\text{in}})$ is the scattering amplitude for a quark on a target with $\underline{p}_{\text{in}}$ and $\underline{p}_{\text{out}}$ the incoming and outgoing quark transverse momenta, respectively, while σ' and σ are the outgoing and incoming quark helicities. The amplitude A is normalized such that $A = M/(2s)$ [60], where M is the conventional textbook scattering amplitude and s is the center-of-mass energy squared.

Neglecting the quark mass, which does not affect small- x evolution, at the sub-eikonal order the quark S -matrix is [3, 63, 64, 66, 70]⁴

$$\begin{aligned} V_{\underline{x}, \underline{y}; \sigma', \sigma} &= V_{\underline{x}} \delta^2(\underline{x} - \underline{y}) \delta_{\sigma, \sigma'} \quad (2.4) \\ &+ \frac{iP^+}{s} \int_{-\infty}^{\infty} dz^- d^2 z V_{\underline{x}}[\infty, z^-] \delta^2(\underline{x} - \underline{z}) \left[-\delta_{\sigma, \sigma'} \overleftarrow{D}^i D^i + g \sigma \delta_{\sigma, \sigma'} F^{12} \right] (z^-, \underline{z}) V_{\underline{y}}[z^-, -\infty] \delta^2(\underline{y} - \underline{z}) \\ &- \frac{g^2 P^+}{2s} \delta^2(\underline{x} - \underline{y}) \int_{-\infty}^{\infty} dz_1^- \int_{z_1^-}^{\infty} dz_2^- V_{\underline{x}}[\infty, z_2^-] t^b \psi_\beta(z_2^-, \underline{x}) U_{\underline{x}}^{ba}[z_2^-, z_1^-] [\delta_{\sigma, \sigma'} \gamma^+ - \sigma \delta_{\sigma, \sigma'} \gamma^+ \gamma^5]_{\alpha\beta} \bar{\psi}_\alpha(z_1^-, \underline{x}) t^a V_{\underline{x}}[z_1^-, -\infty], \end{aligned}$$

where $D^i = \partial^i - igA^i$, and $\overleftarrow{D}^i = \overleftarrow{\partial}^i + igA^i$.

The S -matrix in eq. (2.4) has two distinct polarization-dependent structures, $\sigma \delta_{\sigma, \sigma'}$ and $\delta_{\sigma, \sigma'}$. At the sub-eikonal level (that is, for everything except for the first term on the right-hand side of eq. (2.4)), we define the ‘‘polarized Wilson lines’’ $V_{\underline{x}}^{\text{pol}[1]}$ and $V_{\underline{x}, \underline{y}}^{\text{pol}[2]}$ by [3, 70]

$$V_{\underline{x}, \underline{y}; \sigma', \sigma} \Big|_{\text{sub-eikonal}} \equiv \sigma \delta_{\sigma, \sigma'} V_{\underline{x}}^{\text{pol}[1]} \delta^2(\underline{x} - \underline{y}) + \delta_{\sigma, \sigma'} V_{\underline{x}, \underline{y}}^{\text{pol}[2]}. \quad (2.5)$$

³Helicity basis refers to the (\pm) -interchanged Brodsky-Lepage spinor basis defined below in eq. (3.27), which is commonly used in LCPT. In LCPT, the e_z spatial direction is used for spin quantization: we refer to the projection of particle’s spin onto the z -axis as ‘‘helicity’’. We note that the proper helicity is the projection of spin onto the momentum of the particle. This difference between the true helicity and LCPT ‘‘helicity’’ requires us to keep both $\delta_{\sigma, \sigma'}$ and $\sigma \delta_{\sigma, \sigma'}$ structures in, e.g., eq. (2.4), even when only helicity-dependent quantities are considered. In the rest of the manuscript, both helicity basis and (\pm) -interchanged Brodsky-Lepage spinor basis are used interchangeably.

⁴Note that the sign in front of the $\gamma^+ \gamma^5$ term in eq. (2.4) is different from that in [3, 70] while in agreement with [92]. In [3] one has to correct eq. (45) by replacing $\rho(\sigma) \rightarrow \rho(-\sigma)$ on its right-hand side. Similarly, one should replace $\rho^T(\sigma') \rightarrow \rho^T(-\sigma')$ in eq. (48) of [3]. This would modify eq. (51) of [3] to agree with our eq. (2.4).

$V_{\underline{x}}^{\text{pol}[1]}$ and $V_{\underline{x},\underline{y}}^{\text{pol}[2]}$ can be read off eq. (2.4) using their definition in eq. (2.5). In the following it will be helpful to separate the gluon and quark contributions to $V_{\underline{x}}^{\text{pol}[1]}$ and $V_{\underline{x},\underline{y}}^{\text{pol}[2]}$. Therefore, we define

$$V_{\underline{x}}^{\text{pol}[1]} = V_{\underline{x}}^{\text{G}[1]} + V_{\underline{x}}^{\text{q}[1]}, \quad V_{\underline{x},\underline{y}}^{\text{pol}[2]} = V_{\underline{x},\underline{y}}^{\text{G}[2]} + V_{\underline{x},\underline{y}}^{\text{q}[2]} \delta^2(\underline{x} - \underline{y}), \quad (2.6)$$

such that

$$V_{\underline{x}}^{\text{G}[1]} = \frac{igP^+}{s} \int_{-\infty}^{\infty} dx^- V_{\underline{x}}[\infty, x^-] F^{12}(x^-, \underline{x}) V_{\underline{x}}[x^-, -\infty], \quad (2.7a)$$

$$V_{\underline{x}}^{\text{q}[1]} = \frac{g^2 P^+}{2s} \int_{-\infty}^{\infty} dx_1^- \int_{x_1^-}^{\infty} dx_2^- V_{\underline{x}}[\infty, x_2^-] t^b \psi_\beta(x_2^-, \underline{x}) U_{\underline{x}}^{ba}[x_2^-, x_1^-] [\gamma^+ \gamma^5]_{\alpha\beta} \bar{\psi}_\alpha(x_1^-, \underline{x}) t^a V_{\underline{x}}[x_1^-, -\infty], \quad (2.7b)$$

$$V_{\underline{x},\underline{y}}^{\text{G}[2]} = -\frac{iP^+}{s} \int_{-\infty}^{\infty} dz^- d^2 z V_{\underline{x}}[\infty, z^-] \delta^2(\underline{x} - \underline{z}) \overleftarrow{D}^i(z^-, \underline{z}) D^i(z^-, \underline{z}) V_{\underline{y}}[z^-, -\infty] \delta^2(\underline{y} - \underline{z}), \quad (2.7c)$$

$$V_{\underline{x},\underline{y}}^{\text{q}[2]} = -\frac{g^2 P^+}{2s} \int_{-\infty}^{\infty} dx_1^- \int_{x_1^-}^{\infty} dx_2^- V_{\underline{x}}[\infty, x_2^-] t^b \psi_\beta(x_2^-, \underline{x}) U_{\underline{x}}^{ba}[x_2^-, x_1^-] [\gamma^+]_{\alpha\beta} \bar{\psi}_\alpha(x_1^-, \underline{x}) t^a V_{\underline{x}}[x_1^-, -\infty]. \quad (2.7d)$$

Curiously, only $V_{\underline{x},\underline{y}}^{\text{G}[2]}$ is truly a non-local operator in the transverse plane.

Similar to eq. (2.3) we define the S -matrix for the gluon-target scattering by

$$U_{\underline{x},\underline{y};\lambda',\lambda} \equiv \int \frac{d^2 p_{\text{in}}}{(2\pi)^2} \frac{d^2 p_{\text{out}}}{(2\pi)^2} e^{i\mathbf{p}_{\text{out}} \cdot \underline{x} - i\mathbf{p}_{\text{in}} \cdot \underline{y}} \left[\delta_{\lambda,\lambda'} (2\pi)^2 \delta^2(\underline{p}_{\text{out}} - \underline{p}_{\text{in}}) + i A_{\lambda',\lambda}^G(\underline{p}_{\text{out}}, \underline{p}_{\text{in}}) \right], \quad (2.8)$$

with the gluon scattering amplitude $A_{\lambda',\lambda}^G(\underline{p}_{\text{out}}, \underline{p}_{\text{in}})$ on the background-field target normalized in the same way as the quark one above. At the sub-eikonal level the S -matrix is [3, 39, 64, 66, 70]⁵

$$\begin{aligned} (U_{\underline{x},\underline{y};\lambda',\lambda})^{ba} &= (U_{\underline{x}})^{ba} \delta^2(\underline{x} - \underline{y}) \delta_{\lambda,\lambda'} \\ &+ \frac{iP^+}{s} \int_{-\infty}^{\infty} dz^- d^2 z (U_{\underline{x}}[\infty, z^-])^{bb'} \delta^2(\underline{x} - \underline{z}) \left[2g\lambda\delta_{\lambda,\lambda'} (\mathcal{F}^{12})^{b'a'} - \delta_{\lambda,\lambda'} \overleftarrow{\mathcal{D}}^{b'c} \cdot \overleftarrow{\mathcal{D}}^{ca'} \right] (z^-, \underline{z}) (U_{\underline{y}}[z^-, -\infty])^{a'a} \delta^2(\underline{y} - \underline{z}) \\ &- \frac{g^2 P^+}{2s} \delta^2(\underline{x} - \underline{y}) \int_{-\infty}^{\infty} dz_1^- \int_{z_1^-}^{\infty} dz_2^- \\ &\quad \times (U_{\underline{x}}[\infty, z_2^-])^{bb'} \bar{\psi}(z_2^-, \underline{x}) t^{b'} V_{\underline{x}}[z_2^-, z_1^-] [\delta_{\lambda,\lambda'} \gamma^+ - \lambda \delta_{\lambda,\lambda'} \gamma^+ \gamma^5] t^{a'} \psi(z_1^-, \underline{x}) (U_{\underline{x}}[z_1^-, -\infty])^{a'a} - \text{c.c.} \end{aligned} \quad (2.9)$$

Here $\mathcal{F}^{12} = \sum_a F^{a12} T^a$ is the adjoint gluon field strength tensor, while the adjoint covariant derivatives are $\overleftarrow{\mathcal{D}}^{ab} = \overleftarrow{\nabla}^{ab} + g f^{acb} \underline{A}^c$ and $\overleftarrow{\mathcal{D}}^{ab} = \overleftarrow{\nabla}^{ab} - g f^{acb} \underline{A}^c$ (or, simply, $\overleftarrow{\mathcal{D}}_i^{ab} = \partial_i \delta^{ab} - ig(T^c)_{ab} A_i^c$ and $\overleftarrow{\mathcal{D}}_i^{ab} = \partial_i \delta^{ab} + ig(T^c)_{ab} A_i^c$, using $(T^c)_{ab} = -if^{abc}$ with $\underline{A} = (A^1, A^2) = -(A_1, A_2)$).

⁵Similar to eq. (2.4), the sign of the $\gamma^+ \gamma^5$ term in eq. (2.9) is different from that in eq. (64) of [3]: correcting $\rho^T(\sigma) \rightarrow \rho^T(-\sigma)$ in eq. (58) and $\rho(\sigma) \rightarrow \rho(-\sigma)$ in eq. (60), both in [3], would change the sign of the $\gamma^+ \gamma^5$ term in eq. (64) of [3], making it agree with our eq. (2.9).

Just as in the fundamental representation, for the adjoint S -matrix at hand we can identify two polarization structures, $\lambda \delta_{\lambda, \lambda'}$ and $\delta_{\lambda, \lambda'}$, and define $U_{\underline{x}}^{\text{pol}[1]}$ and $U_{\underline{x}, \underline{y}}^{\text{pol}[2]}$ by

$$(U_{\underline{x}, \underline{y}; \lambda', \lambda})^{ba} \Big|_{\text{sub-eikonal}} \equiv \lambda \delta_{\lambda, \lambda'} (U_{\underline{x}}^{\text{pol}[1]})^{ba} \delta^2(\underline{x} - \underline{y}) + \delta_{\lambda, \lambda'} (U_{\underline{x}, \underline{y}}^{\text{pol}[2]})^{ba} \quad (2.10)$$

at the sub-eikonal order, excluding the eikonal term in eq. (2.9). Again, we separate the quark and gluon operator contributions by writing

$$U_{\underline{x}}^{\text{pol}[1]} = U_{\underline{x}}^{\text{G}[1]} + U_{\underline{x}}^{\text{q}[1]}, \quad U_{\underline{x}, \underline{y}}^{\text{pol}[2]} = U_{\underline{x}, \underline{y}}^{\text{G}[2]} + U_{\underline{x}, \underline{y}}^{\text{q}[2]} \delta^2(\underline{x} - \underline{y}), \quad (2.11)$$

with

$$(U_{\underline{x}}^{\text{G}[1]})^{ba} = \frac{2igP^+}{s} \int_{-\infty}^{\infty} dx^- (U_{\underline{x}}[\infty, x^-])^{bb'} (\mathcal{F}^{12})^{b'a'}(x^-, \underline{x}) (U_{\underline{x}}[x^-, -\infty])^{a'a}, \quad (2.12a)$$

$$(U_{\underline{x}}^{\text{q}[1]})^{ba} = \frac{g^2 P^+}{2s} \int_{-\infty}^{\infty} dx_1^- \int_{x_1^-}^{\infty} dx_2^- (U_{\underline{x}}[\infty, x_2^-])^{bb'} \bar{\psi}(x_2^-, \underline{x}) t^{b'} V_{\underline{x}}[x_2^-, x_1^-] \gamma^+ \gamma^5 t^{a'} \psi(x_1^-, \underline{x}) (U_{\underline{x}}[x_1^-, -\infty])^{a'a} \\ + \text{c.c.}, \quad (2.12b)$$

$$(U_{\underline{x}, \underline{y}}^{\text{G}[2]})^{ba} = -\frac{iP^+}{s} \int_{-\infty}^{\infty} dz^- d^2z (U_{\underline{x}}[\infty, z^-])^{bb'} \delta^2(\underline{x} - \underline{z}) \overleftarrow{\mathcal{D}}^{b'c}(z^-, \underline{z}) \overrightarrow{\mathcal{D}}^{ca'}(z^-, \underline{z}) (U_{\underline{y}}[z^-, -\infty])^{a'a} \delta^2(\underline{y} - \underline{z}), \quad (2.12c)$$

$$(U_{\underline{x}}^{\text{q}[2]})^{ba} = -\frac{g^2 P^+}{2s} \int_{-\infty}^{\infty} dx_1^- \int_{x_1^-}^{\infty} dx_2^- (U_{\underline{x}}[\infty, x_2^-])^{bb'} \bar{\psi}(x_2^-, \underline{x}) t^{b'} V_{\underline{x}}[x_2^-, x_1^-] \gamma^+ t^{a'} \psi(x_1^-, \underline{x}) (U_{\underline{x}}[x_1^-, -\infty])^{a'a} \\ - \text{c.c.} \quad (2.12d)$$

Once more, only $U_{\underline{x}, \underline{y}}^{\text{G}[2]}$ is non-local in the transverse plane.

3 Quark and gluon helicity distributions and g_1 structure function at small x

3.1 Gluon helicity distribution

We begin with the dipole gluon helicity TMD, defined as [93]

$$g_{1L}^{\text{G dip}}(x, k_T^2) = \frac{-2i}{x P^+} \frac{1}{(2\pi)^3} \frac{1}{2} \sum_{S_L} S_L \int d\xi^- d^2\xi e^{ixP^+ \xi^-} e^{-ik \cdot \underline{\xi}} \quad (3.1) \\ \times \langle P, S_L | \epsilon^{ij} \text{tr} [F^{+i}(0) \mathcal{U}^{[+]}[0, \xi] F^{+j}(\xi) \mathcal{U}^{[-]}[\xi, 0]] | P, S_L \rangle_{\xi^+=0},$$

where $\mathcal{U}^{[+]}$ and $\mathcal{U}^{[-]}$ are the future- and past-pointing Wilson line staples, $k_T = |\underline{k}|$, and ϵ^{ij} is the transverse Levi-Civita symbol with $\epsilon^{12} = +1$. The Jaffe-Manohar (JM) gluon helicity PDF is then [4]

$$\Delta G(x, Q^2) = \int d^2k g_{1L}^{\text{G dip}}(x, k_T^2) = \frac{-2i}{x P^+} \frac{1}{4\pi} \frac{1}{2} \sum_{S_L} S_L \int_{-\infty}^{\infty} d\xi^- e^{ixP^+ \xi^-} \quad (3.2) \\ \times \langle P, S_L | \epsilon^{ij} F^{a+i}(0^+, 0^-, \underline{0}) U_0^{ab}[0, \xi^-] F^{b+j}(0^+, \xi^-, \underline{0}) | P, S_L \rangle,$$

where U_0^{ab} now is a regular adjoint light-cone Wilson line (2.2) connecting the two points in the correlator.

We rewrite eq. (3.1) as

$$g_{1L}^{G dip}(x, k_T^2) = \frac{-2i}{x P^+ V^-} \frac{1}{(2\pi)^3} \frac{1}{2} \sum_{S_L} S_L \int d\xi^- d^2\xi d\zeta^- d^2\zeta e^{ixP^+(\xi^- - \zeta^-)} e^{-ik_\perp \cdot (\xi - \zeta)} \quad (3.3)$$

$$\times \langle P, S_L | \epsilon^{ij} \text{tr} \left[F^{+i}(\zeta) \mathcal{U}^{[+]}[\zeta, \xi] F^{+j}(\xi) \mathcal{U}^{[-]}[\xi, \zeta] \right] | P, S_L \rangle_{\xi^+ = \zeta^+ = 0},$$

with the (infinite) volume factor $V^- = \int dx^- d^2x$. The JM gluon helicity PDF is now given by

$$\Delta G(x, Q^2) = \int^{Q^2} d^2k g_{1L}^{G dip}(x, k_T^2) = \frac{-2i}{x P^+ L^-} \frac{1}{4\pi} \frac{1}{2} \sum_{S_L} S_L \int d\xi^- d\zeta^- e^{ixP^+(\xi^- - \zeta^-)} \quad (3.4)$$

$$\times \langle P, S_L | \epsilon^{ij} F^{a+i}(0^+, \zeta^-, \underline{0}) U_0^{ab}[\zeta^-, \xi^-] F^{b+j}(0^+, \xi^-, \underline{0}) | P, S_L \rangle,$$

where $L^- = \int dx^-$.

In any gauge where the field A^\perp is zero at $x^- \rightarrow \pm\infty$ we can rewrite eq. (3.4) as

$$\Delta G(x, Q^2) = \frac{-2i}{x P^+ L^-} \frac{1}{2\pi} \frac{1}{2} \sum_{S_L} S_L \int_{-\infty}^{\infty} d\xi^- d\zeta^- e^{ixP^+(\xi^- - \zeta^-)} \quad (3.5)$$

$$\times \langle P, S_L | \epsilon^{ij} \text{tr} \left[V_0[-\infty, \zeta^-] F^{+i}(0^+, \zeta^-, \underline{0}) V_0[\zeta^-, \infty] V_0[\infty, \xi^-] F^{+j}(0^+, \xi^-, \underline{0}) V_0[\xi^-, -\infty] \right] | P, S_L \rangle.$$

We further note that in a gauge where the field A^\perp is zero at $x^- \rightarrow \pm\infty$ we have [30, 33]

$$\int_{-\infty}^{\infty} d\xi^- e^{ixP^+\xi^-} V_0[\infty, \xi^-] F^{+j}(0^+, \xi^-, \underline{0}) V_0[\xi^-, -\infty] \quad (3.6)$$

$$= \int_{-\infty}^{\infty} d\xi^- e^{ixP^+\xi^-} \left\{ \partial^+ \left(V_0[\infty, \xi^-] A^j(0^+, \xi^-, \underline{0}) V_0[\xi^-, -\infty] \right) - V_0[\infty, \xi^-] (\partial^j A^+) V_0[\xi^-, -\infty] \right\}$$

$$= - \int_{-\infty}^{\infty} d\xi^- e^{ixP^+\xi^-} V_0[\infty, \xi^-] (\partial^j A^+ + ixP^+ A^j) V_0[\xi^-, -\infty],$$

such that

$$\Delta G(x, Q^2) = \frac{-2i}{x P^+ L^-} \frac{1}{2\pi} \frac{1}{2} \sum_{S_L} S_L \int_{-\infty}^{\infty} d\xi^- d\zeta^- e^{ixP^+(\xi^- - \zeta^-)} \quad (3.7)$$

$$\times \langle P, S_L | \epsilon^{ij} \text{tr} \left[(\partial^i A^+ - ixP^+ A^i) V_0[\zeta^-, \xi^-] (\partial^j A^+ + ixP^+ A^j) V_0[\xi^-, \zeta^-] \right] | P, S_L \rangle.$$

Similarly, for the dipole gluon helicity TMD we write

$$g_{1L}^{G dip}(x, k_T^2) = \frac{-2i}{x P^+ V^-} \frac{1}{(2\pi)^3} \frac{1}{2} \sum_{S_L} S_L \int_{-\infty}^{\infty} d\xi^- d^2\xi d\zeta^- d^2\zeta e^{ixP^+(\xi^- - \zeta^-)} e^{-ik_\perp \cdot (\xi - \zeta)} \quad (3.8)$$

$$\times \langle P, S_L | \epsilon^{ij} \text{tr} \left[V_\zeta[-\infty, \zeta^-] (\partial^i A^+ - ixP^+ A^i) V_\zeta[\zeta^-, \infty] V_\xi[\infty, \xi^-] (\partial^j A^+ + ixP^+ A^j) V_\xi[\xi^-, -\infty] \right] | P, S_L \rangle.$$

Let us simplify the gluon helicity TMD operator (3.8) at small x , expanding it down to sub-eikonal order. Start by defining a ‘‘Lipatov vertex’’

$$L^j(x, \underline{k}) \equiv \int_{-\infty}^{\infty} d\xi^- d^2\xi e^{ixP^+ \xi^- - ik \cdot \underline{\xi}} V_{\underline{\xi}}[\infty, \xi^-] (\partial^j A^+ + ixP^+ A^j) V_{\underline{\xi}}[\xi^-, -\infty] \quad (3.9)$$

and rewriting the gluon dipole helicity TMD as

$$g_{1L}^{G \text{ dip}}(x, k_T^2) = \frac{-2i}{xP^+ V^-} \frac{1}{(2\pi)^3} \frac{1}{2} \sum_{S_L} S_L \langle P, S_L | \epsilon^{ij} \text{tr} [L^{i\dagger}(x, \underline{k}) L^j(x, \underline{k})] | P, S_L \rangle. \quad (3.10)$$

Next let us expand the Lipatov vertex (3.9) in powers of x , that is, in *eikonality*. We get

$$L^j(x, \underline{k}) = \int_{-\infty}^{\infty} d\xi^- d^2\xi e^{-ik \cdot \underline{\xi}} V_{\underline{\xi}}[\infty, \xi^-] \left[\partial^j A^+ + ixP^+ (\xi^- \partial^j A^+ + A^j) + \mathcal{O}(x^2) \right] V_{\underline{\xi}}[\xi^-, -\infty]. \quad (3.11)$$

At order- x^0 we get the standard result,

$$\int_{-\infty}^{\infty} d\xi^- d^2\xi e^{-ik \cdot \underline{\xi}} V_{\underline{\xi}}[\infty, \xi^-] (\partial^j A^+) V_{\underline{\xi}}[\xi^-, -\infty] = \int d^2\xi e^{-ik \cdot \underline{\xi}} \frac{1}{ig} \partial^j V_{\underline{\xi}} = -\frac{k^j}{g} \int d^2\xi e^{-ik \cdot \underline{\xi}} V_{\underline{\xi}}. \quad (3.12)$$

At order- x , let us simplify the $\xi^- \partial^j A^+$ term. Writing

$$\xi^- = \lim_{L^- \rightarrow +\infty} \frac{1}{2} \left[- \int_{\xi^-}^{L^-/2} dz^- + \int_{-L^-/2}^{\xi^-} dz^- \right] \quad (3.13)$$

we obtain

$$\begin{aligned} ixP^+ \int_{-\infty}^{\infty} d\xi^- d^2\xi e^{-ik \cdot \underline{\xi}} V_{\underline{\xi}}[\infty, \xi^-] \left[\xi^- \partial^j A^+(\xi) \right] V_{\underline{\xi}}[\xi^-, -\infty] \\ = -\frac{xP^+}{2g} \int d^2\xi e^{-ik \cdot \underline{\xi}} \int_{-\infty}^{\infty} dz^- V_{\underline{\xi}}[\infty, z^-] \left[\partial^j - \overleftarrow{\partial}^j \right] V_{\underline{\xi}}[z^-, -\infty]. \end{aligned} \quad (3.14)$$

The entire Lipatov vertex becomes

$$L^j(x, \underline{k}) = -\frac{k^j}{g} \int d^2\xi e^{-ik \cdot \underline{\xi}} V_{\underline{\xi}} - \frac{xP^+}{2g} \int d^2\xi e^{-ik \cdot \underline{\xi}} \int_{-\infty}^{\infty} dz^- V_{\underline{\xi}}[\infty, z^-] \left[D^j - \overleftarrow{D}^j \right] V_{\underline{\xi}}[z^-, -\infty] + \mathcal{O}(x^2), \quad (3.15)$$

where we have employed the right-acting covariant derivative $D^j = \partial^j - igA^j$ and the left-acting covariant derivative $\overleftarrow{D}^j = \overleftarrow{\partial}^j + igA^j$ (see [94] for the $D^j - \overleftarrow{D}^j$ operator arising in the definitions of quark OAM in the proton). Substituting eq. (3.15) into eq. (3.10) and

expanding the latter to order- x , we see that only the cross-talk between the leading-order term and the $D^j - \overleftarrow{D}^j$ term in eq. (3.15) survives, yielding

$$g_{1L}^{G dip}(x, k_T^2) = \frac{-2is}{P+V^-g^2} \frac{1}{(2\pi)^3} \frac{1}{2} \sum_{S_L} S_L \epsilon^{ij} k^i \int d^2\zeta d^2\xi e^{-ik \cdot (\underline{\xi} - \underline{\zeta})} \langle P, S_L | \text{tr} \left[V_{\underline{\zeta}}^\dagger V_{\underline{\xi}}^{j \text{pol}[2]} - \left(V_{\underline{\zeta}}^{j \text{pol}[2]} \right)^\dagger V_{\underline{\xi}} \right] | P, S_L \rangle, \quad (3.16)$$

where we have defined the fundamental polarized Wilson line of a different type from those in eqs. (2.7) above, by

$$V_{\underline{z}}^{i G[2]} \equiv \frac{P^+}{2s} \int_{-\infty}^{\infty} dz^- V_{\underline{z}}[\infty, z^-] \left[D^i(z^-, \underline{z}) - \overleftarrow{D}^i(z^-, \underline{z}) \right] V_{\underline{z}}[z^-, -\infty]. \quad (3.17)$$

Defining the standard (but polarization-dependent) ‘‘CGC averaging’’ by

$$\langle \dots \rangle \equiv \frac{1}{2} \sum_{S_L} S_L \frac{1}{2P^+V^-} \langle P, S_L | \dots | P, S_L \rangle \quad (3.18)$$

and the sub-eikonal one by [1]

$$\langle\langle \dots \rangle\rangle \equiv s \langle \dots \rangle \quad (3.19)$$

we recast eq. (3.16) as

$$g_{1L}^{G dip}(x, k_T^2) = \frac{-4i}{g^2 (2\pi)^3} \epsilon^{ij} k^i \int d^2\zeta d^2\xi e^{-ik \cdot (\underline{\xi} - \underline{\zeta})} \langle\langle \text{tr} \left[V_{\underline{\zeta}}^\dagger V_{\underline{\xi}}^{j G[2]} - \left(V_{\underline{\zeta}}^{j G[2]} \right)^\dagger V_{\underline{\xi}} \right] \rangle\rangle. \quad (3.20)$$

This result should be compared to eq. (35) in [33]. The definition of the polarized Wilson line in eq. (34) of [33] is different from our eq. (3.17) by keeping only $2ig A^i$ instead of the covariant derivative difference, $D^i - \overleftarrow{D}^i$ and excluding the normalization factor of $\frac{1}{s}$. The former explains the sign difference between our eq. (3.20) and eq. (35) in [33].

Finally, interchanging $\underline{\zeta} \leftrightarrow \underline{\xi}$ in the second term of eq. (3.20) and replacing $\underline{k} \rightarrow -\underline{k}$ in the same term (which we can do since each term in eq. (3.20) depends on k_T^2 and does not depend on the direction of \underline{k}), we arrive at

$$g_{1L}^{G dip}(x, k_T^2) = \frac{-4i}{g^2 (2\pi)^3} \epsilon^{ij} k^i \int d^2\zeta d^2\xi e^{-ik \cdot (\underline{\xi} - \underline{\zeta})} \langle\langle \text{tr} \left[V_{\underline{\zeta}}^\dagger V_{\underline{\xi}}^{j G[2]} + \left(V_{\underline{\xi}}^{j G[2]} \right)^\dagger V_{\underline{\zeta}} \right] \rangle\rangle. \quad (3.21)$$

Defining the polarized dipole amplitude of the second kind

$$G_{10}^j(zs) \equiv \frac{1}{2N_c} \langle\langle \text{tr} \left[V_{\underline{0}}^\dagger V_{\underline{1}}^{j G[2]} + \left(V_{\underline{1}}^{j G[2]} \right)^\dagger V_{\underline{0}} \right] \rangle\rangle \quad (3.22)$$

we obtain (cf. eq. (38) in [33])

$$g_{1L}^{G dip}(x, k_T^2) = \frac{-8iN_c}{g^2 (2\pi)^3} \epsilon^{ij} k^i \int d^2x_0 d^2x_1 e^{-ik \cdot \underline{x}_{10}} G_{10}^j \left(zs = \frac{Q^2}{x} \right). \quad (3.23)$$

Here $\underline{x}_{10} = \underline{x}_1 - \underline{x}_0$ for the transverse-plane position vectors \underline{x}_1 and \underline{x}_0 , with $x_{10} = |\underline{x}_{10}|$ to be used later on.

Similar to [33] we can introduce the following decomposition of the impact-parameter integrated amplitude G^j :

$$\int d^2 \left(\frac{x_1 + x_0}{2} \right) G_{10}^i(zs) = (x_{10})_{\perp}^i G_1(x_{10}^2, zs) + \epsilon^{ij} (x_{10})_{\perp}^j G_2(x_{10}^2, zs). \quad (3.24)$$

Substituting this into eq. (3.21) we see that G_1 does not contribute. We get (cf. eqs. (40) and (41) in [33])

$$\begin{aligned} g_{1L}^{G \text{ dip}}(x, k_T^2) &= \frac{8iN_c}{g^2 (2\pi)^3} \int d^2 x_{10} e^{-ik \cdot x_{10}} \underline{k} \cdot \underline{x}_{10} G_2 \left(x_{10}^2, zs = \frac{Q^2}{x} \right) \\ &= \frac{N_c}{\alpha_s 2\pi^4} \int d^2 x_{10} e^{-ik \cdot x_{10}} \left[1 + x_{10}^2 \frac{\partial}{\partial x_{10}^2} \right] G_2 \left(x_{10}^2, zs = \frac{Q^2}{x} \right). \end{aligned} \quad (3.25)$$

The gluon helicity PDF is obtained by integrating over \underline{k} , which yields (cf. eq. (124) in [33])

$$\Delta G(x, Q^2) = \frac{2N_c}{\alpha_s \pi^2} \left[\left(1 + x_{10}^2 \frac{\partial}{\partial x_{10}^2} \right) G_2 \left(x_{10}^2, zs = \frac{Q^2}{x} \right) \right]_{x_{10}^2 = \frac{1}{Q^2}}. \quad (3.26)$$

We conclude, just as in [33], that the amplitude G_2 gives us both the gluon dipole helicity TMD (3.25) and the gluon helicity PDF (3.26) at small x . The difference here is in the definition of the operator in eq. (3.17), which is different here from that employed in [33], where the partial-derivative part of the full covariant derivative was discarded as a term independent of helicity.

3.2 Quark helicity distribution

To include both sub-eikonal terms from eq. (2.4) into quark helicity distribution we can employ the analysis carried out in [3], which applies here as well, with the diagram B from [3] (see figure 1 below) again giving the only contribution we need to keep. Just as in [3, 92], we will work with the (\pm)-interchanged Brodsky-Lepage spinors [71] (referred there as the anti-BL spinors)

$$u_{\sigma}(p) = \frac{1}{\sqrt{\sqrt{2}p^-}} [\sqrt{2}p^- + m\gamma^0 + \gamma^0 \underline{\gamma} \cdot \underline{p}] \rho(\sigma), \quad v_{\sigma}(p) = \frac{1}{\sqrt{\sqrt{2}p^-}} [\sqrt{2}p^- - m\gamma^0 + \gamma^0 \underline{\gamma} \cdot \underline{p}] \rho(-\sigma), \quad (3.27)$$

with $p^{\mu} = \left(\frac{p^2 + m^2}{2p^-}, p^-, \underline{p} \right)$ and

$$\rho(+1) = \frac{1}{\sqrt{2}} \begin{pmatrix} 1 \\ 0 \\ -1 \\ 0 \end{pmatrix}, \quad \rho(-1) = \frac{1}{\sqrt{2}} \begin{pmatrix} 0 \\ 1 \\ 0 \\ 1 \end{pmatrix}. \quad (3.28)$$

We begin with eq. (15) in [3], which we modify by replacing (for the massless quarks we will consider from now on) [70]

$$\bar{v}_{\sigma_1}(k_1) \left(\hat{V}_{\underline{w}}^{\dagger} \right)^{ji} v_{\sigma_2}(k_2) \rightarrow 2 \sqrt{k_1^- k_2^-} \int d^2 z \left(V_{\underline{z}, \underline{w}; \sigma_2, \sigma_1}^{\dagger} \right)^{ji}, \quad (3.29)$$

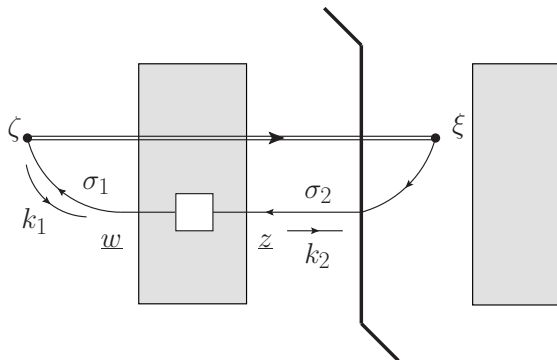


Figure 1. Diagram of class B with kinematics specified. The antiquark propagates from ζ to \underline{w} with momentum k_1 , undergoes a sub-eikonal interaction with the proton which changes its transverse position from \underline{w} on the left of the shock wave (the left shaded rectangle) to \underline{z} on the right of the shock wave, and then propagates from \underline{z} to ξ with momentum k_2 . The sub-eikonal interaction with the proton shock wave (shaded rectangle) is denoted by the white box.

which accounts for both the notation change (to the quark S -matrix from eq. (2.4)) and the fact that the anti-quark position may be different on the two sides of the shock wave, as depicted in figure 1. (Here i, j are the anti-quark color indices. The shock wave, representing the proton target, is shown by the shaded rectangle in figure 1.) Additionally, we need to replace $e^{i\mathbf{k}\cdot(\underline{w}-\underline{\zeta})} \rightarrow e^{i\mathbf{k}\cdot(\underline{z}-\underline{\zeta})}$ in the same eq. (15) of [3]. We end up with

$$g_{1L}^q(x, k_T^2) = -\frac{2P^+}{(2\pi)^3} \int d^2\zeta d^2w d^2z \frac{d^2k_1 dk_1^-}{(2\pi)^3} e^{i\mathbf{k}_1\cdot(\underline{w}-\underline{\zeta}) + i\mathbf{k}\cdot(\underline{z}-\underline{\zeta})} \theta(k_1^-) \sum_{\sigma_1, \sigma_2} \bar{v}_{\sigma_2}(k_2) \frac{1}{2} \gamma^+ \gamma^5 v_{\sigma_1}(k_1) 2\sqrt{k_1^- k_2^-} \times \left\langle \text{Tr} [V_{\underline{\zeta}} V_{\underline{z}, \underline{w}}^\dagger] \right\rangle \frac{1}{[2k_1^- x P^+ + \underline{k}_1^2 - i\epsilon k_1^-] [2k_1^- x P^+ + \underline{k}^2 + i\epsilon k_1^-]} \Big|_{k_2^- = k_1^-, k_1^2 = 0, k_2^2 = 0, \underline{k}_2 = -\underline{k}} + \text{c.c.} \quad (3.30)$$

for the quark helicity TMD with a future-pointing (semi-inclusive Deep Inelastic Scattering, or SIDIS) Wilson-line staple.

Using

$$2\sqrt{k_1^- k_2^-} \bar{v}_{\sigma_2}(k_2) \frac{1}{2} \gamma^+ \gamma^5 v_{\sigma_1}(k_1) = \sigma_1 \delta_{\sigma_2 \sigma_1} (\underline{k}_2 \cdot \underline{k}_1) - i \delta_{\sigma_2 \sigma_1} (\underline{k}_2 \times \underline{k}_1), \quad (3.31)$$

in eq. (3.30), along with eq. (2.5), and assuming that $2k_1^- x P^+ \ll \underline{k}^2, \underline{k}_1^2$ to simplify the denominators at small x , we obtain

$$g_{1L}^q(x, k_T^2) = -\frac{4P^+}{(2\pi)^3} \int d^2\zeta d^2w d^2z \frac{d^2k_1 dk_1^-}{(2\pi)^3} e^{i\mathbf{k}_1\cdot(\underline{w}-\underline{\zeta}) + i\mathbf{k}\cdot(\underline{z}-\underline{\zeta})} \theta(k_1^-) \frac{1}{\underline{k}_1^2 \underline{k}^2} \times \left[-\underline{k} \cdot \underline{k}_1 \delta^2(\underline{z} - \underline{w}) \left\langle \text{Tr} [V_{\underline{\zeta}} V_{\underline{w}}^{\text{pol}[1]\dagger}] \right\rangle + i \underline{k} \times \underline{k}_1 \left\langle \text{Tr} [V_{\underline{\zeta}} V_{\underline{z}, \underline{w}}^{\text{pol}[2]\dagger}] \right\rangle \right] + \text{c.c.} \quad (3.32)$$

Note that the contribution of the eikonal term in eq. (2.4) to eq. (3.30) is zero, as was shown in [3].

Performing the \underline{k}_1 integration and adding the complex conjugate terms explicitly in eq. (3.32) we arrive at

$$g_{1L}^q(x, k_T^2) = -\frac{4iP^+}{(2\pi)^5} \int d^2\zeta d^2w \int_0^{p_2^-} dk_1^- \left\{ e^{i\mathbf{k}\cdot(\underline{w}-\underline{\zeta})} \frac{\underline{k}}{k^2} \cdot \frac{\underline{\zeta}-\underline{w}}{|\underline{\zeta}-\underline{w}|^2} \left\langle \text{T tr} [V_{\underline{\zeta}} V_{\underline{w}}^{\text{pol}[1]\dagger}] + \bar{\text{T}} \text{tr} [V_{\underline{\zeta}}^{\text{pol}[1]} V_{\underline{w}}^\dagger] \right\rangle \right. \\ \left. - i \frac{\underline{k}}{k^2} \times \frac{\underline{\zeta}-\underline{w}}{|\underline{\zeta}-\underline{w}|^2} \int d^2z \left\langle e^{i\mathbf{k}\cdot(\underline{z}-\underline{\zeta})} \text{T tr} [V_{\underline{\zeta}} V_{\underline{z},\underline{w}}^{\text{pol}[2]\dagger}] + e^{-i\mathbf{k}\cdot(\underline{z}-\underline{\zeta})} \bar{\text{T}} \text{tr} [V_{\underline{z},\underline{w}}^{\text{pol}[2]} V_{\underline{\zeta}}^\dagger] \right\rangle \right\}. \quad (3.33)$$

We have also integrated over \underline{z} in the first term in the curly brackets of eq. (3.33) and replaced $\underline{\zeta} \leftrightarrow \underline{w}$ in the term containing the second trace from the first angle brackets.

We concentrate on the second term on the right of eq. (3.33). Employing eq. (2.6), we see that the quark operator contribution to that term is proportional to

$$\propto \int d^2\zeta d^2w \frac{\underline{k}}{k^2} \times \frac{\underline{\zeta}-\underline{w}}{|\underline{\zeta}-\underline{w}|^2} \left\langle e^{i\mathbf{k}\cdot(\underline{w}-\underline{\zeta})} \text{T tr} [V_{\underline{\zeta}} V_{\underline{w}}^{\text{q}[2]\dagger}] + e^{-i\mathbf{k}\cdot(\underline{w}-\underline{\zeta})} \bar{\text{T}} \text{tr} [V_{\underline{w}}^{\text{q}[2]} V_{\underline{\zeta}}^\dagger] \right\rangle. \quad (3.34)$$

For a longitudinally polarized target proton, the expectation values of the impact-parameter integrated traces in eq. (3.34) are functions of the dipole size only. Let us illustrate this with the first such trace: the absence of any preferred transverse direction in the longitudinally polarized target means

$$\int d^2 \left(\frac{\underline{\zeta} + \underline{w}}{2} \right) \left\langle \text{T tr} [V_{\underline{\zeta}} V_{\underline{w}}^{\text{q}[2]\dagger}] \right\rangle = f(|\underline{\zeta} - \underline{w}|^2), \quad (3.35)$$

such that

$$\int d^2\zeta d^2w \frac{\underline{k}}{k^2} \times \frac{\underline{\zeta}-\underline{w}}{|\underline{\zeta}-\underline{w}|^2} \left\langle e^{i\mathbf{k}\cdot(\underline{w}-\underline{\zeta})} \text{T tr} [V_{\underline{\zeta}} V_{\underline{w}}^{\text{q}[2]\dagger}] \right\rangle \\ = \frac{\underline{k}}{k^2} \times \int d^2(\zeta - w) e^{i\mathbf{k}\cdot(\underline{w}-\underline{\zeta})} \frac{\underline{\zeta}-\underline{w}}{|\underline{\zeta}-\underline{w}|^2} f(|\underline{\zeta}-\underline{w}|^2) \propto \underline{k} \times \underline{k} = 0. \quad (3.36)$$

Applying a similar argument to the second term in eq. (3.34), we see that the quark operator $V_{\underline{w}}^{\text{q}[2]}$ does not contribute to the quark dipole TMD at small x in eq. (3.33).

We next consider the gluon contribution to the second term on the right of eq. (3.33). To evaluate this term, it is easier to go back to eq. (3.32), the second term of which can be written as

$$\frac{4(P^+)^2}{s(2\pi)^6} \int_0^{p_2^-} dk_1^- \int d^2\zeta d^2w d^2k_1 e^{i(\underline{k}_1+\underline{k})\cdot(\underline{w}-\underline{\zeta})} \frac{\underline{k} \times \underline{k}_1}{k^2 k_1^2} \int_{-\infty}^{\infty} dy^- \\ \times \left\langle \text{T tr} [V_{\underline{\zeta}} V_{\underline{w}}[-\infty, y^-] \left(\overleftarrow{D}_{\underline{w}}^i - ik_1^i \right) \left(D_{\underline{w}}^i - ik^i \right) V_{\underline{w}}[y^-, \infty]] \right\rangle + \text{c.c.} \quad (3.37)$$

with the help of eq. (2.7c). Further, writing $D_{\underline{w}}^i = (D_{\underline{w}}^i/2) + (D_{\underline{w}}^i/2)$ and integrating one of these terms by parts, while performing the same operation for $\overleftarrow{D}_{\underline{w}}^i$, we arrive at

$$\begin{aligned} & \frac{(P^+)^2}{s(2\pi)^6} \int_0^{p_2^-} dk_1^- \int d^2\zeta d^2w d^2k_1 e^{i(\underline{k}_1+\underline{k})\cdot(\underline{w}-\underline{\zeta})} \frac{\underline{k}\times\underline{k}_1}{\underline{k}^2\underline{k}_1^2} \int_{-\infty}^{\infty} dy^- \\ & \times \left\langle \text{Ttr} \left[V_{\underline{\zeta}} V_{\underline{w}}[-\infty, y^-] \left(\overleftarrow{D}_{\underline{w}}^i - D_{\underline{w}}^i + i(k_1^i - k_1^i) \right) \left(D_{\underline{w}}^i - \overleftarrow{D}_{\underline{w}}^i + i(k_1^i - k_1^i) \right) V_{\underline{w}}[y^-, \infty] \right] \right\rangle + \text{c.c.} \end{aligned} \quad (3.38)$$

The arguments similar to those used to show that the quark operator contribution to this term vanishes apply here to the $(D_{\underline{w}}^i - \overleftarrow{D}_{\underline{w}}^i)^2$ and $(k_1^i - k_1^i)^2$ terms as well, leaving only the ‘‘cross-talk’’ between the $D_{\underline{w}}^i - \overleftarrow{D}_{\underline{w}}^i$ and $k_1^i - k_1^i$ in eq. (3.38). Employing the definition (3.17), we recast those remaining non-zero terms in eq. (3.38) as

$$\frac{4iP^+}{(2\pi)^6} \int_0^{p_2^-} dk_1^- \int d^2\zeta d^2w d^2k_1 e^{i(\underline{k}_1+\underline{k})\cdot(\underline{w}-\underline{\zeta})} \frac{\underline{k}\times\underline{k}_1}{\underline{k}^2\underline{k}_1^2} (k_1^i - k_1^i) \left\langle \text{Ttr} [V_{\underline{\zeta}} V_{\underline{w}}^{iG[2]\dagger}] - \bar{\text{T}}\text{tr} [V_{\underline{\zeta}}^{iG[2]} V_{\underline{w}}^\dagger] \right\rangle. \quad (3.39)$$

Further, employing

$$- \partial_2^j \left(\frac{x_{20}^i}{x_{20}^2} \right) = \frac{\delta^{ij} x_{20}^2 - 2x_{20}^i x_{20}^j}{x_{20}^4} + \delta^{ij} \pi \delta^2(x_{20}) \quad (3.40)$$

we perform the Fourier transform over \underline{k}_1 , obtaining

$$\begin{aligned} & - \frac{4P^+}{(2\pi)^5} \int_0^{p_2^-} dk_1^- \int d^2\zeta d^2w e^{i\underline{k}\cdot(\underline{w}-\underline{\zeta})} \frac{\epsilon^{mj} k^m}{\underline{k}^2} \left[k^i \frac{(\underline{w}-\underline{\zeta})^j}{|\underline{w}-\underline{\zeta}|^2} + i \frac{\delta^{ij} |\underline{w}-\underline{\zeta}|^2 - 2(\underline{w}-\underline{\zeta})^i (\underline{w}-\underline{\zeta})^j}{|\underline{w}-\underline{\zeta}|^4} \right] \\ & \times \left\langle \text{Ttr} [V_{\underline{\zeta}} V_{\underline{w}}^{iG[2]\dagger}] - \bar{\text{T}}\text{tr} [V_{\underline{\zeta}}^{iG[2]} V_{\underline{w}}^\dagger] \right\rangle, \end{aligned} \quad (3.41)$$

where we have also used the fact that $\text{tr} [V_{\underline{w}} V_{\underline{w}}^{iG[2]\dagger}] = 0$. Interchanging the integration variables $\underline{\zeta} \leftrightarrow \underline{w}$ along with flipping the sign $\underline{k} \rightarrow -\underline{k}$ of the transverse momentum in the second term of eq. (3.41) (which is allowed since each term in eq. (3.41) is a function of k_T^2 only), we obtain

$$\begin{aligned} & - \frac{4P^+}{(2\pi)^5} \int_0^{p_2^-} dk_1^- \int d^2\zeta d^2w e^{i\underline{k}\cdot(\underline{w}-\underline{\zeta})} \frac{\epsilon^{mj} k^m}{\underline{k}^2} \left[k^i \frac{(\underline{w}-\underline{\zeta})^j}{|\underline{w}-\underline{\zeta}|^2} + i \frac{\delta^{ij} |\underline{w}-\underline{\zeta}|^2 - 2(\underline{w}-\underline{\zeta})^i (\underline{w}-\underline{\zeta})^j}{|\underline{w}-\underline{\zeta}|^4} \right] \\ & \times \left\langle \text{Ttr} [V_{\underline{\zeta}} V_{\underline{w}}^{iG[2]\dagger}] + \bar{\text{T}}\text{tr} [V_{\underline{w}}^{iG[2]} V_{\underline{\zeta}}^\dagger] \right\rangle. \end{aligned} \quad (3.42)$$

To further simplify the matrix elements of the traces in eq. (3.42) we can employ the relations given by eqs. (22) of [3] (see also [95]),

$$\left\langle \text{Ttr} [V_{\underline{x}} V_{\underline{y}}^{\text{pol}\dagger}] \right\rangle = \left\langle \text{tr} [V_{\underline{x}} V_{\underline{y}}^{\text{pol}\dagger}] \right\rangle, \quad (3.43a)$$

$$\left\langle \bar{\text{T}}\text{tr} [V_{\underline{x}} V_{\underline{y}}^{\text{pol}\dagger}] \right\rangle = \left\langle \text{tr} [V_{\underline{y}}^{\text{pol}\dagger} V_{\underline{x}}] \right\rangle, \quad (3.43b)$$

where the ordering of the operators on the right is important, since the right Wilson line belongs to the amplitude, while the left one is in the complex conjugate amplitude. Application of eqs. (3.43) yields

$$\left\langle \text{T tr} \left[V_{\underline{\zeta}} V_{\underline{w}}^{iG[2]\dagger} \right] + \bar{\text{T}} \text{tr} \left[V_{\underline{w}}^{iG[2]} V_{\underline{\zeta}}^\dagger \right] \right\rangle = \left\langle \text{tr} \left[V_{\underline{\zeta}} V_{\underline{w}}^{iG[2]\dagger} \right] + \text{tr} \left[V_{\underline{w}}^{iG[2]} V_{\underline{\zeta}}^\dagger \right] \right\rangle. \quad (3.44)$$

Comparing this with eq. (3.22), we see that the objects in the angle brackets in the two equations are similar, but not quite the same: the order of the Wilson lines is different in the trace. As we noted above, the order of Wilson lines matters for the operators here. To remedy this issue, we note that the quark helicity TMD is PT-even: hence, we can substitute eq. (3.44) back into eq. (3.42) and apply the PT-transformation to the latter, leaving it invariant (while, in the process, changing the SIDIS Wilson-line staple to the Drell-Yan (DY) one for the TMD). For infinite Wilson lines in question we have

$$V_{\underline{\zeta}} \xrightarrow{\text{PT}} V_{-\underline{\zeta}}^\dagger, \quad V_{\underline{w}}^{iG[2]} \xrightarrow{\text{PT}} V_{-\underline{w}}^{iG[2]\dagger}. \quad (3.45)$$

This means that, under PT, the expression in eq. (3.44) becomes $(2N_c/s) G_{-\underline{w}, -\underline{\zeta}}^i$ (cf. eq. (3.22)), where the sign change in front of \underline{w} and $\underline{\zeta}$ is not important, since these are integration variables. Due to the PT-invariance of the quark helicity TMD, we obtain for eq. (3.42)

$$-\frac{4N_c}{(2\pi)^5} \int_{\Lambda^2/s}^1 \frac{dz}{z} \int d^2\zeta d^2w e^{ik \cdot (w-\zeta)} \frac{\epsilon^{mj} k^m}{k^2} \left[k^i \frac{(w-\zeta)^j}{|w-\zeta|^2} + i \frac{\delta^{ij} |w-\zeta|^2 - 2(w-\zeta)^i (w-\zeta)^j}{|w-\zeta|^4} \right] G_{\underline{w}, \underline{\zeta}}^i(zs), \quad (3.46)$$

where $z = k_1^-/p_2^-$ and Λ is an infrared (IR) cutoff. (Note that the PT-symmetry argument would not have been needed if we had started with the quark TMD with the DY Wilson-line staple or interchanged the past- and forward-pointing staples in eq. (3.1).)

Replacing the second term in eq. (3.33) by the expression (3.46), and adding the contribution of the anti-quark helicity TMD as it was done in [3] to obtain the flavor-singlet quark helicity TMD, we arrive at

$$g_{1L}^S(x, k_T^2) = -\frac{8N_c N_f}{(2\pi)^5} \int_{\Lambda^2/s}^1 \frac{dz}{z} \int d^2\zeta d^2w e^{ik \cdot (w-\zeta)} \left\{ i \frac{\underline{\zeta} - \underline{w}}{|\underline{\zeta} - \underline{w}|^2} \cdot \frac{\underline{k}}{k^2} Q_{\underline{w}, \underline{\zeta}}(zs) \right. \quad (3.47)$$

$$\left. + \frac{\epsilon^{mj} k^m}{k^2} \left[k^i \frac{(w-\zeta)^j}{|w-\zeta|^2} + i \frac{\delta^{ij} |w-\zeta|^2 - 2(w-\zeta)^i (w-\zeta)^j}{|w-\zeta|^4} \right] G_{\underline{w}, \underline{\zeta}}^i(zs) \right\},$$

where we have also summed over quark flavors, generating a factor of N_f by assuming, for simplicity, that all flavors give equal contributions. As in [3], we have defined the ‘‘original’’ polarized dipole amplitude

$$Q_{\underline{w}, \underline{\zeta}}(zs) \equiv \frac{1}{2N_c} \text{Re} \left\langle \left\langle \text{T tr} \left[V_{\underline{\zeta}} V_{\underline{w}}^{\text{pol}[1]\dagger} \right] + \text{T tr} \left[V_{\underline{w}}^{\text{pol}[1]} V_{\underline{\zeta}}^\dagger \right] \right\rangle \right\rangle. \quad (3.48)$$

While the helicity evolution we will derive below is independent of quark flavor, the initial conditions for $Q_{\underline{w}, \underline{\zeta}}(zs)$ may be flavor-dependent [22], meaning that our simplified

assumption of flavor symmetry may need to be generalized by replacing $N_f \rightarrow \sum_f$ and $Q_{\underline{w}, \underline{\zeta}}(zs) \rightarrow Q_{\underline{w}, \underline{\zeta}}^f(zs)$ in eq. (3.47) to include the potential flavor-dependence of the amplitudes $Q_{\underline{w}, \underline{\zeta}}^f(zs)$.

The flavor-singlet quark helicity PDF (1.3) is

$$\Delta\Sigma(x, Q^2) = \int d^2k_T g_{1L}^S(x, k_T^2). \quad (3.49)$$

Using eq. (3.47) in eq. (3.49) while imposing the $\frac{1}{x} > zsx_{10}^2$ lifetime ordering yields

$$\Delta\Sigma(x, Q^2) = -\frac{N_c N_f}{2\pi^3} \int_{\Lambda^2/s}^1 \frac{dz}{z} \int_{\frac{1}{zs}}^{\min\left\{\frac{1}{zQ^2}, \frac{1}{\Lambda^2}\right\}} \frac{dx_{10}^2}{x_{10}^2} \left[Q(x_{10}^2, zs) + 2 G_2(x_{10}^2, zs) \right] \quad (3.50)$$

where we have employed the decomposition (3.24) and

$$Q(x_{10}^2, zs) \equiv \int d^2 \left(\frac{x_0 + x_1}{2} \right) Q_{10}(zs). \quad (3.51)$$

Equation (3.50) is to be compared to eq. (8b) in [2] or, equivalently, eq. (5) in [31], which contain only the first term in the square brackets of eq. (3.50).

Using the decomposition (3.24) and eq. (3.51), eq. (3.47) can be rewritten as

$$g_{1L}^S(x, k_T^2) = \frac{8 N_c N_f}{(2\pi)^5} \int_{\Lambda^2/s}^1 \frac{dz}{z} \int d^2 x_{10} e^{ik \cdot x_{10}} \left[i \frac{x_{10}}{x_{10}^2} \cdot \frac{k}{k^2} \left[Q(x_{10}^2, zs) + G_2(x_{10}^2, zs) \right] - \frac{(k \times x_{10})^2}{k^2 x_{10}^2} G_2(x_{10}^2, zs) \right]. \quad (3.52)$$

The integral over the angles of x_{10} in the last term on the right of eq. (3.52) can be cast into the same form as in the first term [32]. This yields

$$g_{1L}^S(x, k_T^2) = \frac{8 i N_c N_f}{(2\pi)^5} \int_{\Lambda^2/s}^1 \frac{dz}{z} \int d^2 x_{10} e^{ik \cdot x_{10}} \frac{x_{10}}{x_{10}^2} \cdot \frac{k}{k^2} \left[Q(x_{10}^2, zs) + 2 G_2(x_{10}^2, zs) \right]. \quad (3.53)$$

We see that both the quark and gluon helicity TMDs and PDFs at small x can be expressed in terms of the polarized dipole amplitudes $Q(x_{10}^2, zs)$ and $G_2(x_{10}^2, zs)$. These dipole amplitudes enter the expressions (3.53) and (3.50) for the quark helicity TMD and PDF in a specific linear combination, $Q + 2 G_2$.

3.3 g_1 structure function

Next we consider DIS on a longitudinally polarized proton. The hadronic tensor can be written as (see [96, 97] for a systematic exposition)

$$\begin{aligned} W_{\mu\nu} &\equiv \frac{1}{4\pi M_p} \int d^4x e^{iq \cdot x} \langle P, S_L | j_\mu(x) j_\nu(0) | P, S_L \rangle \\ &= W_{\mu\nu}^{\text{sym}} + i \epsilon_{\mu\nu\rho\sigma} \frac{q^\rho}{M_p P \cdot q} \left[S^\sigma g_1(x, Q^2) + \left(S^\sigma - \frac{S \cdot q}{P \cdot q} P^\sigma \right) g_2(x, Q^2) \right], \end{aligned} \quad (3.54)$$

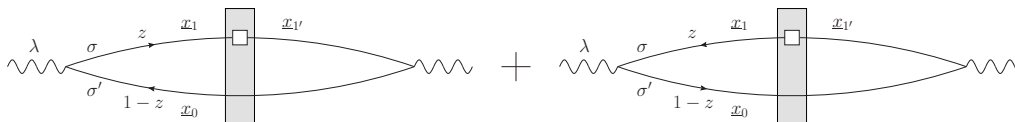


Figure 2. Diagrams needed for the calculation of the g_1 structure function in the dipole picture of DIS. The proton shock wave is denoted by the shaded rectangle, while the white box denotes the sub-eikonal interaction with the target.

where M_p is the proton mass and $W_{\mu\nu}^{\text{sym}}$ denotes the spin-independent ($\mu \leftrightarrow \nu$ symmetric) part of the hadronic tensor, dependent on the F_1 , F_2 structure functions. As usual, j_μ is the quark electromagnetic current operator and the 4-dimensional Levi-Civita symbol is defined with $\epsilon_{0123} = +1$ [98]. We will work in the proton rest frame where $P^\mu = (M_p, \vec{0})$ and the spin 4-vector is $S^\mu = (0, 0, 0, \Sigma M_p)$ for the longitudinally polarized proton with polarization $\Sigma = \pm 1$. Adjusting the frame further such that the virtual photon momentum is $q^\mu = (-Q^2/(2q^-), q^-, \underline{0})$ in the $(+, -, \perp)$ light-cone notation, we have the photon polarizations vectors $\epsilon_{T\lambda}^\mu = (0, 0, \underline{\epsilon}_\lambda)$ for transverse polarizations (with $\underline{\epsilon}_\lambda = (-1/\sqrt{2})(\lambda, i)$ and $\lambda = \pm 1$) and $\epsilon_L^\mu = (Q/(2q^-), q^-/Q, \underline{0})$ for the longitudinal polarization (see e.g. [60]).

Consider the $\gamma^* + p$ scattering cross section,

$$\sigma^{\gamma^*p} = \frac{4\pi^2\alpha_{EM}}{q^0} W_{\mu\nu} \epsilon^{*\mu} \epsilon^\nu \quad (3.55)$$

with α_{EM} the fine structure constant. We are interested in the spin-dependent part of this cross section, which we obtain by using the spin-dependent part of $W_{\mu\nu}$ from eq. (3.54) in eq. (3.55). In the frame we are working in, one can see that only transverse values of μ, ν contribute to the spin-dependent part of σ^{γ^*p} : this means only transverse photon polarizations contribute. Assuming that the virtual photon is transversely polarized with polarization λ , after some algebra we obtain the spin-dependent cross section

$$\sigma^{\gamma^*p}(\lambda, \Sigma) = \frac{4\pi^2\alpha_{EM}}{q^0} W_{\mu\nu} \epsilon_{T\lambda}^{*\mu} \epsilon_{T\lambda}^\nu = -\frac{8\pi^2\alpha_{EM}x}{Q^2} \lambda \Sigma \left[g_1(x, Q^2) - \frac{4x^2M_p^2}{Q^2} g_2(x, Q^2) \right]. \quad (3.56)$$

The object in the square brackets of eq. (3.56) is equal to the virtual photon spin asymmetry A_1 multiplied by the spin-independent structure function $F_1(x, Q^2)$ [97]. The factor of x in the prefactor of eq. (3.56), which is absent in the analogue of this equation for the spin-independent case [60], indicates that the spin-dependent cross section is indeed sub-eikonal at small x . Furthermore, at small x we have $4x^2M_p^2/Q^2 \ll 1$ (which is also true in the standard perturbative approaches which assume large Q^2): this allows us to neglect the second term in the square brackets of eq. (3.56), since it is a sub-sub-sub-eikonal contribution (that is, a contribution suppressed by x^3 compared to the eikonal scattering). We thus write

$$g_1(x, Q^2) = -\frac{Q^2}{16\pi^2\alpha_{EM}x} \left[\sigma^{\gamma^*p}(+, +) - \sigma^{\gamma^*p}(-, +) \right]. \quad (3.57)$$

We see that to obtain the g_1 structure function, we need to find the polarization-dependent part of the $\gamma^* + p$ scattering cross section, σ^{γ^*p} , with the transversely polarized

photon. Working in the dipole picture of DIS, appropriate at small x , we write (cf. [60]), keeping in mind the eikonal and sub-eikonal terms,

$$\begin{aligned} \sigma^{\gamma^* p(\lambda, \Sigma)} = & - \int \frac{d^2 x_1 d^2 x_{1'} d^2 x_0}{4\pi} \int_0^1 \frac{dz}{z(1-z)} \sum_{\sigma, \sigma', f} 2\text{Re} \left\{ \Psi_{\sigma, \sigma'; \lambda}^{\gamma^* \rightarrow q\bar{q}}(\underline{x}_{10}, z) \left[\Psi_{\sigma, \sigma'; \lambda}^{\gamma^* \rightarrow q\bar{q}}(\underline{x}_{1'0}, z) \right]^* \left\langle \text{Ttr} \left[V_{\underline{1}', \underline{1}; \sigma, \sigma}^{\text{pol}} V_{\underline{0}}^\dagger \right] \right\rangle(z) \right. \\ & \left. + \Psi_{\sigma', \sigma; \lambda}^{\gamma^* \rightarrow q\bar{q}}(\underline{x}_{01}, 1-z) \left[\Psi_{\sigma', \sigma; \lambda}^{\gamma^* \rightarrow q\bar{q}}(\underline{x}_{01'}, 1-z) \right]^* \left\langle \text{Ttr} \left[V_{\underline{0}} V_{\underline{1}', \underline{1}; \sigma, \sigma}^{\text{pol}\dagger} \right] \right\rangle(z) \right\}, \quad (3.58) \end{aligned}$$

where the light-cone wave function of a transversely polarized virtual photon in the conventions of [60] is

$$\Psi_{\sigma, \sigma'; \lambda}^{\gamma^* \rightarrow q\bar{q}}(\underline{x}_{10}, z) = \frac{eZ_f}{2\pi} \sqrt{z(1-z)} \left[\delta_{\sigma, -\sigma'} (1-2z-\sigma\lambda) i a_f \frac{\underline{\varepsilon}_\lambda \cdot \underline{x}_{10}}{x_{10}} K_1(x_{10} a_f) + \delta_{\sigma\sigma'} \frac{m_f}{\sqrt{2}} (1+\sigma\lambda) K_0(x_{10} a_f) \right]. \quad (3.59)$$

Equation (3.58) is illustrated in figure 2. For each quark flavor f , m_f is the quark mass, Z_f is the fractional charge of the quark, and $a_f^2 = z(1-z)Q^2 + m_f^2$ with z the fraction of the photon's light-cone ($-$) momentum carried by the quark or by the antiquark, as labeled in the diagrams in figure 2. The overall minus sign in eq. (3.58) reflects the sign difference between the real part of (the interaction term in) the S -matrix and the imaginary part of the forward scattering amplitude.

The light-cone wave function in eq. (3.59) is defined in such a way that the quark is located at \underline{x}_1 in the transverse plane, while the anti-quark is at \underline{x}_0 . As before, $\underline{x}_{ij} = \underline{x}_i - \underline{x}_j$ with $x_{ij} = |\underline{x}_{ij}|$. The dipole sizes before and after scattering on the shock wave in eq. (3.58) are x_{10} and $x_{1'0}$, respectively. In eq. (3.59), the quark and the anti-quark carry polarizations σ and σ' , respectively, while the photon carries polarization λ .

One can easily show that the eikonal part of the S -matrix $V_{\underline{1}', \underline{1}; \sigma, \sigma}^{\text{pol}}$ does not contribute a λ -dependent term in eq. (3.58) that would contribute to eq. (3.57). Therefore, concentrating on the sub-eikonal terms, we substitute eqs. (2.5) and (3.59) into eq. (3.58) and sum over σ, σ' . This gives

$$\begin{aligned} \sigma^{\gamma^* p(+, +)} - \sigma^{\gamma^* p(-, +)} = & - \sum_f \frac{2\alpha_{EM} Z_f^2}{\pi^2} \int d^2 x_1 d^2 x_{1'} d^2 x_0 \int_0^1 dz \quad (3.60) \\ & \times \text{Re} \left\{ -i [z^2 + (1-z)^2] a_f^2 \frac{\underline{x}_{10} \times \underline{x}_{1'0}}{x_{10} x_{1'0}} K_1(x_{10} a_f) K_1(x_{1'0} a_f) \left\langle \text{Ttr} \left[V_{\underline{1}', \underline{1}}^{\text{G}[2]} V_{\underline{0}}^\dagger \right] + \text{Ttr} \left[V_{\underline{0}} V_{\underline{1}', \underline{1}}^{\text{G}[2]\dagger} \right] \right\rangle(z) \right. \\ & \left. + \delta^2(\underline{x}_{11'}) [(2z-1) a_f^2 [K_1(x_{10} a_f)]^2 + m_f^2 [K_0(x_{10} a_f)]^2] \left\langle \text{Ttr} \left[V_{\underline{1}}^{\text{pol}[1]} V_{\underline{0}}^\dagger \right] + \text{Ttr} \left[V_{\underline{0}} V_{\underline{1}}^{\text{pol}[1]\dagger} \right] \right\rangle(z) \right\}. \end{aligned}$$

Note that the quark operator $V^{\text{q}[2]}$ does not contribute.

Finally, we employ the definition of $V_{\underline{1}', \underline{1}}^{\text{G}[2]}$ from eq. (2.7c), along with the polarized Wilson line (3.17) and the dipole amplitude definitions (3.22), (3.24), (3.48), and (3.51), in eq. (3.60). Inserting the result into eq. (3.57), after some algebra and after invoking the PT-symmetry argument we employed earlier on, we obtain our final expression for the

small- x structure function g_1 in terms of the polarized dipole amplitudes:

$$g_1(x, Q^2) = - \sum_f \frac{N_c Z_f^2}{4\pi^4} \int d^2x_{10} \int_{\Lambda^2/s}^1 \frac{dz}{z} \left\{ 2 [z^2 + (1-z)^2] a_f^2 [K_1(x_{10} a_f)]^2 G_2(x_{10}^2, zs) + [(1-2z) a_f^2 [K_1(x_{10} a_f)]^2 - m_f^2 [K_0(x_{10} a_f)]^2] Q(x_{10}^2, zs) \right\}. \quad (3.61)$$

We can cross-check the result (3.61) by considering the double-logarithmic limit of its integrals. Expanding the integrand of eq. (3.61) for $z \ll 1$ and $x_{10} a_f \ll 1$ and keeping only the double-logarithmic terms yields

$$g_1(x, Q^2) = - \sum_f \frac{N_c Z_f^2}{4\pi^3} \int_{\Lambda^2/s}^1 \frac{dz}{z} \int_{\frac{1}{zs}}^{\min\left\{\frac{1}{zQ^2}, \frac{1}{\Lambda^2}\right\}} \frac{dx_{10}^2}{x_{10}^2} [Q(x_{10}^2, zs) + 2 G_2(x_{10}^2, zs)], \quad (3.62)$$

where the lower limit of the x_{10}^2 -integral arises from the $zsx_{10}^2 \gg 1$ conditions, which, in turn, follows from the validity of the shock wave (dipole picture of DIS) approximation (see e.g. [36]), and is also implicitly applied to the full eq. (3.61).

Equation (3.62) should be compared to eq. (3.50), also written in the double-logarithmic approximation. One can rewrite eq. (3.50) as eq. (1.3) with

$$\Delta q_f^+(x, Q^2) = - \frac{N_c}{2\pi^3} \int_{\Lambda^2/s}^1 \frac{dz}{z} \int_{\frac{1}{zs}}^{\min\left\{\frac{1}{zQ^2}, \frac{1}{\Lambda^2}\right\}} \frac{dx_{10}^2}{x_{10}^2} [Q(x_{10}^2, zs) + 2 G_2(x_{10}^2, zs)]. \quad (3.63)$$

Comparing eqs. (3.63) and (3.62) we arrive at the well-known relation [97]

$$g_1(x, Q^2) = \frac{1}{2} \sum_f Z_f^2 \Delta q_f^+(x, Q^2), \quad (3.64)$$

thus confirming consistency of our eqs. (3.62) and (3.50). This completes the cross-check of eq. (3.61).

We conclude this section by summarizing its main results: at small x , the flavor-singlet quark and gluon helicity PDFs and TMDs ($\Delta\Sigma(x, Q^2)$, $g_{1L}^S(x, k_T^2)$, $\Delta G(x, Q^2)$, $g_{1L}^{G dip}(x, k_T^2)$) along with the g_1 structure function can all be expressed in terms of the polarized dipole amplitudes $Q(x_{10}^2, zs)$ and $G_2(x_{10}^2, zs)$. Therefore, to describe these observables we need to construct evolution equations for these two polarized dipole amplitudes. In the earlier literature [2, 3, 31], the contributions of the amplitude G_2 to the quark helicity TMD and PDF, and to the g_1 structure function, have been omitted.

4 Helicity evolution at small x

Our next step is to derive small- x evolution equations for the polarized dipole amplitudes in eqs. (3.48) and (3.22), which we summarize here again for convenience:

$$Q_{10}(zs) \equiv \frac{1}{2N_c} \text{Re} \left\langle \left\langle \text{T tr} [V_{\underline{0}} V_{\underline{1}}^{\text{pol}[1]\dagger}] + \text{T tr} [V_{\underline{1}}^{\text{pol}[1]} V_{\underline{0}}^\dagger] \right\rangle \right\rangle (zs), \quad (4.1)$$

$$G_{10}^i(zs) \equiv \frac{1}{2N_c} \left\langle \left\langle \text{tr} [V_{\underline{0}}^\dagger V_{\underline{1}}^{i\text{G}[2]} + (V_{\underline{1}}^{i\text{G}[2]})^\dagger V_{\underline{0}}] \right\rangle \right\rangle (zs). \quad (4.2)$$

Ultimately, in the evolution equations we would replace G^i by G_2 , defined in the decomposition (3.24).

The evolution equations will be derived in the double-logarithmic approximation (DLA), which is defined as resumming powers of $\alpha_s \ln^2(1/x)$. We will then compare our results to those obtained earlier in [1–3, 31, 33].

4.1 Evolution equations in the operator form

4.1.1 Evolution equations for fundamental and adjoint $Q_{10}(zs)$

Following the procedure outlined in [3, 33], we construct the evolution in the operator language using the shock wave approximation for the polarized target. We suggest that the procedure we employ, which uses the operator language in light cone time-ordered Feynman diagrams (cf. also [95]), could be called the light-cone operator treatment (LCOT). We will again work in the frame where the target proton has a large P^+ momentum, while the projectile Wilson lines are oriented along the x^- -axis. To construct the evolution we will need gluon and quark propagators in the shock wave background. The operators in the polarized dipole amplitudes Q_{10} and G_{10}^i depend on the gluon field components A^+ , \underline{A} and on the quark fields ψ , $\bar{\psi}$: we will need propagators connecting those fields. (We are working in $A^- = 0$ light-cone gauge.)

We begin with the amplitude $Q_{10}(zs)$. Diagrams contributing to its evolution are shown in figure 3. These are the same diagrams as in the earlier works on the subject [1, 3, 33], except now the square box on the line going through the shock wave indicates both terms in eq. (2.10) for the gluon line and both terms in eq. (2.5) for the quark line. In the past works [1, 3, 33], only the first term in each of those equations was included.

In the gluon sector, the sub-eikonal propagator contributing to the evolution of $Q_{10}(zs)$ is $\overline{a^\perp} a^\perp$. It contributes to diagrams I, I', II, II' in figure 3. Following the steps detailed in [3, 33] while including both polarization structures from eq. (2.10) gives (for the propagator in the diagram II)

$$\int_{-\infty}^0 dx_{2'}^- \int_0^\infty dx_2^- \overline{a^\perp} a^\perp(x_{2'}^-, x_1^-) a^\perp(x_2^-, x_0^-) = \sum_{\lambda, \lambda'} \int d^2 x_2 d^2 x_{2'} \left[\int_{-\infty}^0 dx_{2'}^- \int \frac{d^4 k_{2'}}{(2\pi)^4} e^{ik_{2'}^+ x_{2'}^-} e^{ik_{2'}^- x_{2'}^+} \frac{-i}{k_{2'}^2 + i\epsilon} \epsilon_{\lambda'}^{i*} \right] \\ \times \left[(U_{2,2';\lambda,\lambda'}^{\text{pol}})^{ba} 2\pi(2k_2^-) \delta(k_2^- - k_{2'}^-) \right] \left[\int_0^\infty dx_2^- \int \frac{d^4 k_2}{(2\pi)^4} e^{-ik_2^+ x_2^-} e^{-ik_2^- x_{20}^+} \frac{-i}{k_2^2 + i\epsilon} \frac{\epsilon_\lambda \cdot k_2}{k_2^-} \right]. \quad (4.3)$$

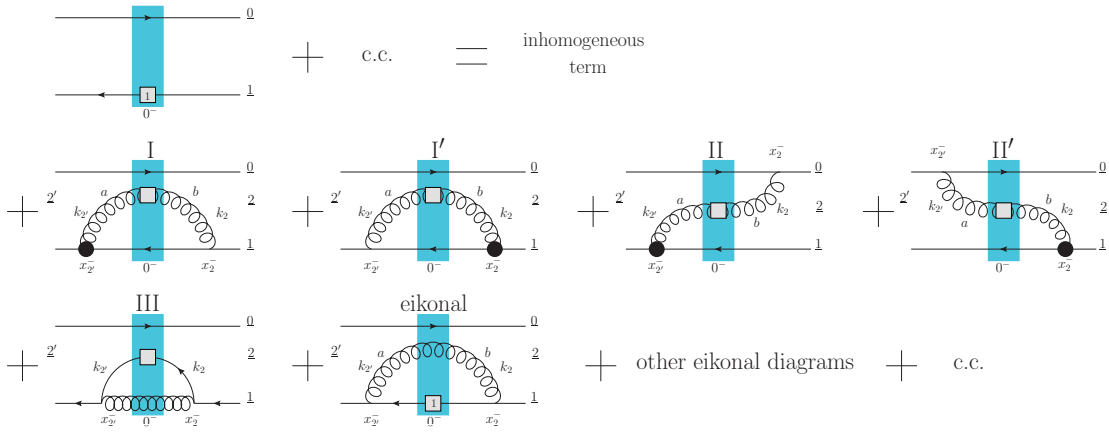


Figure 3. Diagrams representing the evolution of the fundamental polarized dipole amplitude Q_{10} . The vertical shaded rectangle represents the shock wave. The square box on the gluon and quark lines represents the sub-eikonal interaction with the target given by eq. (2.10) for gluons and eq. (2.5) for quarks. The same square box, but with number 1 in it, on the quark line denotes the interaction described by $V_{\perp}^{\text{pol}[1]}$ only. The black circle denotes the sub-eikonal quark-gluon vertex generated by the F^{12} operator in eq. (2.7a), that is, by the F^{12} part of $V_{\perp}^{\text{pol}[1]}$, which, in turn, contributes to Q_{10} through eq. (4.1). All momenta flow to the right.

The propagator (4.3) is separated by the square brackets into the interaction with the shock wave and two free-gluon propagators on either side of the shock wave. It neglects the instantaneous terms in the free-gluon propagators in the light-cone perturbation theory (LCPT) terminology [71, 72], which is justified since such terms do not generate longitudinal logarithms, and, hence, do not contribute to the DLA evolution.

Substituting eq. (2.10) into eq. (4.3), summing over polarizations and integrating over k_2 and $k_{2'}$ (except for $k^- = k_2^- = k_{2'}^-$) yields

$$\begin{aligned}
 & \int_{-\infty}^0 dx_{2'}^- \int_0^{\infty} dx_2^- \overline{a_{\perp}^{ia}(x_{2'}, x_1)} a^{+b}(x_2^-, x_0) = \\
 & = -\frac{1}{4\pi^3} \int_0^{p_2^-} dk^- \left[\int d^2 x_2 \ln\left(\frac{1}{x_{21}\Lambda}\right) \frac{\epsilon^{ij} x_{20}^j}{x_{20}^2} (U_{\perp}^{\text{pol}[1]})^{ba} - i \int d^2 x_2 d^2 x_{2'} \ln\left(\frac{1}{x_{2'1}\Lambda}\right) \frac{x_{20}^i}{x_{20}^2} (U_{\perp}^{\text{pol}[2]})^{ba} \right].
 \end{aligned} \tag{4.4}$$

The first term on the right of eq. (4.4) was obtained before in [33].

As can be seen from the diagrams I and I', or II and II' in figure 3, the propagator (4.4) enters the evolution of $Q_{10}(zs)$ together with the similar propagator, with the x^- -ordering of the endpoints reversed, along with the color indices a, b of the gluon fields interchanged,

$$\begin{aligned}
 & \int_{-\infty}^0 dx_{2'}^- \int_0^{\infty} dx_2^- \overline{a_{\perp}^{ib}(x_2^-, x_1)} a^{+a}(x_{2'}^-, x_0) = \\
 & = -\frac{1}{4\pi^3} \int_0^{p_2^-} dk^- \left[\int d^2 x_2 \ln\left(\frac{1}{x_{21}\Lambda}\right) \frac{\epsilon^{ij} x_{20}^j}{x_{20}^2} (U_{\perp}^{\text{pol}[1]})^{ba} + i \int d^2 x_2 d^2 x_{2'} \ln\left(\frac{1}{x_{21}\Lambda}\right) \frac{x_{2'0}^i}{x_{2'0}^2} (U_{\perp}^{\text{pol}[2]})^{ba} \right].
 \end{aligned} \tag{4.5}$$

One can clearly see that the eikonal Wilson line contribution $(U_2)^{ba} \delta^2(\underline{x}_{22'})$ from eq. (2.9), which is neglected here as a non-DLA contribution, would have entered eqs. (4.4) and (4.5) in the same way as $(U_{2,2'}^{\text{pol}[2]})^{ba}$ does: this eikonal contribution would exactly vanish in the sum of eqs. (4.4) and (4.5), justifying our neglecting of this contribution.

Adding eqs. (4.4) and (4.5), and employing eq. (2.11), after some algebra we arrive at

$$\begin{aligned}
 & \int_{-\infty}^0 dx_{2'}^- \int_0^\infty dx_2^- \left[\overline{a_{\perp}^{ia}(x_2^-, \underline{x}_1)} a^{+b}(x_2^-, \underline{x}_0) + \overline{a_{\perp}^{ib}(x_2^-, \underline{x}_1)} a^{+a}(x_2^-, \underline{x}_0) \right] \\
 &= -\frac{1}{4\pi^3} \int_0^{p_2^-} dk^- \int d^2 x_2 \left\{ 2 \ln \left(\frac{1}{x_{21}\Lambda} \right) \frac{\epsilon^{ij} x_{20}^j}{x_{20}^2} (U_2^{\text{pol}[1]})^{ba} \right. \\
 & \quad + \frac{P^+}{s} \int_{-\infty}^\infty dz^- \left[\frac{x_{20}^i}{x_{20}^2} \frac{x_{21}^j}{x_{21}^2} + \ln \left(\frac{1}{x_{21}\Lambda} \right) \left(\frac{\delta^{ij} x_{20}^2 - 2x_{20}^i x_{20}^j}{x_{20}^4} + \delta^{ij} \pi \delta^2(\underline{x}_{20}) \right) \right] \\
 & \quad \left. \times \left(U_2[\infty, z^-] \left[\mathcal{D}^j - \overleftarrow{\mathcal{D}}^j \right] (z^-, \underline{x}_2) U_2[z^-, -\infty] \right)^{ba} \right\}, \tag{4.6}
 \end{aligned}$$

where we have used eq. (3.40). Note that the contributions of $U_2^{\text{q}[2]}$ from eq. (2.12d) also canceled in the sum (4.6), similar to how the eikonal contributions disappeared earlier.

Defining the gluon contribution to the adjoint polarized Wilson line of the second kind by (cf. eq. (3.17))

$$U_{\underline{z}}^{i\text{G}[2]} \equiv \frac{P^+}{2s} \int_{-\infty}^\infty dz^- U_{\underline{z}}[\infty, z^-] \left[\mathcal{D}^i(z^-, \underline{z}) - \overleftarrow{\mathcal{D}}^i(z^-, \underline{z}) \right] U_{\underline{z}}[z^-, -\infty] \tag{4.7}$$

we rewrite eq. (4.6) as

$$\begin{aligned}
 & \int_{-\infty}^0 dx_{2'}^- \int_0^\infty dx_2^- \left[\overline{a_{\perp}^{ia}(x_2^-, \underline{x}_1)} a^{+b}(x_2^-, \underline{x}_0) + \overline{a_{\perp}^{ib}(x_2^-, \underline{x}_1)} a^{+a}(x_2^-, \underline{x}_0) \right] \\
 &= -\frac{1}{2\pi^3} \int_0^{p_2^-} dk^- \int d^2 x_2 \left\{ \ln \left(\frac{1}{x_{21}\Lambda} \right) \frac{\epsilon^{ij} x_{20}^j}{x_{20}^2} (U_2^{\text{pol}[1]})^{ba} \right. \\
 & \quad \left. + \left[\frac{x_{20}^i}{x_{20}^2} \frac{x_{21}^j}{x_{21}^2} + \ln \left(\frac{1}{x_{21}\Lambda} \right) \left(\frac{\delta^{ij} x_{20}^2 - 2x_{20}^i x_{20}^j}{x_{20}^4} + \delta^{ij} \pi \delta^2(\underline{x}_{20}) \right) \right] (U_2^{i\text{G}[2]})^{ba} \right\}. \tag{4.8}
 \end{aligned}$$

Let us pose here to review the time-ordering arguments, previously detailed in [36]. For the shock-wave picture to be valid, the light-cone lifetime of a gluon, which is $\sim 2k^-/k_{\perp}^2$ for a gluon with momentum k , should be longer than the extent of the ‘‘core’’ shock wave, the target proton, $\sim 1/P^+$. This gives $2k^-P^+ \gg k_{\perp}^2$. Since $k^- = zp_2^-$ with p_2^- the momentum of the original probe, $2k^-P^+ = zs$. For a dipole, $k_{\perp} \sim 1/x_{\perp}$ with x_{\perp} the dipole size. The lifetime ordering condition becomes $zsx_{\perp}^2 \gg 1$. The delta function in eq. (4.8), which puts $x_{20} = 0$, should be interpreted as putting $x_{20}^2 = 1/zs$, since $1/zs$ is the shortest possible distance squared in the scattering system at hand. This means that $zsx_{20}^2 = 1$ and the

gluon emission, corresponding to the delta-function term, is inside the “core” shock wave (and deep inside the shock wave made out of the subsequent emissions in the evolution). Therefore, the subsequent emissions cannot be outside the shock wave, and, hence, cannot generate longitudinal logarithms of energy. Hence, further evolution stops in the delta-function term in eq. (4.8), and the delta function only contributes to the inhomogeneous term in the evolution equations. A similar observation has already been made in [70]. We will, therefore, discard the contribution of the delta function $\delta^2(\underline{x}_{20})$ to the evolution kernel in the following. It is possible that the delta-function term is canceled by the instantaneous term for the gluon propagator (in the LCPT terminology [71, 72]): we are not including such terms in the DLA calculation at hand and, hence, cannot verify that.

The contribution of the propagator (4.8) to the evolution of $F^{12} = \epsilon^{ij} \partial^i A^j$ (at the Abelian level) is proportional to

$$\begin{aligned} & \epsilon^{ji} \partial_1^j \left[\int_{-\infty}^0 dx_2^- \int_0^\infty dx_2^- \left(\overline{a_\perp^{ia}(x_2^-, \underline{x}_1)} a^{+b}(x_2^-, \underline{x}_0) + \overline{a_\perp^{ib}(x_2^-, \underline{x}_1)} a^{+a}(x_2^-, \underline{x}_0) \right) \right] = \\ & - \frac{1}{2\pi^3} \int_0^{p_2^-} dk^- \int d^2 x_2 \left\{ \frac{x_{21}}{x_{21}^2} \cdot \frac{x_{20}}{x_{20}^2} \left(U_2^{\text{Pol}[1]} \right)^{ba} + \left[\frac{\epsilon^{ij} (x_{20}^j + x_{21}^j)}{x_{20}^2 x_{21}^2} + \frac{2x_{20} \times x_{21}}{x_{20}^2 x_{21}^2} \left(\frac{x_{21}^i}{x_{21}^2} - \frac{x_{20}^i}{x_{20}^2} \right) \right] \left(U_2^{iG[2]} \right)^{ba} \right\}. \end{aligned} \quad (4.9)$$

The first term on the right agrees with (twice) the equation (65) in [33]. Its contribution to the evolution of $Q_{10}(zs)$ in figure 3 has been studied before [3, 33]. Therefore, we need to concentrate on the contribution of the second term on the right of eq. (4.9).

Employing eq. (4.9) we see that the contribution of the diagrams I, I', II and II' from figure 3 to the evolution of $Q_{10}(zs)$ is (cf. [1, 3, 33, 40])

$$\begin{aligned} \text{I+I'+II+II'} &= \frac{\alpha_s N_c}{2\pi^2} \int_{\frac{\Lambda^2}{s}}^z \frac{dz'}{z'} \int d^2 x_2 \left\{ \left[\frac{1}{x_{21}^2} - \frac{x_{21}}{x_{21}^2} \cdot \frac{x_{20}}{x_{20}^2} \right] \frac{1}{N_c^2} \left\langle \left\langle \text{Tr} [t^b V_0 t^a V_1^\dagger] \left(U_2^{\text{Pol}[1]} \right)^{ba} + \text{c.c.} \right\rangle \right\rangle (z's) \right. \\ & \left. + \left[2 \frac{\epsilon^{ij} x_{21}^j}{x_{21}^4} - \frac{\epsilon^{ij} (x_{20}^j + x_{21}^j)}{x_{20}^2 x_{21}^2} - \frac{2x_{20} \times x_{21}}{x_{20}^2 x_{21}^2} \left(\frac{x_{21}^i}{x_{21}^2} - \frac{x_{20}^i}{x_{20}^2} \right) \right] \frac{1}{N_c^2} \left\langle \left\langle \text{Tr} [t^b V_0 t^a V_1^\dagger] \left(U_2^{iG[2]} \right)^{ba} + \text{c.c.} \right\rangle \right\rangle (z's) \right\}. \end{aligned} \quad (4.10)$$

Here the emitted gluon's longitudinal momentum is $k^- = z' p_2^-$, while the minimum minus momentum fraction in the parent dipole is labeled z [1, 3, 33, 40]. The second line of eq. (4.10) was not present in the earlier works [1, 3, 33, 40].

While the eikonal diagrams in figure 3 are evaluated the same way as usual [41–47], the contribution of the diagram III is evaluated using the anti-quark propagator through the shock wave [3]

$$\begin{aligned} & \int_{-\infty}^0 dx_{2'}^- \int_0^\infty dx_2^- \overline{\psi_\alpha^i(x_2^-, \underline{x}_1)} \psi_\beta^j(x_{2'}^-, \underline{x}_1) = \sum_{\sigma, \sigma'} \int d^2 x_2 d^2 x_{2'} \left[\int_{-\infty}^0 dx_{2'}^- \int \frac{d^4 k_{2'}}{(2\pi)^4} e^{ik_{2'}^+ x_{2'}^-} e^{ik_{2'} \cdot \underline{x}_{2'1}} \frac{i}{k_{2'}^2 + i\epsilon} (v_{\sigma'}(k_{2'}))_\beta \right] \\ & \times \left[\left(V_{\underline{2}, \underline{2}'; \sigma, \sigma'}^\dagger \right)^{ji} (2k_2^-) (2\pi) \delta(k_2^- - k_{2'}^-) \right] \left[\int_0^\infty dx_2^- \int \frac{d^4 k_2}{(2\pi)^4} e^{-ik_2^+ x_2^-} e^{-ik_2 \cdot \underline{x}_{21}} \frac{i}{k_2^2 + i\epsilon} (\bar{v}_\sigma(k_2))_\alpha \right], \end{aligned} \quad (4.11)$$

where α, β are the spinor indices, while i, j are the color indices. The propagator (4.11) is taken to be local in the transverse plane, since this is how it always enters our evolution in figure 3. Once again, we neglect the instantaneous terms, as being beyond the DLA we are constructing here.

Simplifying the propagator (4.11) to (again, $k^- = k_2^- = k_{2'}^-$)

$$\int_{-\infty}^0 dx_2^- \int_0^{\infty} dx_2^- \overbrace{\psi_\alpha^i(x_2^-, \underline{x}_1) \psi_\beta^j(x_2^-, \underline{x}_1)} = -\frac{1}{\pi} \sum_\sigma \int dk^- k^- \int d^2 x_2 d^2 x_2' \left[\int \frac{d^2 k_2'}{(2\pi)^2} e^{ik_2' \cdot \underline{x}_2'} \frac{1}{k_2'^2} (v_\sigma(k_2'))_\beta \right] \\ \times \left(\sigma V_{\underline{2}}^{\text{pol}[1]\dagger} \delta^2(\underline{x}_{22'}) + V_{\underline{2}, \underline{2}'}^{\text{pol}[2]\dagger} \right)^{ji} \left[\int \frac{d^2 k_2}{(2\pi)^2} e^{-ik_2 \cdot \underline{x}_{21}} \frac{1}{k_2^2} (\bar{v}_\sigma(k_2))_\alpha \right], \quad (4.12)$$

we use it to contract the quark fields in the definition (4.1) of $Q_{10}(zs)$, where the quark field dependence enters through eq. (2.7b) (see [3]). Employing eq. (3.31), we arrive at the following contribution of the diagram III to the evolution of $Q_{10}(zs)$:

$$\text{III} = \frac{\alpha_s}{4\pi^2 N_c} \int_{\frac{\Lambda^2}{s}}^z \frac{dz'}{z'} \int d^2 x_2 \left\{ \frac{1}{x_{21}^2} \left\langle \left\langle \text{Tr tr} \left[t^b V_{\underline{0}} t^a V_{\underline{2}}^{\text{pol}[1]\dagger} \right] U_{\underline{1}}^{ba} \right\rangle \right\rangle (z's) \right. \\ \left. + i \int d^2 x_2' \frac{x_{21}}{x_{21}^2} \times \frac{x_{2'1}}{x_{2'1}^2} \left\langle \left\langle \text{Tr tr} \left[t^b V_{\underline{0}} t^a V_{\underline{2}, \underline{2}'}^{\text{pol}[2]\dagger} \right] U_{\underline{1}}^{ba} \right\rangle \right\rangle (z's) + \text{c.c.} \right\}. \quad (4.13)$$

Employing eqs. (2.6) and (2.7c) the integral over $\underline{x}_{2'}$ can be carried out, yielding

$$\text{III} = \frac{\alpha_s}{4\pi^2 N_c} \int_{\frac{\Lambda^2}{s}}^z \frac{dz'}{z'} \int d^2 x_2 \left\{ \frac{1}{x_{21}^2} \left\langle \left\langle \text{Tr tr} \left[t^b V_{\underline{0}} t^a V_{\underline{2}}^{\text{pol}[1]\dagger} \right] U_{\underline{1}}^{ba} \right\rangle \right\rangle (z's) \right. \\ \left. + 2 \frac{\epsilon^{ij} x_{21}^j}{x_{21}^4} \left\langle \left\langle \text{Tr tr} \left[t^b V_{\underline{0}} t^a V_{\underline{2}}^{iG[2]\dagger} \right] U_{\underline{1}}^{ba} \right\rangle \right\rangle (z's) + \text{c.c.} \right\}. \quad (4.14)$$

While the first term on the right-hand side of eq. (4.14) was obtained before [1, 3], the second term is new.

Combining eqs. (4.10) and (4.14), while adding the well-known contribution [41–47] of the eikonal diagrams from figure 3, and suppressing the time-ordering sign for brevity, we obtain our final evolution equation for the fundamental polarized dipole amplitude $Q_{10}(zs)$:

$$\frac{1}{2N_c} \left\langle \left\langle \text{tr} \left[V_{\underline{0}} V_{\underline{1}}^{\text{pol}[1]\dagger} \right] + \text{c.c.} \right\rangle \right\rangle (zs) = \frac{1}{2N_c} \left\langle \left\langle \text{tr} \left[V_{\underline{0}} V_{\underline{1}}^{\text{pol}[1]\dagger} \right] + \text{c.c.} \right\rangle \right\rangle_0 (zs) \\ + \frac{\alpha_s N_c}{2\pi^2} \int_{\frac{\Lambda^2}{s}}^z \frac{dz'}{z'} \int d^2 x_2 \left\{ \left[\frac{1}{x_{21}^2} - \frac{x_{21}}{x_{21}^2} \cdot \frac{x_{20}}{x_{20}^2} \right] \frac{1}{N_c^2} \left\langle \left\langle \text{tr} \left[t^b V_{\underline{0}} t^a V_{\underline{1}}^\dagger \right] \left(U_{\underline{2}}^{\text{pol}[1]} \right)^{ba} + \text{c.c.} \right\rangle \right\rangle (z's) \right. \\ \left. + \left[2 \frac{\epsilon^{ij} x_{21}^j}{x_{21}^4} - \frac{\epsilon^{ij} (x_{20}^j + x_{21}^j)}{x_{20}^2 x_{21}^2} - \frac{2x_{20} \times x_{21}}{x_{20}^2 x_{21}^2} \left(\frac{x_{21}^i}{x_{21}^2} - \frac{x_{20}^i}{x_{20}^2} \right) \right] \frac{1}{N_c^2} \left\langle \left\langle \text{tr} \left[t^b V_{\underline{0}} t^a V_{\underline{1}}^\dagger \right] \left(U_{\underline{2}}^{iG[2]} \right)^{ba} + \text{c.c.} \right\rangle \right\rangle (z's) \right\} \\ + \frac{\alpha_s N_c}{4\pi^2} \int_{\frac{\Lambda^2}{s}}^z \frac{dz'}{z'} \int \frac{d^2 x_2}{x_{21}^2} \left\{ \frac{1}{N_c^2} \left\langle \left\langle \text{tr} \left[t^b V_{\underline{0}} t^a V_{\underline{2}}^{\text{pol}[1]\dagger} \right] U_{\underline{1}}^{ba} \right\rangle \right\rangle (z's) + 2 \frac{\epsilon^{ij} x_{21}^j}{x_{21}^2} \frac{1}{N_c^2} \left\langle \left\langle \text{tr} \left[t^b V_{\underline{0}} t^a V_{\underline{2}}^{iG[2]\dagger} \right] U_{\underline{1}}^{ba} \right\rangle \right\rangle (z's) + \text{c.c.} \right\} \\ + \frac{\alpha_s N_c}{2\pi^2} \int_{\frac{\Lambda^2}{s}}^z \frac{dz'}{z'} \int d^2 x_2 \frac{x_{10}^2}{x_{21}^2 x_{20}^2} \left\{ \frac{1}{N_c^2} \left\langle \left\langle \text{tr} \left[t^b V_{\underline{0}} t^a V_{\underline{1}}^{\text{pol}[1]\dagger} \right] U_{\underline{2}}^{ba} \right\rangle \right\rangle (z's) - \frac{C_F}{N_c^2} \left\langle \left\langle \text{tr} \left[V_{\underline{0}} V_{\underline{1}}^{\text{pol}[1]\dagger} \right] \right\rangle \right\rangle (z's) + \text{c.c.} \right\}.$$

Here the 0 subscript on the angle brackets, $\left\langle \left\langle \dots \right\rangle \right\rangle_0$, denotes the inhomogeneous term [1, 3, 33, 40], which is the polarized dipole amplitude calculated in the quasi-classical

approximation of the Glauber-Mueller/McLerran-Venugopalan model [99–102], extended in [38] to include helicity dependence.

For brevity reasons we did not include into eq. (4.15) the θ -functions imposing the lifetime-ordering condition (of the daughter parton lifetime compared to the parent parton lifetime) [1, 3, 33, 36, 40]. We imply that every IR-divergent integral in eq. (4.15) is regulated via multiplication of the integrand by such a condition: e.g., by $\theta(z x_{10}^2 - z' x_{21}^2)$. Similarly, the ultraviolet (UV) divergences are regulated by the lifetime ordering condition discussed above, $\min\{x_{21}^2, x_{20}^2\} > 1/(z's)$.

The equation (4.15) contains the DLA evolution of $Q_{10}(zs)$, resumming all powers of $\alpha_s \ln^2(1/x)$ for this amplitude. In fact, it includes part of the single-logarithmic evolution too, by resumming all terms with the longitudinal logarithms of x : thus, it sums up some of the powers of $\alpha_s \ln(1/x)$. These terms were labeled SLA_L in [40], for the single-logarithmic approximation terms, coming from the longitudinal logarithms.

Note also that the expressions in this section have been written down by ignoring the nuances of properly ordering the Wilson lines in the correlators discussed in detail in [3]. In part, this is due to the PT-symmetry argument presented above, which shows that such issues are not relevant for the helicity operators at hand. Additionally, the ordering of operators is not important in the quasi-classical approximation, which is applicable to helicity observables as shown in [38].

As is the case with Balitsky hierarchy [44, 45], eq. (4.15) is not closed. It will become a closed equation only in the large- N_c and large- $N_c \& N_f$ limits considered below (see also [1, 3, 33, 40]). Additionally, different from the earlier works [1, 3, 33, 40], this evolution equation mixes polarized “Wilson lines” of the first “[1]” and second “[2]” kind, in the notation of eqs. (2.5) and (2.10). Hence, to close this equation, even in the large- N_c and large- $N_c \& N_f$ limits, we will need to develop evolution equations for the polarized “Wilson lines” of the second “[2]” kind.

Before doing that, we need to construct the evolution of the adjoint analogue of the amplitude $Q_{10}(zs)$, defined by [3, 40]

$$G_{10}^{\text{adj}}(zs) \equiv \frac{1}{2(N_c^2 - 1)} \text{Re} \left\langle \left\langle \text{T Tr} \left[U_{\underline{0}} U_{\underline{1}}^{\text{pol}[1]\dagger} \right] + \text{T Tr} \left[U_{\underline{1}}^{\text{pol}[1]} U_{\underline{0}}^\dagger \right] \right\rangle \right\rangle (zs) \quad (4.16)$$

with Tr denoting an adjoint trace, delineating it from the fundamental one. The evolution of $G_{10}^{\text{adj}}(zs)$ is needed because unlike the large- N_c limit, in the large- $N_c \& N_f$ limit there is no simple relationship between the two amplitudes, Q_{10} and G_{10}^{adj} , and both of them enter the corresponding evolution equations [1, 3].

Our discussion of the evolution for G_{10}^{adj} will be brief, since it mirrors the above derivation for the fundamental dipole; in addition, large parts of this calculation were done before in [3], albeit omitting the polarized Wilson lines of the second kind. The relevant diagrams are shown in figure 4 and are similar to figure 3. The notation is the same as in figure 3, with the (minor) differences detailed in the caption of figure 4.

The contribution of diagrams I, I', II, and II' from figure 4 is calculated in the same way as that for the same diagrams in figure 3, employing the propagator in eq. (4.9), with the differences being $N_c^2 - 1$ in the denominator of eq. (4.16) as opposed to N_c in the

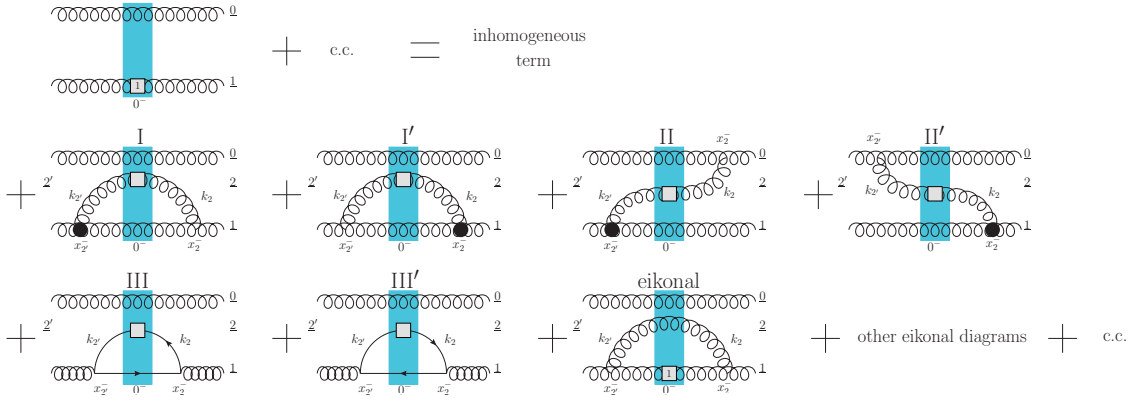


Figure 4. Diagrams representing the evolution of the adjoint polarized dipole amplitude G_{10}^{adj} . Again, the square box on the gluon and quark lines represents the sub-eikonal interaction with the target given by eq. (2.10) for gluons and eq. (2.5) for quarks. The same square box, but with number 1 in it, on the gluon line denotes the interaction described by $U_{\perp}^{\text{pol}[1]}$ only. The black circle denotes the sub-eikonal triple-gluon vertex generated by the F^{12} operator in eq. (2.12a), that is, by the F^{12} part of $U_{\perp}^{\text{pol}[1]}$. All momenta flow to the right.

denominator of eq. (4.1), the overall factor of 2 in eq. (2.12a) absent in eq. (2.7a), and the adjoint representation versus fundamental. We get

$$\begin{aligned}
 \text{I} + \text{I}' + \text{II} + \text{II}' &= \frac{\alpha_s}{\pi^2} \int \frac{dz'}{z'} \int d^2x_2 \left\{ \left[\frac{1}{x_{21}^2} - \frac{x_{21} \cdot x_{20}}{x_{21}^2 x_{20}^2} \right] \frac{1}{N_c^2 - 1} \left\langle \text{Tr} \left[T^b U_0 T^a U_1^\dagger \right] \left(U_2^{\text{pol}[1]} \right)^{ba} + \text{c.c.} \right\rangle (z's) \right. \\
 &+ \left. \left[2 \frac{\epsilon^{ij} x_{21}^j}{x_{21}^4} - \frac{\epsilon^{ij} (x_{20}^j + x_{21}^j)}{x_{20}^2 x_{21}^2} - \frac{2x_{20} \times x_{21}}{x_{20}^2 x_{21}^2} \left(\frac{x_{21}^i}{x_{21}^2} - \frac{x_{20}^i}{x_{20}^2} \right) \right] \frac{1}{N_c^2 - 1} \left\langle \text{Tr} \left[T^b U_0 T^a U_1^\dagger \right] \left(U_2^{iG[2]} \right)^{ba} + \text{c.c.} \right\rangle (z's) \right\}. \quad (4.17)
 \end{aligned}$$

Diagrams III and III' in figure 4 are calculated similar to the diagram III in figure 3, with the propagator (4.12) and the operator (2.12b) coming in particularly handy. This gives

$$\begin{aligned}
 \text{III} + \text{III}' &= -\frac{\alpha_s N_f}{2\pi^2 (N_c^2 - 1)} \int \frac{dz'}{z'} \int d^2x_2 \left\{ \frac{1}{x_{21}^2} \left\langle \text{Tr} \left[t^b V_1 t^a V_2^{\text{pol}[1]\dagger} \right] U_0^{ba} \right\rangle (z's) \right. \\
 &+ \left. 2 \frac{\epsilon^{ij} x_{21}^j}{x_{21}^4} \left\langle \text{Tr} \left[t^b V_1 t^a V_2^{iG[2]\dagger} \right] U_0^{ba} \right\rangle (z's) + \text{c.c.} \right\}, \quad (4.18)
 \end{aligned}$$

where we multiplied everything by the number of quark flavors N_f to account for the sum over flavors in the loop.

Finally, combining eqs. (4.17) and (4.18), adding the well-known contribution of the eikonal diagrams in figure 4, and again suppressing the time-ordering sign for brevity, we arrive at the evolution equation for the adjoint polarized dipole of the first kind,

$$\begin{aligned}
 & \frac{1}{2(N_c^2-1)} \text{Re} \left\langle \left\langle \text{Tr} \left[U_0 U_{\underline{1}}^{\text{Pol}[1]\dagger} \right] + \text{c.c.} \right\rangle \right\rangle (zs) = \frac{1}{2(N_c^2-1)} \text{Re} \left\langle \left\langle \text{Tr} \left[U_0 U_{\underline{1}}^{\text{Pol}[1]\dagger} \right] + \text{c.c.} \right\rangle \right\rangle_0 (zs) \quad (4.19) \\
 & + \frac{\alpha_s}{\pi^2} \int_{\frac{\Delta^2}{s}}^z \frac{dz'}{z'} \int d^2 x_2 \left\{ \left[\frac{1}{x_{21}^2} - \frac{x_{21} \cdot x_{20}}{x_{21}^2 x_{20}^2} \right] \frac{1}{N_c^2-1} \left\langle \left\langle \text{Tr} \left[T^b U_0 T^a U_{\underline{1}}^\dagger \right] \left(U_{\underline{2}}^{\text{Pol}[1]} \right)^{ba} + \text{c.c.} \right\rangle \right\rangle (z's) \right. \\
 & + \left. \left[2 \frac{\epsilon^{ij} x_{21}^j}{x_{21}^4} - \frac{\epsilon^{ij} (x_{20}^j + x_{21}^j)}{x_{20}^2 x_{21}^2} - \frac{2 x_{20} \times x_{21}}{x_{20}^2 x_{21}^2} \left(\frac{x_{21}^i}{x_{21}^2} - \frac{x_{20}^i}{x_{20}^2} \right) \right] \frac{1}{N_c^2-1} \left\langle \left\langle \text{Tr} \left[T^b U_0 T^a U_{\underline{1}}^\dagger \right] \left(U_{\underline{2}}^{iG[2]} \right)^{ba} + \text{c.c.} \right\rangle \right\rangle (z's) \right\} \\
 & - \frac{\alpha_s N_f}{2\pi^2(N_c^2-1)} \int_{\frac{\Delta^2}{s}}^z \frac{dz'}{z'} \int d^2 x_2 \left\{ \frac{1}{x_{21}^2} \left\langle \left\langle \text{tr} \left[t^b V_{\underline{1}} t^a V_{\underline{2}}^{\text{Pol}[1]\dagger} \right] U_0^{ba} \right\rangle \right\rangle (z's) \right. \\
 & \quad \left. + 2 \frac{\epsilon^{ij} x_{21}^j}{x_{21}^4} \left\langle \left\langle \text{tr} \left[t^b V_{\underline{1}} t^a V_{\underline{2}}^{iG[2]\dagger} \right] U_0^{ba} \right\rangle \right\rangle (z's) + \text{c.c.} \right\} \\
 & + \frac{\alpha_s}{2\pi^2} \int_{\frac{\Delta^2}{s}}^z \frac{dz'}{z'} \int d^2 x_2 \frac{x_{10}^2}{x_{21}^2 x_{20}^2} \frac{1}{N_c^2-1} \left\{ \left\langle \left\langle \text{Tr} \left[T^b U_0 T^a U_{\underline{1}}^{\text{Pol}[1]\dagger} \right] U_{\underline{2}}^{ba} \right\rangle \right\rangle (z's) - N_c \left\langle \left\langle \text{Tr} \left[U_0 U_{\underline{1}}^{\text{Pol}[1]\dagger} \right] \right\rangle \right\rangle (z's) + \text{c.c.} \right\}.
 \end{aligned}$$

Just like eq. (4.15), eq. (4.19) resums both the DLA and SLA_L terms. The regulator $\theta(z x_{10}^2 - z' x_{21}^2)$ is implied for the IR-divergent integrals while the $\min\{x_{21}^2, x_{20}^2\} > 1/(z's)$ condition regulates the UV divergences. In the previous version of this evolution in the literature [3], the terms in the third and fifth lines were absent.

4.1.2 Evolution equations for fundamental and adjoint $G_{10}^i(zs)$

Our next step is to construct the evolution equation for the polarized amplitude of the second kind, $G_{10}^i(zs)$, defined in eq. (4.2). The process is very similar to the evolution equations for the polarized dipoles of the first kind constructed above in section 4.1.1. The diagrams contributing to the evolution of $G_{10}^i(zs)$ are shown in figure 5 (cf. figure 3 in [33]). Since the polarized Wilson line of the second kind $V_{\underline{z}}^{iG[2]}$ from eq. (3.17) is a purely gluonic operator, the evolution of $G_{10}^i(zs)$ in figure 5 does not involve soft quark emissions, unlike the evolution of Q_{10} , which contains diagram III in figure 3. Since the eikonal diagrams' contribution is the same as above and in the literature [41–47], we only need to calculate diagrams IV, IV', V, and V' in figure 5.

Start with the operator in eq. (3.17), which we rewrite as

$$\begin{aligned}
 V_{\underline{z}}^{iG[2]} & \equiv \frac{P^+}{2s} \int_{-\infty}^{\infty} dz^- V_{\underline{z}}[\infty, z^-] \left[D^i(z^-, \underline{z}) - \overleftarrow{D}^i(z^-, \underline{z}) \right] V_{\underline{z}}[z^-, -\infty] \quad (4.20) \\
 & = -ig \frac{P^+}{s} \int_{-\infty}^{\infty} dz^- V_{\underline{z}}[\infty, z^-] \left[z^- \partial^i A^+(z^-, \underline{z}) + A^i(z^-, \underline{z}) \right] V_{\underline{z}}[z^-, -\infty].
 \end{aligned}$$

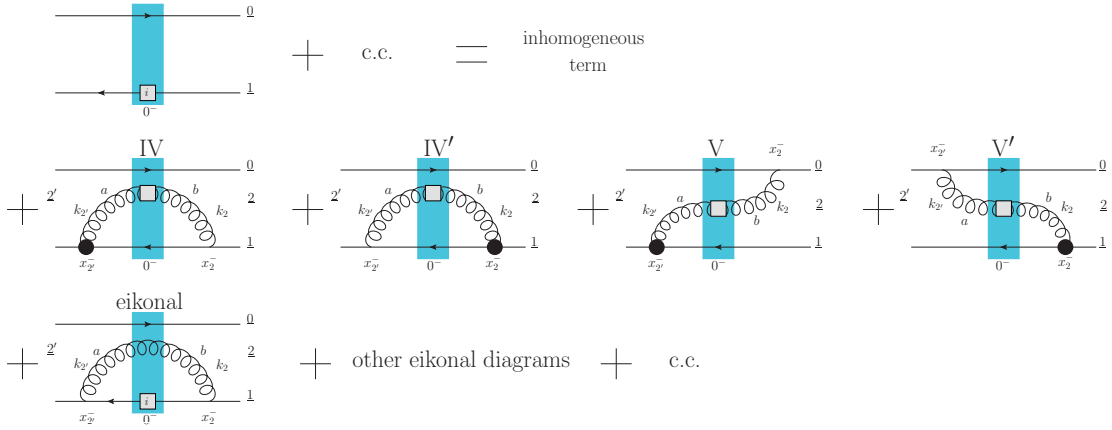


Figure 5. Diagrams representing the evolution of the polarized dipole amplitude of the second kind, $G_{10}^i(zs)$. Once again, the square box on the gluon and quark lines represents the sub-eikonal interaction with the target given by eq. (2.10) for gluons and eq. (2.5) for quarks. The same square box, but with an i in it, on the quark line denotes the interaction described by $V_{\perp}^{iG[2]}$. The black circle denotes the sub-eikonal vertex generated by the $z^- \partial^i A^+(z^-, \underline{z}) + A^i(z^-, \underline{z})$ operator in eq. (4.20), which contributes to G_{10}^i through eq. (4.2). All momenta flow to the right.

Sub-eikonal evolution of the operator in eq. (4.20) depicted in the diagram V of figure 5 includes the following propagator:

$$\begin{aligned}
 & \int_{-\infty}^0 dx_{2'}^- \int_0^{\infty} dx_2^- \left[x_{2'}^- \partial^i a^{+a}(x_{2'}^-, \underline{x}_1) + \overline{a^{ia}(x_{2'}^-, \underline{x}_1)} \right] a^{+b}(x_1^-, \underline{x}_0) \\
 &= \sum_{\lambda, \lambda'} \int d^2 x_2 d^2 x_{2'} \left[\int_{-\infty}^0 dx_{2'}^- \int \frac{d^4 k_1}{(2\pi)^4} e^{ik_1^+ x_{2'}^-} e^{ik_1 \cdot \underline{x}_{2'1}} \frac{-i}{k_{2'}^2 + i\epsilon} \left(\epsilon_{\lambda'}^{*i} + ix_{2'}^- k_2^i \frac{\epsilon_{\lambda'}^* \cdot \underline{k}_{2'}}{k_{2'}^-} \right) \right] \\
 & \times \left[\left(U_{\underline{2}, \underline{2}'; \lambda, \lambda'}^{\text{pol}} \right)^{ba} 2\pi(2k_{2'}^-) \delta(k_2^- - k_{2'}^-) \right] \left[\int_0^{\infty} dx_2^- \int \frac{d^4 k_2}{(2\pi)^4} e^{-ik_2^+ x_2^-} e^{-ik_2 \cdot \underline{x}_{20}} \frac{-i}{k_2^2 + i\epsilon} \frac{\epsilon_{\lambda} \cdot \underline{k}_2}{k_2^-} \right].
 \end{aligned} \tag{4.21}$$

The contraction sign over the square brackets in eq. (4.21) is an abbreviated notation implying the sum of contractions $x_{2'}^- \partial^i \overline{a^{+a}} a^{+b}$ and $\overline{a^{ia}} a^{+b}$.

We integrate eq. (4.21) over $x_{2'}^-$ and x_2^- first, then over $k_2^+, k_{2'}^+, k_2^-$ (note the second-order pole in the $k_{2'}^+$ integral due to the extra power of $x_{2'}^-$), Fourier-transform over \underline{k}_2 and $\underline{k}_{2'}$, and use eq. (2.10) to sum over polarizations. The following Fourier transform integral comes in handy:

$$\int \frac{d^2 k}{(2\pi)^2} \frac{e^{ik \cdot \underline{x}}}{k_{\perp}^2} \left[\delta^{ij} - \frac{2k^i k^j}{k_{\perp}^2} \right] = -\frac{1}{4\pi} \left[\delta^{ij} - \frac{2x^i x^j}{x_{\perp}^2} \right]. \tag{4.22}$$

In the end one arrives at

$$\begin{aligned}
 & \int_{-\infty}^0 dx_{2'}^- \int_0^{\infty} dx_2^- \left[x_2^- \partial^i a^{+a}(x_2^-, \underline{x}_1) \sqrt{a^{ia}(x_2^-, \underline{x}_1)} \right] a^{+b}(x_2^-, \underline{x}_0) \\
 &= \frac{1}{(2\pi)^3} \int_0^{p_2^-} dk^- \left\{ \int d^2 x_2 \left[\frac{\epsilon^{ij} x_{20}^j}{x_{20}^2} - 2x_{21}^i \frac{x_{21} \cdot x_{20}}{x_{21}^2 x_{20}^2} \right] \left(U_{\underline{2}}^{\text{Pol}[1]} \right)^{ba} - i \int d^2 x_2 d^2 x_{2'} \left[\frac{x_{20}^i}{x_{20}^2} - 2x_{21}^i \frac{x_{21} \cdot x_{20}}{x_{21}^2 x_{20}^2} \right] \left(U_{\underline{2}, \underline{2}'}^{\text{Pol}[2]} \right)^{ba} \right\},
 \end{aligned} \tag{4.23}$$

where, as usual, $k^- = k_2^- = k_{2'}^-$.

Similarly, for the other time ordering which enters in diagram V' from figure 5 we obtain

$$\begin{aligned}
 & \int_{-\infty}^0 dx_{2'}^- \int_0^{\infty} dx_2^- \left[x_2^- \partial^i a^{+b}(x_2^-, \underline{x}_1) \sqrt{a^{ib}(x_2^-, \underline{x}_1)} \right] a^{+a}(x_2^-, \underline{x}_0) \\
 &= \frac{1}{(2\pi)^3} \int_0^{p_2^-} dk^- \left\{ \int d^2 x_2 \left[\frac{\epsilon^{ij} x_{20}^j}{x_{20}^2} - 2x_{21}^i \frac{x_{21} \cdot x_{20}}{x_{21}^2 x_{20}^2} \right] \left(U_{\underline{2}}^{\text{Pol}[1]} \right)^{ba} + i \int d^2 x_2 d^2 x_{2'} \left[\frac{x_{2'0}^i}{x_{2'0}^2} - 2x_{21}^i \frac{x_{21} \cdot x_{2'0}}{x_{21}^2 x_{2'0}^2} \right] \left(U_{\underline{2}, \underline{2}'}^{\text{Pol}[2]} \right)^{ba} \right\},
 \end{aligned} \tag{4.24}$$

such that the sum of both time orderings (4.23) and (4.24) is

$$\begin{aligned}
 & \int_{-\infty}^0 dx_{2'}^- \int_0^{\infty} dx_2^- \left\{ \left[x_2^- \partial^i a^{+a}(x_2^-, \underline{x}_1) \sqrt{a^{ia}(x_2^-, \underline{x}_1)} \right] a^{+b}(x_2^-, \underline{x}_0) + \left[x_2^- \partial^i a^{+b}(x_2^-, \underline{x}_1) \sqrt{a^{ib}(x_2^-, \underline{x}_1)} \right] a^{+a}(x_2^-, \underline{x}_0) \right\} \\
 &= \frac{1}{4\pi^3} \int_0^{p_2^-} dk^- \int d^2 x_2 \left\{ \left[\frac{\epsilon^{ij} x_{20}^j}{x_{20}^2} - 2x_{21}^i \frac{x_{21} \cdot x_{20}}{x_{21}^2 x_{20}^2} \right] \left(U_{\underline{2}}^{\text{Pol}[1]} \right)^{ba} \right. \\
 & \quad \left. + \left[\delta^{ij} \left(2 \frac{x_{20} \cdot x_{21}}{x_{20}^2 x_{21}^2} + \frac{1}{x_{20}^2} \right) + 2 \frac{x_{21}^i x_{20}^j}{x_{21}^2 x_{20}^2} \left(2 \frac{x_{20} \cdot x_{21}}{x_{20}^2} + 1 \right) - 2 \frac{x_{21}^i x_{21}^j}{x_{21}^2 x_{20}^2} \left(2 \frac{x_{20} \cdot x_{21}}{x_{21}^2} + 1 \right) - 2 \frac{x_{20}^i x_{20}^j}{x_{20}^4} \right] \left(U_{\underline{2}}^{G[2]} \right)^{ba} \right\}.
 \end{aligned} \tag{4.25}$$

Here we have neglected the delta-function terms, similar to those appearing in eq. (3.40).

Employing the propagator (4.25) to calculate diagrams IV, IV', V, and V' in figure 5, and adding in the eikonal contribution, which is the same as in eq. (4.15), we derive the evolution equation for $G_{10}^i(zs)$:

$$\begin{aligned}
 & \frac{1}{2N_c} \left\langle \left\langle \text{tr} \left[V_0 V_1^{iG[2]\dagger} \right] + \text{c.c.} \right\rangle \right\rangle (zs) = \frac{1}{2N_c} \left\langle \left\langle \text{tr} \left[V_0 V_1^{iG[2]\dagger} \right] + \text{c.c.} \right\rangle \right\rangle_0 (zs) \\
 & + \frac{\alpha_s N_c}{4\pi^2} \int_{\frac{\Lambda_s^2}{s}}^z \frac{dz'}{z'} \int d^2 x_2 \left\{ \left[\frac{\epsilon^{ij} x_{21}^j}{x_{21}^2} - \frac{\epsilon^{ij} x_{20}^j}{x_{20}^2} + 2x_{21}^i \frac{x_{21} \cdot x_{20}}{x_{21}^2 x_{20}^2} \right] \frac{1}{N_c^2} \left\langle \left\langle \text{tr} \left[t^b V_0 t^a V_1^\dagger \right] \left(U_{\underline{2}}^{\text{Pol}[1]} \right)^{ba} + \text{c.c.} \right\rangle \right\rangle (z's) \right. \\
 & + \left[\delta^{ij} \left(\frac{3}{x_{21}^2} - 2 \frac{x_{20} \cdot x_{21}}{x_{20}^2 x_{21}^2} - \frac{1}{x_{20}^2} \right) - 2 \frac{x_{21}^i x_{20}^j}{x_{21}^2 x_{20}^2} \left(2 \frac{x_{20} \cdot x_{21}}{x_{20}^2} + 1 \right) + 2 \frac{x_{21}^i x_{21}^j}{x_{21}^2 x_{20}^2} \left(2 \frac{x_{20} \cdot x_{21}}{x_{21}^2} + 1 \right) + 2 \frac{x_{20}^i x_{20}^j}{x_{20}^4} - 2 \frac{x_{21}^i x_{21}^j}{x_{21}^4} \right] \\
 & \times \frac{1}{N_c^2} \left\langle \left\langle \text{tr} \left[t^b V_0 t^a V_1^\dagger \right] \left(U_{\underline{2}}^{G[2]} \right)^{ba} + \text{c.c.} \right\rangle \right\rangle (z's) \left. \right\} \\
 & + \frac{\alpha_s N_c}{2\pi^2} \int_{\frac{\Lambda_s^2}{s}}^z \frac{dz'}{z'} \int d^2 x_2 \frac{x_{10}^2}{x_{21}^2 x_{20}^2} \left\{ \frac{1}{N_c^2} \left\langle \left\langle \text{tr} \left[t^b V_0 t^a V_1^{iG[2]\dagger} \right] \left(U_{\underline{2}} \right)^{ba} \right\rangle \right\rangle (z's) - \frac{C_F}{N_c^2} \left\langle \left\langle \text{tr} \left[V_0 V_1^{iG[2]\dagger} \right] \right\rangle \right\rangle (z's) + \text{c.c.} \right\}.
 \end{aligned} \tag{4.26}$$

In the version of eq. (4.26) constructed in [33] (see eq. (80) there), the term in the third and fourth lines of eq. (4.26) was missing, and the kernel of the term in the second line was different, since the contributions of the fields $a^{+a}(x_{2'}^-, \underline{x}_1)$ and $a^{+b}(x_2^-, \underline{x}_1)$ in eq. (4.25) was neglected.

The adjoint version of eq. (4.26) can be constructed by analogy. One gets

$$\begin{aligned}
 & \frac{1}{2(N_c^2-1)} \left\langle \left\langle \text{Tr} \left[U_0 U_1^{iG[2]\dagger} \right] + \text{c.c.} \right\rangle \right\rangle (zs) = \frac{1}{2(N_c^2-1)} \left\langle \left\langle \text{Tr} \left[U_0 U_1^{iG[2]\dagger} \right] + \text{c.c.} \right\rangle \right\rangle_0 (zs) \\
 & + \frac{\alpha_s}{4\pi^2} \int \frac{dz'}{z'} \int d^2x_2 \left\{ \left[\frac{\epsilon^{ij} x_{21}^j}{x_{21}^2} - \frac{\epsilon^{ij} x_{20}^j}{x_{20}^2} + 2x_{21}^i \frac{x_{21} \cdot x_{20}}{x_{21}^2 x_{20}^2} \right] \frac{1}{N_c^2-1} \left\langle \left\langle \text{Tr} \left[T^b U_0 T^a U_1^\dagger \right] \left(U_2^{\text{Pol}[1]} \right)^{ba} + \text{c.c.} \right\rangle \right\rangle (z's) \right. \\
 & + \left[\delta^{ij} \left(\frac{3}{x_{21}^2} - 2 \frac{x_{20} \cdot x_{21}}{x_{20}^2 x_{21}^2} - \frac{1}{x_{20}^2} \right) - 2 \frac{x_{21}^i x_{20}^j}{x_{21}^2 x_{20}^2} \left(2 \frac{x_{20} \cdot x_{21}}{x_{20}^2} + 1 \right) + 2 \frac{x_{21}^i x_{21}^j}{x_{21}^2 x_{20}^2} \left(2 \frac{x_{20} \cdot x_{21}}{x_{21}^2} + 1 \right) + 2 \frac{x_{20}^i x_{20}^j}{x_{20}^4} - 2 \frac{x_{21}^i x_{21}^j}{x_{21}^4} \right] \\
 & \times \frac{1}{N_c^2-1} \left\langle \left\langle \text{Tr} \left[T^b U_0 T^a U_1^\dagger \right] \left(U_2^{jG[2]} \right)^{ba} + \text{c.c.} \right\rangle \right\rangle (z's) \left. \right\} \\
 & + \frac{\alpha_s}{2\pi^2} \int \frac{dz'}{z'} \int d^2x_2 \frac{x_{10}^2}{x_{21}^2 x_{20}^2} \frac{1}{N_c^2-1} \left\{ \left\langle \left\langle \text{Tr} \left[T^b U_0 T^a U_1^{iG[2]\dagger} \right] \left(U_2 \right)^{ba} \right\rangle \right\rangle (z's) - N_c \left\langle \left\langle \text{Tr} \left[U_0 U_1^{iG[2]\dagger} \right] \right\rangle \right\rangle (z's) + \text{c.c.} \right\}.
 \end{aligned} \tag{4.27}$$

Equations (4.26) and (4.27) resum both the DLA and SLA_L terms. The regulator $\theta(z x_{10}^2 - z' x_{21}^2)$ is implied again for all the IR-divergent integrals in these equations, while the $\min\{x_{21}^2, x_{20}^2\} > 1/(z's)$ condition again regulates the UV divergences.

Equations (4.15), (4.19), (4.26), and (4.27) form a closed set of equation at the level of (polarized) Wilson lines. To achieve a closed set of equations at the level of (polarized) dipole amplitude, we need to take the large- N_c or the large- $N_c \& N_f$ limits [1, 3, 33, 40]. This is what we will do next.

4.2 Evolution equations in the large- N_c limit

To obtain the large- N_c limit of the helicity evolution at hand, we will follow the standard approach [3]. We start with eq. (4.19), and drop the term proportional to N_f on its right-hand side, as being due to the quark loop correction, suppressed at large N_c . Similarly neglecting all quark loop contribution, we replace

$$U_{\underline{x}}^{\text{Pol}[1]} \rightarrow U_{\underline{x}}^{\text{G}[1]} \tag{4.28}$$

everywhere in eq. (4.19), thus discarding $U_{\underline{x}}^{\text{q}[1]}$ in eq. (2.11). In the same spirit, we define the large- N_c analogue of $Q_{10}(zs)$ from eq. (4.1) by [3]

$$G_{10}(zs) \equiv \frac{1}{2N_c} \text{Re} \left\langle \left\langle \text{T tr} \left[V_0 V_1^{\text{G}[1]\dagger} \right] + \text{T tr} \left[V_1^{\text{G}[1]} V_0^\dagger \right] \right\rangle \right\rangle (zs). \tag{4.29}$$

We employ the well-known relation between the adjoint and fundamental Wilson lines,

$$(U_{\underline{x}})^{ba} = 2 \text{tr} [t^b V_{\underline{x}} t^a V_{\underline{x}}^\dagger]. \tag{4.30}$$

Using eq. (4.30) one can show that (see eq. (73) in [3])

$$\left(U_{\underline{x}}^{\text{G}[1]} \right)^{ba} = 4 \text{tr} \left[t^b V_{\underline{x}} t^a V_{\underline{x}}^{\text{G}[1]\dagger} \right] + 4 \text{tr} \left[t^b V_{\underline{x}}^{\text{G}[1]} t^a V_{\underline{x}}^\dagger \right]. \tag{4.31}$$

This relation, in turn, gives

$$G_{10}^{\text{adj}}(zs) = 4 G_{10}(zs) S_{10}(zs) \quad (4.32)$$

at large N_c . Here we have defined the “standard” unpolarized dipole S -matrix [41–53]

$$S_{10}(zs) = \frac{1}{N_c} \left\langle \text{Tr} \left[V_{\underline{0}} V_{\underline{1}}^\dagger \right] \right\rangle (zs). \quad (4.33)$$

We assume that $S_{10}(zs)$ is real, neglecting the odderon contribution to the imaginary part of $S_{10}(zs)$, as suppressed by a power of α_s [103–114].

Similarly, defining the adjoint version of $G_{10}^i(zs)$ from eq. (4.2) by

$$G_{10}^{i \text{ adj}}(zs) \equiv \frac{1}{2(N_c^2 - 1)} \text{Re} \left\langle \left\langle \text{Tr} \text{Tr} \left[U_{\underline{0}} U_{\underline{1}}^{i \text{ G}[2] \dagger} \right] + \text{Tr} \text{Tr} \left[U_{\underline{1}}^{i \text{ G}[2]} U_{\underline{0}}^\dagger \right] \right\rangle \right\rangle (zs), \quad (4.34)$$

one can use eq. (4.30) to show that

$$\left(U_{\underline{x}}^{i \text{ G}[2]} \right)^{ba} = 2 \text{tr} \left[t^b V_{\underline{x}} t^a V_{\underline{x}}^{i \text{ G}[2] \dagger} \right] + 2 \text{tr} \left[t^b V_{\underline{x}}^{i \text{ G}[2]} t^a V_{\underline{x}}^\dagger \right] \quad (4.35)$$

such that

$$G_{10}^{i \text{ adj}}(zs) = 2 G_{10}^i(zs) S_{10}(zs). \quad (4.36)$$

Using the above results, along with the Fierz identity, we can similarly simplify the operators on the right-hand side of eq. (4.19) at large N_c , obtaining (cf. [3, 40])

$$\frac{1}{N_c^2 - 1} \left\langle \left\langle \text{Tr} \left[T^b U_{\underline{0}} T^a U_{\underline{1}}^\dagger \right] \left(U_{\underline{2}}^{\text{G}[1]} \right)^{ba} + \text{c.c.} \right\rangle \right\rangle (zs) = 4 N_c S_{10}(zs) [S_{20}(zs) G_{21}(zs) + S_{21}(zs) \Gamma_{20,21}(zs)], \quad (4.37a)$$

$$\frac{1}{N_c^2 - 1} \left\langle \left\langle \text{Tr} \left[T^b U_{\underline{0}} T^a U_{\underline{1}}^\dagger \right] \left(U_{\underline{2}}^{i \text{ G}[2]} \right)^{ba} + \text{c.c.} \right\rangle \right\rangle (zs) = 2 N_c S_{10}(zs) [S_{20}(zs) G_{21}^i(zs) + S_{21}(zs) \Gamma_{20,21}^i(zs)], \quad (4.37b)$$

$$\frac{1}{N_c^2 - 1} \left\langle \left\langle \text{Tr} \left[T^b U_{\underline{0}} T^a U_{\underline{1}}^{\text{G}[1] \dagger} \right] \left(U_{\underline{2}} \right)^{ba} + \text{c.c.} \right\rangle \right\rangle (zs) = 4 N_c S_{20}(zs) [S_{10}(zs) G_{21}(zs) + S_{21}(zs) \Gamma_{10,21}(zs)]. \quad (4.37c)$$

Here $\Gamma_{20,21}(zs)$ is the “neighbor” polarized dipole amplitude of the first kind [1–3, 33]: its operator definition is the same as for $G_{20}(zs)$, see eq. (4.29). However, the evolution in $\Gamma_{20,21}(zs)$ is subject to the lifetime of subsequent emissions limited by $z x_{21}^2$ from above. Hence the evolution depends on the size of the neighbor dipole 21, justifying the name of the amplitude. Similarly, the “neighbor” polarized dipole amplitude of the second kind, $\Gamma_{20,21}^i(zs)$, is defined by eq. (4.2) with the same lifetime constraint on the subsequent evolution. The choice of which amplitude in eqs. (4.37) becomes the “neighbor” amplitude is made assuming that $x_{21} \ll x_{20}$ in the DLA, as is justified by the kernel in eq. (4.19).

Employing eqs. (4.32) and (4.37) along with the trick detailed in the appendix D of [40], we arrive at the large- N_c version of eq. (4.19),

$$\begin{aligned} G_{10}(zs) = & G_{10}^{(0)}(zs) + \frac{\alpha_s N_c}{2\pi^2} \int_{\frac{\Lambda^2}{s}}^z \frac{dz'}{z'} \int d^2 x_2 \left\{ 2 \left[\frac{1}{x_{21}^2} - \frac{x_{21}}{x_{21}^2} \cdot \frac{x_{20}}{x_{20}^2} \right] [S_{20}(z's) G_{21}(z's) + S_{21}(z's) \Gamma_{20,21}^{\text{gen}}(z's)] \right. \\ & + \left[2 \frac{\epsilon^{ij} x_{21}^j}{x_{21}^4} - \frac{\epsilon^{ij} (x_{20}^j + x_{21}^j)}{x_{20}^2 x_{21}^2} - \frac{2 x_{20} \times x_{21}}{x_{20}^2 x_{21}^2} \left(\frac{x_{21}^i}{x_{21}^2} - \frac{x_{20}^i}{x_{20}^2} \right) \right] [S_{20}(z's) G_{21}^i(z's) + S_{21}(z's) \Gamma_{20,21}^{i \text{ gen}}(z's)] \\ & \left. + \frac{x_{10}^2}{x_{21}^2 x_{20}^2} [S_{20}(z's) G_{21}(z's) - \Gamma_{10,21}^{\text{gen}}(z's)] \right\}. \quad (4.38) \end{aligned}$$

In spirit with summing up the DLA and SLA_L terms simultaneously, we replaced $\Gamma_{10,21}$ and $\Gamma_{20,21}^i$ in eq. (4.38) by the generalized polarized dipole amplitudes [33, 40]

$$\Gamma_{10,32}^{\text{gen}}(zs) \equiv G_{10}(zs) \theta(x_{32} - x_{10}) + \Gamma_{10,32}(zs) \theta(x_{10} - x_{32}), \quad (4.39a)$$

$$\Gamma_{10,32}^{i\text{ gen}}(zs) \equiv G_{10}^i(zs) \theta(x_{32} - x_{10}) + \Gamma_{10,32}^i(zs) \theta(x_{10} - x_{32}). \quad (4.39b)$$

The amplitudes in eqs. (4.39) become $\Gamma_{10,21}$ and $\Gamma_{20,21}^i$, respectively, in the DLA limit, and reduce back to G_{10} and G_{10}^i for the SLA_L terms, in which the ordering between the dipole size and its neighbor dipole size is not important. Note that in eqs. (4.39), x_{10} and x_{32} can be any general transverse separations, that is, neither of them is necessarily the parent or daughter dipole size.

To extract the DLA contribution from eq. (4.38), we put $S_{21} = S_{20} = 1$ in it, since the evolution of the unpolarized dipole S -matrix is SLA_L [44–53]. In addition, it appears to be more convenient to integrate eq. (4.38) over the impact parameters, while employing eq. (3.24). The same decomposition applies to $\Gamma_{20,21}^i$, since it depends only on the size x_{21} of the dipole 21, and not on its orientation in the transverse plane,

$$\int d^2 \left(\frac{x_1 + x_0}{2} \right) \Gamma_{20,21}^i(zs) = (x_{20})_{\perp}^i \Gamma_1(x_{20}^2, x_{21}^2, zs) + \epsilon^{ij} (x_{20})_{\perp}^j \Gamma_2(x_{20}^2, x_{21}^2, zs). \quad (4.40)$$

Defining (cf. eq. (3.51))

$$G(x_{10}^2, zs) \equiv \int d^2 \left(\frac{x_0 + x_1}{2} \right) G_{10}(zs), \quad \Gamma(x_{20}^2, x_{21}^2, zs) \equiv \int d^2 \left(\frac{x_0 + x_2}{2} \right) \Gamma_{20,21}(zs) \quad (4.41)$$

we write the impact-parameter integrated part of eq. (4.38) as

$$G(x_{10}^2, zs) = G^{(0)}(x_{10}^2, zs) + \frac{\alpha_s N_c}{2\pi^2} \int_{\frac{\Lambda_s^2}{s}}^z \frac{dz'}{z'} \int d^2 x_2 \left\{ \frac{1}{x_{21}^2} \theta(x_{10} - x_{21}) [\Gamma(x_{10}^2, x_{21}^2, z's) + 3G(x_{21}^2, z's)] \right. \quad (4.42)$$

$$+ \left[\frac{2}{x_{21}^2} - \frac{\underline{x}_{21} \cdot (\underline{x}_{20} + \underline{x}_{21})}{x_{20}^2 x_{21}^2} + \frac{2(\underline{x}_{21} \times \underline{x}_{20})^2}{x_{20}^4 x_{21}^2} \right] G_2(x_{21}^2, z's)$$

$$\left. + \left[2 \frac{\underline{x}_{20} \cdot \underline{x}_{21}}{x_{21}^4} - \frac{\underline{x}_{20} \cdot (\underline{x}_{20} + \underline{x}_{21})}{x_{20}^2 x_{21}^2} + \frac{2(\underline{x}_{21} \times \underline{x}_{20})^2}{x_{20}^2 x_{21}^2} \right] \Gamma_2^{\text{gen}}(x_{20}^2, x_{21}^2, z's) \right\}.$$

Here we have applied the DLA simplifications to the parts of the integral kernel containing amplitudes G and Γ . Note that the contributions of G_1 and Γ_1 defined in the decompositions (3.24) and (4.40) vanish, due to a single Levi-Civita symbol ϵ^{ij} multiplying those functions in the x_2 integrals: it is impossible to make a non-zero scalar quantity out of a single transverse vector \underline{x}_{10} and one factor of ϵ^{ij} .

We now need to extract the DLA part of the kernel containing amplitudes G_2 and Γ_2^{gen} in eq. (4.42).⁶ The x_2 -integral in those terms appears to have no IR divergence and no UV

⁶Here and below, when extracting DLA parts of various evolution equations, we will assume that the impact parameter-integrated amplitudes without transverse indices, G, Γ, G_2, Γ_2 , etc., do not contain integer powers of the dipole sizes, x_{10}, x_{21}, x_{20} , etc., and the dependence on these distances enters the amplitudes only as perturbatively small ($\sim \sqrt{\alpha_s}$ or $\sim \alpha_s$) powers or logarithms of x_{10}, x_{21}, x_{20} , etc. This assumption is supported by the Born-level initial conditions (the inhomogeneous terms) shown below (see also [2, 33]).

divergence as $x_{20} \rightarrow 0$. However, there is a divergence at $x_{21} \rightarrow 0$, due to the first term in each square bracket: keeping those terms only we obtain

$$G(x_{10}^2, z s) = G^{(0)}(x_{10}^2, z s) + \frac{\alpha_s N_c}{2\pi^2} \int_{\frac{\Lambda^2}{s}}^z \frac{dz'}{z'} \int d^2 x_2 \theta(x_{10} - x_{21}) \left\{ \frac{1}{x_{21}^2} [\Gamma(x_{10}^2, x_{21}^2, z' s) + 3G(x_{21}^2, z' s)] \right. \\ \left. + \frac{2}{x_{21}^2} G_2(x_{21}^2, z' s) + 2 \frac{x_{20} \cdot x_{21}}{x_{21}^4} \Gamma_2(x_{20}^2, x_{21}^2, z' s) \right\}. \quad (4.43)$$

The last term in eq. (4.43) contains a power-law divergence as $x_{21} \rightarrow 0$: however, this divergence vanishes after angular averaging. Writing $\underline{x}_{20} = \underline{x}_{10} + \underline{x}_{21}$ in that term, and expanding in the powers of $x_{21} \ll x_{10}$ while keeping only divergent terms as $x_{21} \rightarrow 0$, we get

$$\int d^2 x_2 \theta(x_{10} - x_{21}) 2 \frac{x_{20} \cdot x_{21}}{x_{21}^4} \Gamma_2(x_{20}^2, x_{21}^2, z' s) \quad (4.44) \\ \approx \int d^2 x_2 \theta(x_{10} - x_{21}) \frac{2}{x_{21}^2} \left[\Gamma_2(x_{10}^2, x_{21}^2, z' s) + x_{10}^2 \frac{\partial}{\partial x_{10}^2} \Gamma_2(x_{10}^2, x_{21}^2, z' s) \right].$$

The second term on the right of eq. (4.44) contains a logarithmic derivative with respect to x_{10}^2 . Such derivative removes one power of $\ln x_{10}^2$, and is, therefore, outside of the DLA. Therefore, we neglect this term here, keeping in mind that it will need to be reinstated in the single-logarithmic approximation (SLA). Inserting the first term from the right-hand side of eq. (4.44) into eq. (4.43), we arrive at the DLA version of eq. (4.38),

$$G(x_{10}^2, z s) = G^{(0)}(x_{10}^2, z s) + \frac{\alpha_s N_c}{2\pi} \int_{\frac{1}{s x_{10}^2}}^z \frac{dz'}{z'} \int_{\frac{1}{z' s}}^{x_{10}^2} \frac{dx_{21}^2}{x_{21}^2} \left[\Gamma(x_{10}^2, x_{21}^2, z' s) + 3G(x_{21}^2, z' s) \quad (4.45) \right. \\ \left. + 2G_2(x_{21}^2, z' s) + 2\Gamma_2(x_{10}^2, x_{21}^2, z' s) \right].$$

The G and Γ terms in eq. (4.45) agree with that found in the literature [1–3, 33], while the G_2 and Γ_2 terms are new.

The DLA large- N_c evolution equation for the neighbor amplitude Γ can be found by analogy, employing the existing techniques [1–3, 33, 36, 40]. One gets

$$\Gamma(x_{10}^2, x_{21}^2, z' s) = G^{(0)}(x_{10}^2, z' s) + \frac{\alpha_s N_c}{2\pi} \int_{\frac{1}{s x_{10}^2}}^{z'} \frac{dz''}{z''} \int_{\frac{1}{z'' s}}^{\min[x_{10}^2, x_{21}^2 \frac{z'}{z''}]} \frac{dx_{32}^2}{x_{32}^2} \left[\Gamma(x_{10}^2, x_{32}^2, z'' s) + 3G(x_{32}^2, z'' s) \quad (4.46) \right. \\ \left. + 2G_2(x_{32}^2, z'' s) + 2\Gamma_2(x_{10}^2, x_{32}^2, z'' s) \right].$$

Again, the G_2 and Γ_2 terms are new.

Equations (4.45) and (4.46) have to be supplemented by the large- N_c DLA evolution equations for G_2 and Γ_2 . We begin with eq. (4.26) and perform the replacement (4.28) in it, to remove quark loops which are negligible at large N_c . Employing eqs. (4.30), (4.31),

and (4.35), along with the Fierz identity, one can readily show that at large N_c

$$\frac{1}{N_c^2} \left\langle \left\langle \text{tr} \left[t^b V_0 t^a V_1^\dagger \right] \left(U_2^{G[1]} \right)^{ba} + \text{c.c.} \right\rangle \right\rangle (zs) = 2S_{20}(zs)G_{21}(zs) + 2S_{21}(zs)\Gamma_{20,21}(zs), \quad (4.47a)$$

$$\frac{1}{N_c^2} \left\langle \left\langle \text{tr} \left[t^b V_0 t^a V_1^\dagger \right] \left(U_2^{jG[2]} \right)^{ba} + \text{c.c.} \right\rangle \right\rangle (zs) = S_{20}(zs)G_{21}^j(zs) + S_{21}(zs)\Gamma_{20,21}^j(zs), \quad (4.47b)$$

$$\frac{1}{N_c^2} \left\langle \left\langle \text{tr} \left[t^b V_0 t^a V_1^{iG[2]\dagger} \right] \left(U_2 \right)^{ba} + \text{c.c.} \right\rangle \right\rangle (zs) = S_{20}(zs)G_{12}^i(zs). \quad (4.47c)$$

Again, in selecting which dipole amplitude are of the “neighbor” type, we assume that the UV divergences in the DLA limit come only from the $x_{21} \ll x_{10} \approx x_{20}$ region, and do not arise from the $x_{20} \ll x_{10} \approx x_{21}$ region.

Employing eqs. (4.47) in eq. (4.26) we arrive at

$$\begin{aligned} G_{10}^i(zs) &= G_{10}^{i(0)}(zs) \\ &+ \frac{\alpha_s N_c}{4\pi^2} \int_{\frac{\Lambda_s^2}{s}}^z \frac{dz'}{z'} \int d^2 x_2 \left\{ 2 \left[\frac{\epsilon^{ij} x_{21}^j}{x_{21}^2} - \frac{\epsilon^{ij} x_{20}^j}{x_{20}^2} + 2x_{21}^i \frac{x_{21} \times x_{20}}{x_{21}^2 x_{20}^2} \right] \left[S_{20}(z's)G_{21}(z's) + S_{21}(z's)\Gamma_{20,21}^{\text{gen}}(z's) \right] \right. \\ &+ \left[\delta^{ij} \left(\frac{3}{x_{21}^2} - 2 \frac{x_{20} \cdot x_{21}}{x_{20}^2 x_{21}^2} - \frac{1}{x_{20}^2} \right) - 2 \frac{x_{21}^i x_{20}^j}{x_{21}^2 x_{20}^2} \left(2 \frac{x_{20} \cdot x_{21}}{x_{20}^2} + 1 \right) + 2 \frac{x_{21}^i x_{21}^j}{x_{21}^2 x_{20}^2} \left(2 \frac{x_{20} \cdot x_{21}}{x_{21}^2} + 1 \right) + 2 \frac{x_{20}^i x_{20}^j}{x_{20}^4} - 2 \frac{x_{21}^i x_{21}^j}{x_{21}^4} \right] \\ &\left. \times \left[S_{20}(z's)G_{21}^j(z's) + S_{21}(z's)\Gamma_{20,21}^{j\text{gen}}(z's) \right] \right\} \\ &+ \frac{\alpha_s N_c}{2\pi^2} \int_{\frac{\Lambda_s^2}{s}}^z \frac{dz'}{z'} \int d^2 x_2 \frac{x_{10}^2}{x_{21}^2 x_{20}^2} \left[S_{20}(z's)G_{12}^i(z's) - \Gamma_{10,21}^{i\text{gen}}(z's) \right]. \end{aligned} \quad (4.48)$$

Equation (4.48), just like eq. (4.38), resums both the DLA and SLA_L terms.

To extract the DLA contribution from eq. (4.48), we put $S_{21} = S_{20} = 1$ and integrate it over the impact parameters. Since we are interested in the amplitude G_2 , we invert eq. (3.24) to write

$$G_2(x_{10}^2, zs) = \frac{\epsilon^{ij} x_{10}^j}{x_{10}^2} \int d^2 \left(\frac{x_1 + x_0}{2} \right) G_{10}^i(zs). \quad (4.49)$$

Performing the projection (4.49), we arrive at

$$\begin{aligned} G_2(x_{10}^2, zs) &= G_2^{(0)}(x_{10}^2, zs) \\ &+ \frac{\alpha_s N_c}{4\pi^2} \int_{\frac{\Lambda_s^2}{s}}^z \frac{dz'}{z'} \int \frac{d^2 x_2}{x_{10}^2} \left\{ 2 \left[\underline{x}_{10} \cdot \left(\frac{x_{21}}{x_{21}^2} - \frac{x_{20}}{x_{20}^2} \right) + 2 \frac{(x_{21} \times x_{20})^2}{x_{21}^2 x_{20}^2} \right] \left[G(x_{21}^2, z's) + \Gamma^{\text{gen}}(x_{20}^2, x_{21}^2, z's) \right] \right. \\ &+ \left[\underline{x}_{10} \cdot x_{21} \left(\frac{3}{x_{21}^2} - 2 \frac{x_{20} \cdot x_{21}}{x_{20}^2 x_{21}^2} - \frac{1}{x_{20}^2} \right) + 2 \frac{(x_{21} \times x_{20})^2}{x_{20}^2} \left(\frac{1}{x_{21}^2} + 2 \frac{x_{20} \cdot x_{21}}{x_{20}^2 x_{21}^2} - \frac{1}{x_{20}^2} \right) \right] G_2(x_{21}^2, z's) \\ &+ \left. \left[\underline{x}_{10} \cdot x_{20} \left(\frac{3}{x_{21}^2} - 2 \frac{x_{20} \cdot x_{21}}{x_{20}^2 x_{21}^2} - \frac{1}{x_{20}^2} \right) + 2 \frac{(x_{21} \times x_{20})^2}{x_{21}^2} \left(-\frac{1}{x_{21}^2} + 2 \frac{x_{20} \cdot x_{21}}{x_{20}^2 x_{21}^2} + \frac{1}{x_{20}^2} \right) \right] \Gamma_2^{\text{gen}}(x_{20}^2, x_{21}^2, z's) \right\} \\ &- \frac{\alpha_s N_c}{2\pi^2} \int_{\frac{\Lambda_s^2}{s}}^z \frac{dz'}{z'} \int \frac{d^2 x_2}{x_{21}^2 x_{20}^2} \left[\underline{x}_{10} \cdot x_{21} G_2(x_{21}^2, z's) + x_{10}^2 \Gamma_2^{\text{gen}}(x_{10}^2, x_{21}^2, z's) \right]. \end{aligned} \quad (4.50)$$

Next we need to extract the DLA part of the integral kernels in eq. (4.50). We start with the first term in the kernel on the right-hand side of eq. (4.50), the one multiplying $G + \Gamma^{\text{gen}}$: it has no UV divergences, neither at $x_{21} \rightarrow 0$ nor at $x_{20} \rightarrow 0$. It does have an IR divergence when $x_{21} \approx x_{20} \gg x_{10}$. We proceed to the next term in the kernel, the one multiplying G_2 : it also has no UV divergences, but it does have an IR divergence. The term multiplying Γ_2 contains an IR divergence as well, along with the UV divergence at $x_{21} \rightarrow 0$. Finally, the term in the last line of eq. (4.50) has neither an IR divergence nor a UV divergence at $x_{20} \rightarrow 0$: it does contain a UV divergence at $x_{21} \rightarrow 0$. The two UV divergences cancel. Performing all these DLA simplification yields the DLA large- N_c evolution for G_2 :

$$G_2(x_{10}^2, zs) = G_2^{(0)}(x_{10}^2, zs) + \frac{\alpha_s N_c}{\pi} \int_{\frac{\Lambda^2}{s}}^z \frac{dz'}{z'} \int_{\max[x_{10}^2, \frac{1}{z's}]}^{\min[\frac{z}{z'}x_{10}^2, \frac{1}{\Lambda^2}]} \frac{dx_{21}^2}{x_{21}^2} \left[G(x_{21}^2, z's) + 2G_2(x_{21}^2, z's) \right]. \quad (4.51)$$

In arriving at eq. (4.51) we have also employed the fact that for $x_{21} \approx x_{20} \gg x_{10}$ we have $\Gamma^{\text{gen}}(x_{20}^2, x_{21}^2, z's) \approx G(x_{21}^2, z's)$ and $\Gamma_2^{\text{gen}}(x_{20}^2, x_{21}^2, z's) \approx G_2(x_{21}^2, z's)$, since the two daughter dipole sizes are comparable to each other. We have also imposed light-cone time ordering conditions, $zx_{10}^2 \gg z'x_{21}^2 \gg 1/s$, along with the $1/\Lambda^2$ IR cutoff on the x_{21}^2 integration. Equation (4.51) is different from the corresponding equation for G_2 derived earlier in [33], for the reasons stated above.

The analogue of eq. (4.51) for the neighbor dipole amplitude Γ_2 is constructed similarly. We get

$$\Gamma_2(x_{10}^2, x_{21}^2, z's) = G_2^{(0)}(x_{10}^2, z's) + \frac{\alpha_s N_c}{\pi} \int_{\frac{\Lambda^2}{s}}^{\frac{z'}{x_{10}^2}} \frac{dz''}{z''} \int_{\max[x_{10}^2, \frac{1}{z''s}]}^{\min[\frac{z'}{z''}x_{21}^2, \frac{1}{\Lambda^2}]} \frac{dx_{32}^2}{x_{32}^2} \left[G(x_{32}^2, z''s) + 2G_2(x_{32}^2, z''s) \right]. \quad (4.52)$$

Equations (4.45), (4.46), (4.51), and (4.52) form a closed system of DLA evolution equations for helicity at large N_c . For convenience, we list them all here,

$$G(x_{10}^2, zs) = G^{(0)}(x_{10}^2, zs) + \frac{\alpha_s N_c}{2\pi} \int_{\frac{1}{sx_{10}^2}}^z \frac{dz'}{z'} \int_{\frac{1}{z's}}^{x_{10}^2} \frac{dx_{21}^2}{x_{21}^2} \left[\Gamma(x_{10}^2, x_{21}^2, z's) + 3G(x_{21}^2, z's) \right. \\ \left. + 2G_2(x_{21}^2, z's) + 2\Gamma_2(x_{10}^2, x_{21}^2, z's) \right], \quad (4.53a)$$

$$\Gamma(x_{10}^2, x_{21}^2, z's) = G^{(0)}(x_{10}^2, z's) + \frac{\alpha_s N_c}{2\pi} \int_{\frac{1}{sx_{10}^2}}^{z'} \frac{dz''}{z''} \int_{\frac{1}{z''s}}^{\min[x_{10}^2, x_{21}^2 \frac{z'}{z''}]} \frac{dx_{32}^2}{x_{32}^2} \left[\Gamma(x_{10}^2, x_{32}^2, z''s) + 3G(x_{32}^2, z''s) \right. \\ \left. + 2G_2(x_{32}^2, z''s) + 2\Gamma_2(x_{10}^2, x_{32}^2, z''s) \right], \quad (4.53b)$$

$$G_2(x_{10}^2, zs) = G_2^{(0)}(x_{10}^2, zs) + \frac{\alpha_s N_c}{\pi} \int_{\frac{\Lambda^2}{s}}^z \frac{dz'}{z'} \int_{\max[x_{10}^2, \frac{1}{z's}]}^{\min[\frac{z}{z'} x_{10}^2, \frac{1}{\Lambda^2}]} \frac{dx_{21}^2}{x_{21}^2} [G(x_{21}^2, z's) + 2G_2(x_{21}^2, z's)], \quad (4.53c)$$

$$\Gamma_2(x_{10}^2, x_{21}^2, z's) = G_2^{(0)}(x_{10}^2, z's) + \frac{\alpha_s N_c}{\pi} \int_{\frac{\Lambda^2}{s}}^{\frac{z' x_{21}^2}{x_{10}^2}} \frac{dz''}{z''} \int_{\max[x_{10}^2, \frac{1}{z''s}]}^{\min[\frac{z'}{z''} x_{21}^2, \frac{1}{\Lambda^2}]} \frac{dx_{32}^2}{x_{32}^2} [G(x_{32}^2, z''s) + 2G_2(x_{32}^2, z''s)]. \quad (4.53d)$$

Note that $\Gamma(x_{10}^2, x_{21}^2, z's)$ and $\Gamma_2(x_{10}^2, x_{21}^2, z's)$ are only defined for $x_{10} \geq x_{21}$. Let us also stress here that Λ is taken here to be the IR cutoff, such that eqs. (4.53), as written, are only valid for $x_{10} < 1/\Lambda$.

The equations (4.53) have to be solved with the appropriate initial conditions (inhomogeneous terms). At Born level, these are [2, 33]

$$G^{(0)}(x_{10}^2, zs) = \frac{\alpha_s^2 C_F}{2N_c} \pi \left[C_F \ln \frac{zs}{\Lambda^2} - 2 \ln(zs x_{10}^2) \right], \quad G_2^{(0)}(x_{10}^2, zs) = \frac{\alpha_s^2 C_F}{N_c} \pi \ln \frac{1}{x_{10} \Lambda}. \quad (4.54)$$

(The sign difference in $G_2^{(0)}$ compared to that in [33] is due to the sign difference of the A^i term in the definition of G^i employed here and in that work.)

The solution of eqs. (4.53) would give us the gluon and quark helicity TMD and PDF along with the g_1 structure function at small x by using eqs. (3.25), (3.26), (3.50), (3.52), and (3.61) (or eq. (3.62)). In using the latter formulas we have to assume that, at large N_c , $Q(x_{10}^2, zs) \approx G(x_{10}^2, zs)$ (see section VI of [37] for a brief discussion of the subtleties associated with taking the large- N_c limit of small- x helicity evolution).

4.3 Evolution equations in the large- N_c & N_f limit

In this section, we consider another limit under which equations (4.15), (4.19), (4.26), and (4.27) form a closed set of equations, following the standard approach described in [3]. Since N_f and N_c are taken to be comparable in this limit, we include both gluon and quark loop contributions. We also notice the distinction between the fundamental and adjoint dipole amplitudes. The fundamental dipole amplitudes we consider in this section are

$$Q_{10}(zs) = \frac{1}{2N_c} \text{Re} \left\langle \left\langle \text{T tr} [V_0 V_1^{\text{pol}[1] \dagger}] + \text{T tr} [V_1^{\text{pol}[1]} V_0^\dagger] \right\rangle \right\rangle (zs), \quad (4.55a)$$

$$G_{10}^i(zs) = \frac{1}{2N_c} \text{Re} \left\langle \left\langle \text{T tr} [V_0 V_1^{iG[2] \dagger}] + \text{T tr} [V_1^{iG[2]} V_0^\dagger] \right\rangle \right\rangle (zs). \quad (4.55b)$$

Since the polarized Wilson line of the second kind, $V_x^{iG[2]}$, contains no sub-eikonal quark operator, the evolution equation for $G_{10}^i(zs)$ in the large- N_c & N_f limit will be the same as in the large- N_c limit given above in eq. (4.48). Furthermore, the relation (4.36) still holds in the large- N_c & N_f limit, allowing us to consider only the fundamental dipole amplitude, $G_{10}^i(zs)$. As for the dipole amplitudes of the first kind, the large- N_c & N_f analogue of $G_{10}(zs)$ from eq. (4.29) is defined as [40]

$$\tilde{G}_{10}(zs) = \frac{1}{2N_c} \text{Re} \left\langle \left\langle \text{T tr} [V_0 W_1^{\text{pol}[1] \dagger}] + \text{T tr} [W_1^{\text{pol}[1]} V_0^\dagger] \right\rangle \right\rangle (zs), \quad (4.56)$$

where

$$W_{\underline{x}}^{\text{pol}[1]} = V_{\underline{x}}^{\text{G}[1]} + \frac{g^2 p_1^+}{4s} \int_{-\infty}^{\infty} dx_1^- \int_{x_1^-}^{\infty} dx_2^- V_{\underline{x}}[\infty, x_2^-] \psi_{\alpha}(x_2^-, \underline{x}) \left(\frac{1}{2} \gamma^+ \gamma_5 \right)_{\beta\alpha} \bar{\psi}_{\beta}(x_1^-, \underline{x}) V_{\underline{x}}[x_1^-, -\infty]. \quad (4.57)$$

In the large- N_c & N_f limit the amplitude (4.56) is related to that in eq. (4.16) by $G_{10}^{\text{adj}}(zs) = 4 S_{10}(zs) \tilde{G}_{10}(zs)$. Note that there is no simple relation between $\tilde{G}_{10}(zs)$ and $Q_{10}(zs)$ even at the large N_c & N_f [3]. The main argument in favor of the definitions (4.56) and (4.57) is that the following relation holds at large N_c & N_f (cf. eqs. (74) and (83) in [3] along with eq. (4.31) above),

$$\left(U_{\underline{x}}^{\text{pol}[1]} \right)^{ba} = 4 \text{tr} \left[W_{\underline{x}}^{\text{pol}[1] \dagger} t^b V_{\underline{x}} t^a \right] + 4 \text{tr} \left[V_{\underline{x}}^{\dagger} t^b W_{\underline{x}}^{\text{pol}[1]} t^a \right], \quad (4.58)$$

which will simplify our derivations below. For each amplitude of $Q_{10}(zs)$, $\tilde{G}_{10}(zs)$ and $G_{10}^i(zs)$, we will derive below its DLA evolution equation in the large- N_c & N_f limit, together with the evolution equation for its neighbor dipole amplitude.

The evolution of the fundamental dipole amplitude, $Q_{10}(zs)$, follows from the evolution equation (4.15). At large- N_c & N_f , by employing Fierz identity several times along with eq. (4.36), the expectation values of the operators in eq. (4.15) can be written as

$$\frac{1}{N_c^2} \left\langle \left\langle \text{tr} \left[t^b V_{\underline{0}} t^a V_{\underline{1}}^{\dagger} \right] \left(U_{\underline{2}}^{\text{pol}[1]} \right)^{ba} + \text{c.c.} \right\rangle \right\rangle (zs) = 2 \left[S_{21}(zs) \tilde{\Gamma}_{20,21}(zs) + S_{20}(zs) \tilde{G}_{21}(zs) \right], \quad (4.59a)$$

$$\frac{1}{N_c^2} \left\langle \left\langle \text{tr} \left[t^b V_{\underline{0}} t^a V_{\underline{1}}^{\dagger} \right] \left(U_{\underline{2}}^{i\text{G}[2]} \right)^{ba} + \text{c.c.} \right\rangle \right\rangle (zs) = S_{21}(zs) \Gamma_{20,21}^i(zs) + S_{20}(zs) G_{21}^i(zs), \quad (4.59b)$$

$$\frac{1}{N_c^2} \left\langle \left\langle \text{tr} \left[t^b V_{\underline{0}} t^a V_{\underline{2}}^{\text{pol}[1] \dagger} \right] U_{\underline{1}}^{ba} + \text{c.c.} \right\rangle \right\rangle (zs) = S_{10}(zs) Q_{21}(zs), \quad (4.59c)$$

$$\frac{1}{N_c^2} \left\langle \left\langle \text{tr} \left[t^b V_{\underline{0}} t^a V_{\underline{2}}^{i\text{G}[2] \dagger} \right] U_{\underline{1}}^{ba} + \text{c.c.} \right\rangle \right\rangle (zs) = S_{10}(zs) G_{21}^i(zs). \quad (4.59d)$$

Here, $\tilde{\Gamma}_{20,21}$ is the neighbour counterpart of \tilde{G}_{10} defined in eq. (4.56), while $\Gamma_{20,21}^i$ is, again, the neighbour amplitude for G_{10}^i from eq. (4.55b). Below we will also employ $\bar{\Gamma}_{20,21}$, the neighbour counterpart of the amplitude Q_{10} .

Employing eqs. (4.59) along with (at large N_c & N_f)

$$\frac{1}{N_c^2} \left\langle \left\langle \text{tr} \left[t^b V_{\underline{0}} t^a V_{\underline{1}}^{\text{pol}[1] \dagger} \right] U_{\underline{2}}^{ba} + \text{c.c.} \right\rangle \right\rangle (zs) = S_{20}(zs) Q_{12}(zs), \quad (4.60)$$

we rewrite eq. (4.15) as

$$\begin{aligned}
 Q_{10}(zs) &= Q_{10}^{(0)}(zs) \\
 &+ \frac{\alpha_s N_c}{2\pi^2} \int_{\frac{\Lambda^2}{s}}^z \frac{dz'}{z'} \int d^2x_2 \left\{ 2 \left[\frac{1}{x_{21}^2} - \frac{x_{21}}{x_{21}^2} \cdot \frac{x_{20}}{x_{20}^2} \right] \left(S_{21}(z's) \tilde{\Gamma}_{20,21}^{\text{gen}}(z's) + S_{20}(z's) \tilde{G}_{21}(z's) \right) \right. \\
 &+ \left. \left[2 \frac{\epsilon^{ij} x_{21}^j}{x_{21}^4} - \frac{\epsilon^{ij} (x_{20}^j + x_{21}^j)}{x_{20}^2 x_{21}^2} - \frac{2x_{20} \times x_{21}}{x_{20}^2 x_{21}^2} \left(\frac{x_{21}^i}{x_{21}^2} - \frac{x_{20}^i}{x_{20}^2} \right) \right] \left(S_{21}(z's) \Gamma_{20,21}^{i \text{ gen}}(z's) + S_{20}(z's) G_{21}^i(z's) \right) \right\} \\
 &+ \frac{\alpha_s N_c}{4\pi^2} \int_{\frac{\Lambda^2}{s}}^z \frac{dz'}{z'} \int \frac{d^2x_2}{x_{21}^2} S_{10}(z's) \left\{ Q_{21}(z's) + \frac{2\epsilon^{ij} x_{21}^j}{x_{21}^2} G_{21}^i(z's) \right\} \\
 &+ \frac{\alpha_s N_c}{2\pi^2} \int_{\frac{\Lambda^2}{s}}^z \frac{dz'}{z'} \int d^2x_2 \frac{x_{10}^2}{x_{21}^2 x_{20}^2} \left\{ S_{20}(z's) Q_{12}(z's) - \bar{\Gamma}_{10,21}^{\text{gen}}(z's) \right\}.
 \end{aligned} \tag{4.61}$$

In eq. (4.61), similar to what we did in eq. (4.38), we replaced neighbor dipole amplitudes by their generalized polarized dipole amplitude counterparts. For the purposes of this section, the generalized dipole amplitudes in eq. (4.61) are defined as [33]

$$\bar{\Gamma}_{10,32}^{\text{gen}}(zs) \equiv Q_{10}(zs) \theta(x_{32} - x_{10}) + \bar{\Gamma}_{10,32}(zs) \theta(x_{10} - x_{32}), \tag{4.62a}$$

$$\tilde{\Gamma}_{10,32}^{\text{gen}}(zs) \equiv \tilde{G}_{10}(zs) \theta(x_{32} - x_{10}) + \tilde{\Gamma}_{10,32}(zs) \theta(x_{10} - x_{32}), \tag{4.62b}$$

$$\Gamma_{10,32}^{i \text{ gen}}(zs) \equiv G_{10}^i(zs) \theta(x_{32} - x_{10}) + \Gamma_{10,32}^i(zs) \theta(x_{10} - x_{32}). \tag{4.62c}$$

Similar to eqs. (4.39), neither x_{10} nor x_{32} is necessarily the size of the parent or daughter dipole. Rather, they can be any general transverse separations. As one can infer from their definitions in eqs. (4.62), the generalized dipole amplitudes only reduce to the neighbor dipole amplitudes when $x_{32} \ll x_{10}$, as it is the only regime where the lifetime ordering needs to be expressed using a different transverse separation from the current dipole size. Otherwise, the generalized dipole amplitudes reduce to their “regular” counterparts.

To further simplify the evolution equation (4.61) in preparation for rewriting it in the DLA form, we neglect the single-logarithmic unpolarized evolution [41–53, 88, 89] and put all the unpolarized dipole S -matrices to 1. Subsequently, we integrate eq. (4.61) over the impact parameter, $\underline{b} = \frac{\underline{x}_1 + \underline{x}_0}{2}$. Upon such integration, $G_{10}^i(zs)$ and $\Gamma_{20,21}^i(zs)$ decompose in a similar fashion to eqs. (3.24) and (4.40), that is,

$$\int d^2 \left(\frac{x_1 + x_0}{2} \right) G_{10}^i(zs) = (x_{10})_{\perp}^i G_1(x_{10}^2, zs) + \epsilon^{ij} (x_{10})_{\perp}^j G_2(x_{10}^2, zs), \tag{4.63a}$$

$$\int d^2 \left(\frac{x_1 + x_0}{2} \right) \Gamma_{20,21}^i(zs) = (x_{20})_{\perp}^i \Gamma_1(x_{20}^2, x_{21}^2, zs) + \epsilon^{ij} (x_{20})_{\perp}^j \Gamma_2(x_{20}^2, x_{21}^2, zs). \tag{4.63b}$$

Performing all the mentioned steps in eq. (4.61), we obtain (cf. eq. (4.42))

$$\begin{aligned}
 Q(x_{10}^2, zs) &= Q^{(0)}(x_{10}^2, zs) \\
 &+ \frac{\alpha_s N_c}{2\pi^2} \int_{\frac{\Lambda^2}{s}}^z \frac{dz'}{z'} \int d^2 x_2 \left\{ 2 \left[\frac{1}{x_{21}^2} - \frac{\underline{x}_{21} \cdot \underline{x}_{20}}{x_{21}^2 x_{20}^2} \right] \left[\tilde{\Gamma}^{\text{gen}}(x_{20}^2, x_{21}^2, z's) + \tilde{G}(x_{21}^2, z's) \right] \right. \\
 &+ \left[\frac{2 \underline{x}_{20} \cdot \underline{x}_{21}}{x_{21}^4} - \frac{1}{x_{21}^2} - \frac{\underline{x}_{20} \cdot \underline{x}_{21}}{x_{20}^2 x_{21}^2} + \frac{2(\underline{x}_{20} \times \underline{x}_{21})^2}{x_{20}^2 x_{21}^4} \right] \Gamma_2^{\text{gen}}(x_{20}^2, x_{21}^2, z's) \\
 &+ \left. \left[\frac{2}{x_{21}^2} - \frac{\underline{x}_{20} \cdot \underline{x}_{21}}{x_{20}^2 x_{21}^2} - \frac{1}{x_{20}^2} + \frac{2(\underline{x}_{20} \times \underline{x}_{21})^2}{x_{20}^4 x_{21}^2} \right] G_2(x_{21}^2, z's) \right\} \\
 &+ \frac{\alpha_s N_c}{4\pi^2} \int_{\frac{\Lambda^2}{s}}^z \frac{dz'}{z'} \int \frac{d^2 x_2}{x_{21}^2} \left[Q(x_{21}^2, z's) + 2G_2(x_{21}^2, z's) \right] \\
 &+ \frac{\alpha_s N_c}{2\pi^2} \int_{\frac{\Lambda^2}{s}}^z \frac{dz'}{z'} \int d^2 x_2 \frac{x_{10}^2}{x_{21}^2 x_{20}^2} \left[Q(x_{21}^2, z's) - \bar{\Gamma}^{\text{gen}}(x_{10}^2, x_{21}^2, z's) \right],
 \end{aligned} \tag{4.64}$$

where we defined the impact-parameter integrated dipole amplitudes in a similar fashion to (3.51) and (4.41). In particular,

$$\bar{\Gamma}(x_{20}^2, x_{21}^2, zs) \equiv \int d^2 \left(\frac{x_0 + x_2}{2} \right) \bar{\Gamma}_{20,21}(zs), \tag{4.65a}$$

$$\tilde{G}(x_{10}^2, zs) \equiv \int d^2 \left(\frac{x_0 + x_1}{2} \right) \tilde{G}_{10}(zs), \tag{4.65b}$$

$$\tilde{\Gamma}(x_{20}^2, x_{21}^2, zs) \equiv \int d^2 \left(\frac{x_0 + x_2}{2} \right) \tilde{\Gamma}_{20,21}(zs). \tag{4.65c}$$

Note that, similar to eq. (4.42), all the terms in eq. (4.64) involving G_1 or Γ_1 vanish upon integration over \underline{x}_2 because each of them contains a single Levi-Civita symbol, ϵ^{ij} , along with a single transverse vector \underline{x}_{10} : it is impossible to construct a non-zero scalar quantity out of such ingredients.

Eq. (4.64) has no DLA term in the $x_{20} \ll x_{10}$ regime. However, there is at least one DLA term in both $x_{10} \ll x_{21} \approx x_{20}$ and $x_{21} \ll x_{10}$ regimes. Combining all the DLA terms together and taking lifetime ordering into account to specify the integration limits, we obtain the following DLA evolution equation for $Q(x_{10}^2, zs)$ in the large- N_c & N_f limit,

$$\begin{aligned}
 Q(x_{10}^2, zs) &= Q^{(0)}(x_{10}^2, zs) + \frac{\alpha_s N_c}{2\pi} \int_{\max\{\Lambda^2, 1/x_{10}^2\}/s}^z \frac{dz'}{z'} \int_{1/z's}^{x_{10}^2} \frac{dx_{21}^2}{x_{21}^2} \left[2\tilde{\Gamma}(x_{10}^2, x_{21}^2, z's) + 2\tilde{G}(x_{21}^2, z's) \right. \\
 &+ \left. Q(x_{21}^2, z's) - \bar{\Gamma}(x_{10}^2, x_{21}^2, z's) + 2\Gamma_2(x_{10}^2, x_{21}^2, z's) + 2G_2(x_{21}^2, z's) \right] \\
 &+ \frac{\alpha_s N_c}{4\pi} \int_{\Lambda^2/s}^z \frac{dz'}{z'} \int_{1/z's}^{x_{10}^2 z'/z'} \frac{dx_{21}^2}{x_{21}^2} \left[Q(x_{21}^2, z's) + 2G_2(x_{21}^2, z's) \right],
 \end{aligned} \tag{4.66}$$

where we changed the lower limit of the z' -integral in the first term of eq. (4.66) in order to ensure that $z's$ remains larger than Λ^2 for any value of x_{10}^2 . A feature of eq. (4.66),

which is similar to previous treatments of the evolution equations at large- N_c & N_f [1, 3], is that the squared dipole size, x_{10}^2 , can exceed the scale $\frac{1}{\Lambda^2}$ [37]. In contrast to the large- N_c evolution (4.53), we no longer consider Λ as the infrared cutoff in this regime. Rather, $1/\Lambda$ is understood as the typical transverse size of the target [37, 115], which may or may not be larger than the size x_{10} of the projectile dipole.

Similar to what we did in the large- N_c limit, we deduce the evolution equation for $\bar{\Gamma}(x_{10}^2, x_{21}^2, z's)$ by analogy to eq. (4.66), obtaining

$$\begin{aligned} \bar{\Gamma}(x_{10}^2, x_{21}^2, z's) &= Q^{(0)}(x_{10}^2, z's) + \frac{\alpha_s N_c}{2\pi} \int_{\max\{\Lambda^2, 1/x_{10}^2\}/s}^{z'} \frac{dz''}{z''} \int_{1/z''s}^{\min\{x_{10}^2, x_{21}^2 z'/z''\}} \frac{dx_{32}^2}{x_{32}^2} \left[2\tilde{\Gamma}(x_{10}^2, x_{32}^2, z''s) \right. \\ &\quad \left. + 2\tilde{G}(x_{32}^2, z''s) + Q(x_{32}^2, z''s) - \bar{\Gamma}(x_{10}^2, x_{32}^2, z''s) + 2\Gamma_2(x_{10}^2, x_{32}^2, z''s) + 2G_2(x_{32}^2, z''s) \right] \\ &\quad + \frac{\alpha_s N_c}{4\pi} \int_{\Lambda^2/s}^{z'} \frac{dz''}{z''} \int_{1/z''s}^{x_{21}^2 z'/z''} \frac{dx_{32}^2}{x_{32}^2} \left[Q(x_{32}^2, z''s) + 2G_2(x_{32}^2, z''s) \right]. \end{aligned} \quad (4.67)$$

Now, we move on to consider the other polarized dipole amplitude of the first kind, $\tilde{G}_{10}(zs)$. The general evolution equation we need for the large- N_c & N_f evolution of $\tilde{G}_{10}(zs)$ has been derived in eq. (4.19) for the related $G_{10}^{\text{adj}}(zs)$. We simplify the equation in the large- N_c & N_f limit: we first apply the Fierz identity several times, together with eq. (4.58), to obtain the following relations (where we, again, suppress the time-ordering sign for brevity):

$$\frac{1}{N_c^2 - 1} \left\langle \left\langle \text{Tr} \left[U_{\underline{0}} U_{\underline{1}}^{\text{pol}[1]\dagger} \right] + \text{c.c.} \right\rangle \right\rangle (zs) = 8S_{10}(zs) \tilde{G}_{10}(zs), \quad (4.68a)$$

$$\frac{1}{N_c^2 - 1} \left\langle \left\langle \text{Tr} \left[T^b U_{\underline{0}} T^a U_{\underline{1}}^\dagger \right] \left(U_{\underline{2}}^{\text{pol}[1]} \right)^{ba} + \text{c.c.} \right\rangle \right\rangle (zs) = 4N_c S_{10}(zs) \left[S_{20}(zs) \tilde{G}_{21}(zs) + S_{21}(zs) \tilde{\Gamma}_{20,21}(zs) \right], \quad (4.68b)$$

$$\frac{1}{N_c^2 - 1} \left\langle \left\langle \text{Tr} \left[T^b U_{\underline{0}} T^a U_{\underline{1}}^{\text{pol}[1]\dagger} \right] U_{\underline{2}}^{ba} + \text{c.c.} \right\rangle \right\rangle (zs) = 4N_c S_{20}(zs) \left[S_{10}(zs) \tilde{G}_{12}(zs) + S_{21}(zs) \tilde{\Gamma}_{10,21}(zs) \right]. \quad (4.68c)$$

Applying eqs. (4.37), (4.59) and (4.68) to eq. (4.19), we obtain

$$\begin{aligned} 4S_{10}(zs) \tilde{G}_{10}(zs) &= 4S_{10}^{(0)}(zs) \tilde{G}_{10}^{(0)}(zs) \\ &\quad + \frac{\alpha_s N_c}{\pi^2} \int_{\frac{\Lambda^2}{s}}^z \frac{dz'}{z'} \int d^2x_2 \left\{ 4 \left[\frac{1}{x_{21}^2} - \frac{x_{21}}{x_{21}^2} \cdot \frac{x_{20}}{x_{20}^2} \right] S_{10}(z's) \left[S_{20}(z's) \tilde{G}_{21}(z's) + S_{21}(z's) \tilde{\Gamma}_{20,21}^{\text{gen}}(z's) \right] \right. \\ &\quad \left. + 2 \left[2 \frac{\epsilon^{ij} x_{21}^j}{x_{21}^4} - \frac{\epsilon^{ij} (x_{20}^j + x_{21}^j)}{x_{20}^2 x_{21}^2} - \frac{2x_{20} \times x_{21}}{x_{20}^2 x_{21}^2} \left(\frac{x_{21}^i}{x_{21}^2} - \frac{x_{20}^i}{x_{20}^2} \right) \right] S_{10}(z's) \left[S_{20}(z's) G_{21}^i(z's) + S_{21}(z's) \Gamma_{20,21}^{\text{igen}}(z's) \right] \right\} \\ &\quad - \frac{\alpha_s N_f}{2\pi^2} \int_{\frac{\Lambda^2}{s}}^z \frac{dz'}{z'} \int d^2x_2 S_{10}(z's) \left\{ \frac{1}{x_{21}^2} \tilde{\Gamma}_{20,21}^{\text{gen}}(z's) + \frac{2\epsilon^{ij} x_{21}^j}{x_{21}^4} \Gamma_{20,21}^{\text{igen}}(z's) \right\} \\ &\quad + \frac{2\alpha_s N_c}{\pi^2} \int_{\frac{\Lambda^2}{s}}^z \frac{dz'}{z'} \int d^2x_2 \frac{x_{10}^2}{x_{21}^2 x_{20}^2} \left\{ S_{20}(z's) \left[S_{10}(z's) \tilde{G}_{12}(z's) + S_{21}(z's) \tilde{\Gamma}_{10,21}^{\text{gen}}(z's) \right] - 2S_{10}(z's) \tilde{\Gamma}_{10,21}^{\text{gen}}(z's) \right\}. \end{aligned} \quad (4.69)$$

Once again, employing the trick from appendix D of [40], we simplify eq. (4.69) to

$$\begin{aligned} \tilde{G}_{10}(zs) &= \tilde{G}_{10}^{(0)}(zs) \\ &\quad + \frac{\alpha_s N_c}{2\pi^2} \int_{\frac{\Lambda^2}{s}}^z \frac{dz'}{z'} \int d^2x_2 \left\{ 2 \left[\frac{1}{x_{21}^2} - \frac{x_{21}}{x_{21}^2} \cdot \frac{x_{20}}{x_{20}^2} \right] \left[S_{20}(z's) \tilde{G}_{21}(z's) + S_{21}(z's) \tilde{\Gamma}_{20,21}^{\text{gen}}(z's) \right] \right. \end{aligned} \quad (4.70)$$

$$\begin{aligned}
 & + \left[2 \frac{\epsilon^{ij} x_{21}^j}{x_{21}^4} - \frac{\epsilon^{ij} (x_{20}^j + x_{21}^j)}{x_{20}^2 x_{21}^2} - \frac{2 \underline{x}_{20} \times \underline{x}_{21}}{x_{20}^2 x_{21}^2} \left(\frac{x_{21}^i}{x_{21}^2} - \frac{x_{20}^i}{x_{20}^2} \right) \right] \left[S_{20}(z's) G_{21}^i(z's) + S_{21}(z's) \Gamma_{20,21}^{i \text{ gen}}(z's) \right] \Big\} \\
 & - \frac{\alpha_s N_f}{8\pi^2} \int_{\frac{\Lambda^2}{s}}^z \frac{dz'}{z'} \int d^2 x_2 \left\{ \frac{1}{x_{21}^2} \bar{\Gamma}_{20,21}^{\text{gen}}(z's) + \frac{2\epsilon^{ij} x_{21}^j}{x_{21}^4} \Gamma_{20,21}^{\text{gen}}(z's) \right\} \\
 & + \frac{\alpha_s N_c}{2\pi^2} \int_{\frac{\Lambda^2}{s}}^z \frac{dz'}{z'} \int d^2 x_2 \frac{x_{10}^2}{x_{21}^2 x_{20}^2} \left\{ S_{20}(z's) \tilde{G}_{12}(z's) - \tilde{\Gamma}_{10,21}^{\text{gen}}(z's) \right\}.
 \end{aligned}$$

This is the DLA+SLA_L large- N_c & N_f evolution equation for $\tilde{G}_{10}(zs)$.

To extract the DLA limit, we put the unpolarized dipole S -matrices in eq. (4.70) to 1. Then, we integrate the resulting equation over the impact parameters, employing the definitions from eqs. (3.51), (4.41), (4.63) and (4.65). As a result, eq. (4.70) becomes

$$\begin{aligned}
 \tilde{G}(x_{10}^2, zs) & = \tilde{G}^{(0)}(x_{10}^2, zs) \tag{4.71} \\
 & + \frac{\alpha_s N_c}{2\pi^2} \int_{\frac{\Lambda^2}{s}}^z \frac{dz'}{z'} \int d^2 x_2 \left\{ 2 \left[\frac{1}{x_{21}^2} - \frac{\underline{x}_{21} \cdot \underline{x}_{20}}{x_{21}^2} \cdot \frac{\underline{x}_{20}}{x_{20}^2} \right] \left[\tilde{G}(x_{21}^2, z's) + \tilde{\Gamma}^{\text{gen}}(x_{20}^2, x_{21}^2, z's) \right] \right. \\
 & + \left[\frac{2}{x_{21}^2} - \frac{\underline{x}_{21} \cdot \underline{x}_{20}}{x_{20}^2 x_{21}^2} - \frac{1}{x_{20}^2} + \frac{2(\underline{x}_{20} \times \underline{x}_{21})^2}{x_{20}^4 x_{21}^2} \right] G_2(x_{21}^2, z's) \\
 & + \left. \left[2 \frac{\underline{x}_{21} \cdot \underline{x}_{20}}{x_{21}^4} - \frac{1}{x_{21}^2} - \frac{\underline{x}_{21} \cdot \underline{x}_{20}}{x_{20}^2 x_{21}^2} + \frac{2(\underline{x}_{20} \times \underline{x}_{21})^2}{x_{20}^2 x_{21}^4} \right] \Gamma_2^{\text{gen}}(x_{20}^2, x_{21}^2, z's) \right\} \\
 & - \frac{\alpha_s N_f}{8\pi^2} \int_{\frac{\Lambda^2}{s}}^z \frac{dz'}{z'} \int d^2 x_2 \left\{ \frac{1}{x_{21}^2} \bar{\Gamma}^{\text{gen}}(x_{20}^2, x_{21}^2, z's) + 2 \frac{\underline{x}_{21} \cdot \underline{x}_{20}}{x_{21}^4} \Gamma_2^{\text{gen}}(x_{20}^2, x_{21}^2, z's) \right\} \\
 & + \frac{\alpha_s N_c}{2\pi^2} \int_{\frac{\Lambda^2}{s}}^z \frac{dz'}{z'} \int d^2 x_2 \frac{x_{10}^2}{x_{21}^2 x_{20}^2} \left\{ \tilde{G}(x_{21}^2, z's) - \tilde{\Gamma}^{\text{gen}}(x_{10}^2, x_{21}^2, z's) \right\}.
 \end{aligned}$$

For the same reason as in eq. (4.64), all the terms involving G_1 and Γ_1 vanish.

In the $x_{20} \ll x_{10}$ regime, eq. (4.71) contains no DLA terms and is exclusively SLA_L. However, the equation contains DLA terms in both $x_{10} \ll x_{21} \approx x_{20}$ and $x_{21} \ll x_{10}$ regimes. Combining all the DLA terms with lifetime ordering taken into account to obtain the integration limits, we have

$$\begin{aligned}
 \tilde{G}(x_{10}^2, zs) & = \tilde{G}^{(0)}(x_{10}^2, zs) + \frac{\alpha_s N_c}{2\pi} \int_{\max\{\Lambda^2, 1/x_{10}^2\}/s}^z \frac{dz'}{z'} \int_{1/z's}^{x_{10}^2} \frac{dx_{21}^2}{x_{21}^2} \tag{4.72} \\
 & \quad \times \left[3 \tilde{G}(x_{21}^2, z's) + \tilde{\Gamma}(x_{10}^2, x_{21}^2, z's) + 2 G_2(x_{21}^2, z's) + 2 \Gamma_2(x_{10}^2, x_{21}^2, z's) \right] \\
 & \quad - \frac{\alpha_s N_f}{8\pi} \int_{\Lambda^2/s}^z \frac{dz'}{z'} \int_{1/z's}^{x_{10}^2 z'/z'} \frac{dx_{21}^2}{x_{21}^2} \left[\bar{\Gamma}^{\text{gen}}(x_{20}^2, x_{21}^2, z's) + 2 \Gamma_2^{\text{gen}}(x_{20}^2, x_{21}^2, z's) \right].
 \end{aligned}$$

Notice that the lower limit of the longitudinal integral in the first term of eq. (4.72) is modified in a similar fashion to the first term of eq. (4.66).

By analogy, the DLA evolution equation for the adjoint neighbor dipole amplitude of the first kind is

$$\begin{aligned} \tilde{\Gamma}(x_{10}^2, x_{21}^2, z' s) = & \tilde{G}^{(0)}(x_{10}^2, z' s) + \frac{\alpha_s N_c}{2\pi} \int_{\max\{\Lambda^2, 1/x_{10}^2\}/s}^{z'} \frac{dz''}{z''} \int_{1/z'' s}^{\min\{x_{10}^2, x_{21}^2 z'/z''\}} \frac{dx_{32}^2}{x_{32}^2} \\ & \times \left[3\tilde{G}(x_{32}^2, z'' s) + \tilde{\Gamma}(x_{10}^2, x_{32}^2, z'' s) + 2G_2(x_{32}^2, z'' s) + 2\Gamma_2(x_{10}^2, x_{32}^2, z'' s) \right] \\ & - \frac{\alpha_s N_f}{8\pi} \int_{\Lambda^2/s}^{z'} \frac{dz''}{z''} \int_{1/z'' s}^{x_{21}^2 z'/z''} \frac{dx_{32}^2}{x_{32}^2} \left[\Gamma^{\text{gen}}(x_{30}^2, x_{32}^2, z'' s) + 2\Gamma_2^{\text{gen}}(x_{30}^2, x_{32}^2, z'' s) \right]. \end{aligned} \quad (4.73)$$

Finally, we consider the adjoint dipole amplitude of the second kind. Since, as we mentioned above, the polarized Wilson line of this kind does not contain a sub-eikonal quark operator, the DLA evolution equation for $G_2(x_{10}^2, z s)$ and $\Gamma_2(x_{10}^2, x_{21}^2, z' s)$ can be taken directly from eqs. (4.51) and (4.52), respectively, by replacing G with \tilde{G} in them due to the difference in the definitions (4.56) and (4.29). This gives

$$G_2(x_{10}^2, z s) = G_2^{(0)}(x_{10}^2, z s) + \frac{\alpha_s N_c}{\pi} \int_{\frac{\Lambda^2}{s}}^z \frac{dz'}{z'} \int_{\max[x_{10}^2, \frac{1}{z'} s]}^{\frac{z'}{z'} x_{10}^2} \frac{dx_{21}^2}{x_{21}^2} \left[\tilde{G}(x_{21}^2, z' s) + 2G_2(x_{21}^2, z' s) \right], \quad (4.74a)$$

$$\Gamma_2(x_{10}^2, x_{21}^2, z' s) = G_2^{(0)}(x_{10}^2, z' s) + \frac{\alpha_s N_c}{\pi} \int_{\frac{\Lambda^2}{s}}^{\frac{z'}{x_{10}^2} x_{21}^2} \frac{dz''}{z''} \int_{\max[x_{10}^2, \frac{1}{z''} s]}^{\frac{z''}{z''} x_{21}^2} \frac{dx_{32}^2}{x_{32}^2} \left[\tilde{G}(x_{32}^2, z'' s) + 2G_2(x_{32}^2, z'' s) \right]. \quad (4.74b)$$

A caveat in arriving at eq. (4.74) is that all the terms involving polarized Wilson lines of the first kind in eqs. (4.26) and (4.27) got absorbed into the adjoint dipole amplitudes \tilde{G} , that is, the amplitude Q does not appear. Diagrammatically, this is due to the fact that there is no sub-eikonal emission of a polarized soft quark in any of the diagrams in figure 5. Another difference between the large- N_c counterparts, eqs. (4.26) and (4.27), and eq. (4.74) is in the upper limit of the transverse integrals, where the constraints imposed by the infrared cutoff, Λ^2 , in eqs. (4.26) and (4.27) were removed because Λ^2 no longer acts as the infrared cutoff in the large- N_c & N_f limit.

Equations (4.66), (4.67), (4.72), (4.73) and (4.74) form a closed system of DLA evolution equations involving six polarized (neighbor) dipole amplitudes in the large- N_c & N_f limit. To summarize, we rewrite all the equations below, utilizing eqs. (4.62) to separate all integrals into the UV and IR regions.

$$\begin{aligned} Q(x_{10}^2, z s) = & Q^{(0)}(x_{10}^2, z s) + \frac{\alpha_s N_c}{2\pi} \int_{\max\{\Lambda^2, 1/x_{10}^2\}/s}^z \frac{dz'}{z'} \int_{1/z' s}^{x_{10}^2} \frac{dx_{21}^2}{x_{21}^2} \left[2\tilde{G}(x_{21}^2, z' s) + 2\tilde{\Gamma}(x_{10}^2, x_{21}^2, z' s) \right. \\ & \left. + Q(x_{21}^2, z' s) - \bar{\Gamma}(x_{10}^2, x_{21}^2, z' s) + 2\Gamma_2(x_{10}^2, x_{21}^2, z' s) + 2G_2(x_{21}^2, z' s) \right] \\ & + \frac{\alpha_s N_c}{4\pi} \int_{\Lambda^2/s}^z \frac{dz'}{z'} \int_{1/z' s}^{x_{10}^2 z'/z'} \frac{dx_{21}^2}{x_{21}^2} \left[Q(x_{21}^2, z' s) + 2G_2(x_{21}^2, z' s) \right], \end{aligned} \quad (4.75a)$$

$$\begin{aligned} \bar{\Gamma}(x_{10}^2, x_{21}^2, z' s) = & Q^{(0)}(x_{10}^2, z' s) + \frac{\alpha_s N_c}{2\pi} \int_{\max\{\Lambda^2, 1/x_{10}^2\}/s}^{z'} \frac{dz''}{z''} \int_{1/z'' s}^{\min\{x_{10}^2, x_{21}^2 z'/z''\}} \frac{dx_{32}^2}{x_{32}^2} \left[2\tilde{G}(x_{32}^2, z'' s) \right. \\ & \left. + 2\tilde{\Gamma}(x_{10}^2, x_{32}^2, z'' s) + Q(x_{32}^2, z'' s) - \bar{\Gamma}(x_{10}^2, x_{32}^2, z'' s) + 2\Gamma_2(x_{10}^2, x_{32}^2, z'' s) + 2G_2(x_{32}^2, z'' s) \right] \\ & + \frac{\alpha_s N_c}{4\pi} \int_{\Lambda^2/s}^{z'} \frac{dz''}{z''} \int_{1/z'' s}^{x_{21}^2 z'/z''} \frac{dx_{32}^2}{x_{32}^2} \left[Q(x_{32}^2, z'' s) + 2G_2(x_{32}^2, z'' s) \right], \end{aligned} \quad (4.75b)$$

$$\begin{aligned}
 \tilde{G}(x_{10}^2, zs) = & \tilde{G}^{(0)}(x_{10}^2, zs) + \frac{\alpha_s N_c}{2\pi} \int_{\max\{\Lambda^2, 1/x_{10}^2\}/s}^z \frac{dz'}{z'} \int_{1/z's}^{x_{10}^2} \frac{dx_{21}^2}{x_{21}^2} \left[3\tilde{G}(x_{21}^2, z's) + \tilde{\Gamma}(x_{10}^2, x_{21}^2, z's) \right] \\
 & + 2G_2(x_{21}^2, z's) + \left(2 - \frac{N_f}{2N_c} \right) \Gamma_2(x_{10}^2, x_{21}^2, z's) - \frac{N_f}{4N_c} \bar{\Gamma}(x_{10}^2, x_{21}^2, z's) \\
 & - \frac{\alpha_s N_f}{8\pi} \int_{\Lambda^2/s}^z \frac{dz'}{z'} \int_{\max\{x_{10}^2, 1/z's\}}^{x_{10}^2 z'/z'} \frac{dx_{21}^2}{x_{21}^2} \left[Q(x_{21}^2, z's) + 2G_2(x_{21}^2, z's) \right],
 \end{aligned} \tag{4.75c}$$

$$\begin{aligned}
 \tilde{\Gamma}(x_{10}^2, x_{21}^2, z's) = & \tilde{G}^{(0)}(x_{10}^2, z's) + \frac{\alpha_s N_c}{2\pi} \int_{\max\{\Lambda^2, 1/x_{10}^2\}/s}^{z'} \frac{dz''}{z''} \int_{1/z''s}^{\min\{x_{10}^2, x_{21}^2 z'/z''\}} \frac{dx_{32}^2}{x_{32}^2} \left[3\tilde{G}(x_{32}^2, z''s) \right] \\
 & + \tilde{\Gamma}(x_{10}^2, x_{32}^2, z''s) + 2G_2(x_{32}^2, z''s) + \left(2 - \frac{N_f}{2N_c} \right) \Gamma_2(x_{10}^2, x_{32}^2, z''s) - \frac{N_f}{4N_c} \bar{\Gamma}(x_{10}^2, x_{32}^2, z''s) \\
 & - \frac{\alpha_s N_f}{8\pi} \int_{\Lambda^2/s}^{z' x_{21}^2/x_{10}^2} \frac{dz''}{z''} \int_{\max\{x_{10}^2, 1/z''s\}}^{x_{21}^2 z'/z''} \frac{dx_{32}^2}{x_{32}^2} \left[Q(x_{32}^2, z''s) + 2G_2(x_{32}^2, z''s) \right],
 \end{aligned} \tag{4.75d}$$

$$G_2(x_{10}^2, zs) = G_2^{(0)}(x_{10}^2, zs) + \frac{\alpha_s N_c}{\pi} \int_{\frac{\Lambda^2}{s}}^z \frac{dz'}{z'} \int_{\max[x_{10}^2, \frac{1}{z's}]}^{\frac{z'}{z'} x_{10}^2} \frac{dx_{21}^2}{x_{21}^2} \left[\tilde{G}(x_{21}^2, z's) + 2G_2(x_{21}^2, z's) \right], \tag{4.75e}$$

$$\Gamma_2(x_{10}^2, x_{21}^2, z's) = G_2^{(0)}(x_{10}^2, z's) + \frac{\alpha_s N_c}{\pi} \int_{\frac{\Lambda^2}{s}}^{z' \frac{x_{21}^2}{x_{10}^2}} \frac{dz''}{z''} \int_{\max[x_{10}^2, \frac{1}{z''s}]}^{z' x_{21}^2} \frac{dx_{32}^2}{x_{32}^2} \left[\tilde{G}(x_{32}^2, z''s) + 2G_2(x_{32}^2, z''s) \right]. \tag{4.75f}$$

Similar to eq. (4.54) for the large- N_c limit, the inhomogeneous terms of eqs. (4.75) are given by the following expressions at Born level [2, 33]:

$$\tilde{G}^{(0)}(x_{10}^2, zs) = Q^{(0)}(x_{10}^2, zs) = \frac{\alpha_s^2 C_F}{2N_c} \pi \left[C_F \ln \frac{zs}{\Lambda^2} - 2 \ln(zs x_{10}^2) \right], \quad G_2^{(0)}(x_{10}^2, zs) = \frac{\alpha_s^2 C_F}{N_c} \pi \ln \frac{1}{x_{10} \Lambda}. \tag{4.76}$$

These initial conditions assume that the projectile is much smaller than the target, $x_{10} \ll 1/\Lambda$. To be used in eqs. (4.75), the expressions (4.76) may need to be generalized to also describe the large-projectile case, $x_{10} \gg 1/\Lambda$.

4.4 Cross-check against the spin-dependent DGLAP evolution

Let us cross-check our results against the spin-dependent DGLAP evolution equation [73–75]. We are interested in the gluon sector only, since this is where the previous works' [1, 2] agreement with DGLAP evolution was not completely clear. To this end we put the flavor-singlet quark helicity PDF to zero, $\Delta\Sigma(x, Q^2) = 0$, (for instance, by putting $N_f = 0$) and write the DGLAP equation for the gluon helicity PDF only

$$\frac{\partial \Delta G(x, Q^2)}{\partial \ln Q^2} = \int \frac{dz}{z} \Delta P_{GG}(z) \Delta G\left(\frac{x}{z}, Q^2\right). \tag{4.77}$$

We would like to stress that discarding $\Delta\Sigma$ is not a physical approximation. Rather, it is a mathematical step to verify that our evolution agrees with that driven by the splitting function $\Delta P_{GG}(z)$. The latter is known up to three loops [90, 91] (see also [116]). At small z and large N_c it reduces to

$$\Delta P_{GG}(z) = \frac{\alpha_s}{2\pi} 4N_c + \left(\frac{\alpha_s}{2\pi} \right)^2 4N_c^2 \ln^2 z + \left(\frac{\alpha_s}{2\pi} \right)^3 \frac{7}{3} N_c^3 \ln^4 z + \dots \tag{4.78}$$

Since our goal is to check that our evolution in the gluon sector agrees with DGLAP, we will consider the large- N_c evolution in eqs. (4.53). We choose the initial conditions to be

$$G^{(0)}(x_{10}^2, zs) = 0, \quad G_2^{(0)}(x_{10}^2, z's) = 1. \quad (4.79)$$

Employing eq. (3.26), we see that this choice of the initial conditions corresponds to the initial PDF $\Delta G^{(0)}(x, Q^2) = \text{const}$, where the value of the constant is not important for us.

Inserting eq. (4.79) into the right-hand sides of eqs. (4.53a) and (4.53c) yields the result of one iteration of our evolution

$$G^{(1)}(x_{10}^2, zs) = \frac{\alpha_s N_c}{\pi} \ln^2(zsx_{10}^2), \quad (4.80a)$$

$$G_2^{(1)}(x_{10}^2, zs) = 2 \frac{\alpha_s N_c}{\pi} \ln(zsx_{10}^2) \ln\left(\frac{1}{x_{10}^2 \Lambda^2}\right). \quad (4.80b)$$

In arriving at eqs. (4.80) it is convenient to rewrite the kernel of eq. (4.53c) as

$$\int_{\frac{\Lambda^2}{s}}^z \frac{dz'}{z'} \int_{\max[x_{10}^2, \frac{1}{z's}]}^{\min[\frac{z}{z'}x_{10}^2, \frac{1}{\Lambda^2}]} \frac{dx_{21}^2}{x_{21}^2} = \int_{x_{10}^2}^{\frac{1}{\Lambda^2}} \frac{dx_{21}^2}{x_{21}^2} \int_{\frac{1}{sx_{21}^2}}^{\frac{x_{10}^2}{x_{21}^2}} \frac{dz'}{z'}. \quad (4.81)$$

Identifying

$$\frac{1}{x_{10}^2} \rightarrow Q^2, \quad zsx_{10}^2 \rightarrow \frac{zs}{Q^2} \rightarrow \frac{1}{x} \quad (4.82)$$

we see that eq. (4.80b), via eq. (3.26), gives

$$\Delta G^{(1)}(x, Q^2) = 2 \frac{\alpha_s N_c}{\pi} \ln\left(\frac{1}{x}\right) \ln\left(\frac{Q^2}{\Lambda^2}\right) \text{const}. \quad (4.83)$$

This is in complete agreement with one iteration of leading-order (LO) spin-dependent DGLAP equation: indeed, using $\Delta G^{(0)}(x, Q^2) = \text{const}$ on the right of eq. (4.77) with the order- α_s part of the splitting function (4.78) gives us eq. (4.83). We see that we are in complete agreement with the one-loop DGLAP equation.

To check the result at two loops, we substitute eqs. (4.80) into the right-hand side of eq. (4.53c). Employing eq. (4.81) to simplify the integration we get

$$G_2^{(2)}(x_{10}^2, zs) = \left(\frac{\alpha_s N_c}{\pi}\right)^2 \left[\frac{1}{3} \ln^3(zsx_{10}^2) \ln\left(\frac{1}{x_{10}^2 \Lambda^2}\right) + \ln^2(zsx_{10}^2) \ln^2\left(\frac{1}{x_{10}^2 \Lambda^2}\right) \right], \quad (4.84)$$

which, with the help of eq. (4.82), corresponds to

$$\Delta G^{(2)}(x, Q^2) = \left(\frac{\alpha_s N_c}{\pi}\right)^2 \left[\frac{1}{3} \ln^3\left(\frac{1}{x}\right) \ln\left(\frac{Q^2}{\Lambda^2}\right) + \ln^2\left(\frac{1}{x}\right) \ln^2\left(\frac{Q^2}{\Lambda^2}\right) \right] \text{const}. \quad (4.85)$$

Inserting $\Delta G^{(0)}(x, Q^2) = \text{const}$ into the right side of eq. (4.77) and employing the order- α_s^2 part of the splitting function (4.78) we arrive at the first term on the right of eq. (4.85): hence, we agree with the next-to-leading order (NLO) spin-dependent DGLAP evolution

(at large- N_c and small- x) as well. The last term on the right of eq. (4.85) results from two iterations of the LO DGLAP, as can be verified explicitly as well.

Let us push the comparison one step further. To compare our evolution with the next-to-next-to-leading order (NNLO) DGLAP equation, we need to find $G_2^{(3)}$. To construct it, we first employ eqs. (4.79) in eqs. (4.53b) and (4.53d) to obtain

$$\Gamma^{(1)}(x_{10}^2, x_{21}^2, z's) = 2 \frac{\alpha_s N_c}{\pi} \left[\frac{1}{2} \ln^2(z's x_{21}^2) + \ln(z's x_{21}^2) \ln \frac{x_{10}^2}{x_{21}^2} \right], \quad (4.86a)$$

$$\Gamma_2^{(1)}(x_{10}^2, x_{21}^2, z's) = 2 \frac{\alpha_s N_c}{\pi} \ln(z's x_{21}^2) \ln \frac{1}{x_{10}^2 \Lambda^2}. \quad (4.86b)$$

The calculation is simplified if one notices that the kernel of eq. (4.53d) can be rewritten as

$$\int_{\frac{\Lambda^2}{s}}^{z' \frac{x_{21}^2}{x_{10}^2}} \frac{dz''}{z''} \int_{\max[x_{10}^2, \frac{1}{z''s}]}^{\min[\frac{z'}{z''} x_{21}^2, \frac{1}{\Lambda^2}]} \frac{dx_{32}^2}{x_{32}^2} = \int_{x_{10}^2}^{\frac{1}{\Lambda^2}} \frac{dx_{32}^2}{x_{32}^2} \int_{\frac{1}{s x_{32}^2}}^{z' \frac{x_{21}^2}{x_{32}^2}} \frac{dz''}{z''}. \quad (4.87)$$

Employing eqs. (4.86) and (4.80) in eq. (4.53a) we arrive at

$$G^{(2)}(x_{10}^2, z s) = \left(\frac{\alpha_s N_c}{\pi} \right)^2 \left[\frac{7}{24} \ln^4(z s x_{10}^2) + \frac{2}{3} \ln^3(z s x_{10}^2) \ln \left(\frac{1}{x_{10}^2 \Lambda^2} \right) \right]. \quad (4.88)$$

Finally, inserting eqs. (4.84) and (4.88) into the right-hand side of eq. (4.53c) yields

$$G_2^{(3)}(x_{10}^2, z s) = \left(\frac{\alpha_s N_c}{\pi} \right)^3 \left[\frac{7}{120} \ln^5(z s x_{10}^2) \ln \left(\frac{1}{x_{10}^2 \Lambda^2} \right) + \frac{1}{6} \ln^4(z s x_{10}^2) \ln^2 \left(\frac{1}{x_{10}^2 \Lambda^2} \right) + \frac{2}{9} \ln^3(z s x_{10}^2) \ln^3 \left(\frac{1}{x_{10}^2 \Lambda^2} \right) \right], \quad (4.89)$$

which, using eq. (4.82), translates into

$$\Delta G^{(3)}(x, Q^2) = \left(\frac{\alpha_s N_c}{\pi} \right)^3 \left[\frac{7}{120} \ln^5 \left(\frac{1}{x} \right) \ln \left(\frac{Q^2}{\Lambda^2} \right) + \frac{1}{6} \ln^4 \left(\frac{1}{x} \right) \ln^2 \left(\frac{Q^2}{\Lambda^2} \right) + \frac{2}{9} \ln^3 \left(\frac{1}{x} \right) \ln^3 \left(\frac{Q^2}{\Lambda^2} \right) \right] \text{const.} \quad (4.90)$$

The first term on the right of eq. (4.90) exactly corresponds to the contribution of the order- α_s^3 part of the splitting function (4.78) to eq. (4.77): our evolution (4.53) thus agrees with the NNLO DGLAP gluon-gluon splitting function (at large- N_c and small- x). One can also readily verify that the last term on the right of eq. (4.90) corresponds to three iterations of the LO DGLAP kernel, LO^3 , while the second term on the right of eq. (4.90) is a sum of applying LO and NLO DGLAP in different orders, that is, $\text{LO} \times \text{NLO} + \text{NLO} \times \text{LO}$.

Therefore, the agreement between our evolution and the small- x limit of spin-dependent DGLAP equation in the gluon sector has been verified to three loops, the same order as the IREE of [5, 28, 29]. Further iterations in the solution of our eqs. (4.53) can be used to generate new higher-order corrections to the small- x anomalous dimension (4.78), which have not been derived yet (but can also be extracted using the technique of [5, 28, 29]). In addition, let us note here that the amplitude $G_2(x_{10}^2, z s)$

obtained here in eqs. (4.83), (4.85), and (4.90) appears to only contain the solution of the spin-dependent DGLAP equation (4.77) at small x : if an exact analytic solution of eqs. (4.53) is constructed in the future work, it would contain the *exact* expression for the small- x large- N_c spin-dependent gluon-gluon splitting function, generalizing eq. (4.78) to all orders in the coupling.

5 Helicity evolution at small x : the background field method

In the previous section we derived the helicity evolution equations at small x in the LCOT approach. The key element of the calculation was the observation that in the helicity evolution quarks and gluons couple to the background shock-wave fields through the polarized Wilson lines (2.6) and (2.11). This is a non-trivial statement which requires further explanation. The most powerful framework which allows to unambiguously determine the form of the operators which define the coupling of “quantum” quarks and gluons to the background field is the background field method [76, 77]. In this approach the separation of “quantum” and background fields is done at the level of the QCD Lagrangian which allows to obtain the most general form of the propagator in the external background.

In this section we will show how the polarized Wilson lines (2.6) and (2.11) appear in this approach and present an alternative derivation of the helicity evolution equations (4.15) and (4.26). We will thus show that the helicity evolution equations obtained in the background field method are in full agreement with the above results obtained in the LCOT approach.

5.1 The background field method

To introduce the background field method, let us start with a matrix element of an arbitrary operator $\mathcal{O}(A, \psi, \bar{\psi})$ (corresponding to some observable) which is constructed out of quark and gluon fields. The matrix element can be represented as a functional integral over those fields,⁷

$$\langle P_1 | \mathcal{O} | P_2 \rangle = \int \mathcal{D}A \int \mathcal{D}\psi \Psi_{P_1}^*(\vec{A}(t_f), \psi(t_f)) \mathcal{O}(A, \psi) \Psi_{P_2}(\vec{A}(t_i), \psi(t_i)) e^{iS_{QCD}(A, \psi)}, \quad (5.1)$$

where Ψ_{P_2} is the initial state wave function at the initial time $t_i \rightarrow -\infty$ and, similarly, Ψ_{P_1} is the final state wave function at the final time $t_f \rightarrow \infty$.

The main idea of the background field method is that the fields in (5.1) can be separated into the “quantum” and background parts,

$$A_\mu \rightarrow A_\mu^q + A_\mu^{\text{bg}}, \quad \psi \rightarrow \psi^q + \psi^{\text{bg}}. \quad (5.2)$$

The way we separate the fields is completely arbitrary, see for example [117–121]. However, in the context of small- x physics the most efficient approach is to separate the fields based on their longitudinal momentum fraction (or, equivalently, rapidity). This is the rapidity factorization approach [44, 45]. In this approach the “quantum” fields are defined to have

⁷For brevity we do not explicitly show the dependence on (and integrals over) the anti-quark fields $\bar{\psi}$.

momenta $p^- > \sigma$, and background fields are characterized by $p^- < \sigma$, where σ is some rapidity factorization scale.⁸ Note that in the small- x limit, due to Lorentz contraction, the background fields have a shock-wave form with a limited support in the x^- direction (for the plus-direction moving proton).

Assuming that the wave functions depend only on the background fields, we rewrite the matrix element as

$$\langle P_1 | \mathcal{O} | P_2 \rangle = \int \mathcal{D}A^{\text{bg}} \int \mathcal{D}\psi^{\text{bg}} \Psi_{P_1}^*(\vec{A}^{\text{bg}}(t_f), \psi^{\text{bg}}(t_f)) \tilde{\mathcal{O}}(A^{\text{bg}}, \psi^{\text{bg}}, \sigma) \Psi_{P_2}(\vec{A}^{\text{bg}}(t_i), \psi^{\text{bg}}(t_i)) e^{iS_{QCD}(A^{\text{bg}}, \psi^{\text{bg}})}, \quad (5.3)$$

where

$$\tilde{\mathcal{O}}(A^{\text{bg}}, \psi^{\text{bg}}, \sigma) = \int \mathcal{D}A^{\text{q}} \int \mathcal{D}\psi^{\text{q}} \mathcal{O}(A^{\text{q}} + A^{\text{bg}}, \psi^{\text{q}} + \psi^{\text{bg}}) e^{iS_{bQCD}(A^{\text{q}}, \psi^{\text{q}}; A^{\text{bg}}, \psi^{\text{bg}})} \quad (5.4)$$

and the QCD action in the background fields is

$$S_{bQCD}(A^{\text{q}}, \psi^{\text{q}}; A^{\text{bg}}, \psi^{\text{bg}}) = S_{QCD}(A^{\text{q}} + A^{\text{bg}}, \psi^{\text{q}} + \psi^{\text{bg}}) - S_{QCD}(A^{\text{bg}}, \psi^{\text{bg}}). \quad (5.5)$$

Now we can fix the background fields and evaluate the functional integral over the “quantum” fields perturbatively to a certain order in the number of loops. This perturbative calculation in the background field is the essence of the background field method. In general, the result of calculating the functional integrals has a form of a product of the coefficient functions (“impact” factors) and the Wilson-line operators constructed from background fields which describe interaction of “quantum” fields with the background,

$$\tilde{\mathcal{O}}(A^{\text{bg}}, \psi^{\text{bg}}, \sigma) = \sum_i C_i(\sigma) \otimes \mathcal{V}_i(A^{\text{bg}}, \psi^{\text{bg}}, \sigma). \quad (5.6)$$

The sum goes over the different operators. Equation (5.6) should be substituted back into eq. (5.3). In particular, as we will see in our calculation below, the helicity-dependent interaction of quarks and gluons with the shock-wave background is described by polarized Wilson lines (2.6) and (2.11).

To study the dependence of the Wilson-line operators on the rapidity factorization scale σ one can repeat the procedure described above. We introduce a new scale σ' and redefine the background fields as

$$A_\mu^{\text{bg}} \rightarrow \hat{A}_\mu^{\text{q}} + \hat{A}_\mu^{\text{bg}}, \quad \psi^{\text{bg}} \rightarrow \hat{\psi}^{\text{q}} + \hat{\psi}^{\text{bg}}, \quad (5.7)$$

where the “quantum” fields now have momenta $\sigma > p^- > \sigma'$ and the background fields have $p^- < \sigma'$. After this we can perform the integration over new “quantum” fields \hat{A}_μ^{q} , $\hat{\psi}^{\text{q}}$ (keeping \hat{A}_μ^{bg} and $\hat{\psi}^{\text{bg}}$ fixed) in eq. (5.3) which corresponds to the functional integral

$$\text{T} [\mathcal{V}_i(A^{\text{bg}}, \psi^{\text{bg}}, \sigma)] \equiv \int \mathcal{D}\hat{A}^{\text{q}} \int \mathcal{D}\hat{\psi}^{\text{q}} \mathcal{V}_i(\hat{A}^{\text{q}} + \hat{A}^{\text{bg}}, \hat{\psi}^{\text{q}} + \hat{\psi}^{\text{bg}}, \sigma) e^{iS_{bQCD}(\hat{A}^{\text{q}}, \hat{\psi}^{\text{q}}; \hat{A}^{\text{bg}}, \hat{\psi}^{\text{bg}})}. \quad (5.8)$$

⁸In the rapidity factorization approach the “quantum” fields are usually called “slow” fields, and the background fields are called “fast” fields [66].

This integral can be evaluated by a perturbative calculation in the background field which yields an evolution equation of the following form

$$T[\mathcal{V}_i(A^{\text{bg}}, \psi^{\text{bg}}, \sigma)] = \int_{\sigma'}^{\sigma} \frac{dp^-}{p^-} \sum_j \mathcal{K}_{ij} \otimes \mathcal{V}_j(\hat{A}^{\text{bg}}, \hat{\psi}^{\text{bg}}, \sigma'), \quad (5.9)$$

with some kernels \mathcal{K}_{ij} . In particular, in this paper we derive the evolution equation for the polarized Wilson lines (2.6) and (2.11).

For perturbative calculations of the functional integral (5.8) we need to know the propagators of “quantum” particles in the background field. Note that the form of such propagators unambiguously fixes the set of the Wilson-line operators on the right-hand side of the evolution equation (5.9). In the next section we will derive the quark and gluon propagators in the shock-wave background and later use them to construct helicity evolution equations for operators (2.6) and (2.11).

5.2 Quark and gluon propagators in the shock-wave background

In this section we will construct quark and gluon propagators in the external background field by direct resummation of the corresponding Feynman diagrams. While to solve this problem in full generality is a formidable task, see [39, 62–67, 122–124], it is still possible to separate a contribution which dominates at small x . To find this contribution we construct an expansion of the propagators in inverse powers of p^- and find the first few terms in this expansion. Indeed, at small x , the p^- component of the “quantum” field is assumed to be large. As a result, the leading terms of the expansion in inverse powers of p^- dominate at small x yielding a large logarithm $\int \frac{dp^-}{p^-}$. In general, the expansion in the inverse powers of p^- corresponds to the expansion in the powers of x or in eikonality we employed above.

The technique we use is similar to the one developed in refs. [66, 67] for the unpolarized evolution. However, for the helicity evolution we need to extend the approach and assume the most general form of the background field. In particular, we take into account the transverse component A_i of the field, which was neglected in [66, 67]. In our calculation we fix the gauge of the background field as $A_+ = A_- = 0$ and assume that the fields are independent of x^+ , $A_\mu = A_\mu(x^-, \underline{x})$.

5.2.1 Scalar propagator in the shock-wave background

Before we consider quark and gluon propagators in the background field, let us start with a simpler problem and calculate the scalar propagator in the background field. In the Schwinger’s notation, see appendix A, we write the scalar propagator in the background field A_μ as⁹

$$(x|\frac{1}{\hat{P}^2 + i\epsilon}|y) = (x|\frac{1}{\hat{p}^2 + g\{\hat{p}^\mu, A_\mu(\hat{x})\} + g^2 A^\mu(\hat{x})A_\mu(\hat{x}) + i\epsilon}|y), \quad (5.10)$$

where $\hat{P}_\mu = \hat{p}_\mu + gA_\mu(\hat{x})$. Note that in the Schwinger’s notation \hat{p} and $A(\hat{x})$ are operators so one should take into account their ordering. In particular, one can immediately recognize

⁹From here on we do not explicitly show the “q” and “bg” labels for “quantum” and background fields.

in $\{\hat{p}^\mu, A_\mu(\hat{x})\}$ and $A^\mu(\hat{x})A_\mu(\hat{x})$ the two vertices of scalar QED, where the latter is the “seagull” vertex. Of course eq. (5.10) can be obtained by resummation of an infinite number of interactions of the background field A_μ with the propagating scalar particle.

Indeed, expanding the propagator we write¹⁰

$$\begin{aligned} (x|\frac{1}{P^2+i\epsilon}|y) &= (x|\frac{1}{p^2+i\epsilon}|y) - (x|\frac{1}{p^2+i\epsilon}(g\{p^\mu, A_\mu\} + g^2 A^\mu A_\mu)\frac{1}{p^2+i\epsilon}|y) \\ &\quad + (x|\frac{1}{p^2+i\epsilon}(g\{p^\mu, A_\mu\} + g^2 A^\mu A_\mu)\frac{1}{p^2+i\epsilon}(\{p^\mu, A_\mu\} + A^\mu A_\mu)\frac{1}{p^2+i\epsilon}|y) + \dots \end{aligned} \quad (5.11)$$

Let us start with the first term of this expansion which is a free propagator of the scalar particle. Using eq. (A.5) and performing the integration over p^+ we find

$$\begin{aligned} (x|\frac{1}{p^2+i\epsilon}|y) &= \left(-\frac{i}{2\pi}\theta(x^- - y^-) \int_0^\infty \frac{dp^-}{2p^-} + \frac{i}{2\pi}\theta(y^- - x^-) \int_{-\infty}^0 \frac{dp^-}{2p^-} \right) e^{-ip^-(x-y)^+} \\ &\quad \times (\underline{x}|e^{-i\frac{p_1^2}{2p^-}x^-} e^{i\frac{p_1^2}{2p^-}y^-}|\underline{y}). \end{aligned} \quad (5.12)$$

Substituting this result for each free propagator¹¹ in eq. (5.11) one finds the following form of the scalar propagator in the background field

$$\begin{aligned} (x|\frac{1}{P^2+i\epsilon}|y) &= \left(-\frac{i}{2\pi}\theta(x^- - y^-) \int_0^\infty \frac{dp^-}{2p^-} + \frac{i}{2\pi}\theta(y^- - x^-) \int_{-\infty}^0 \frac{dp^-}{2p^-} \right) e^{-ip^-(x-y)^+} \\ &\quad \times (\underline{x}|e^{-i\frac{p_1^2}{2p^-}x^-} \mathcal{S}(x^-, y^-) e^{i\frac{p_1^2}{2p^-}y^-}|\underline{y}), \end{aligned} \quad (5.13)$$

where the operator \mathcal{S} is constructed out of the background fields and describes the interaction of the “quantum” scalar field with the background gluons. In general, this operator has a form of an expansion in inverse powers of p^- ,

$$\mathcal{S}(x^-, y^-) = \mathcal{S}_0(x^-, y^-) + \frac{1}{p^-}\mathcal{S}_1(x^-, y^-) + \frac{1}{(p^-)^2}\mathcal{S}_2(x^-, y^-) + \dots \quad (5.14)$$

As we discussed above, the dominant contribution at small x corresponds to the first few orders of expansion (5.14). Fortunately, it is possible to obtain the exact form of those terms by considering the first few orders of the expansion in the coupling constant (5.11).

¹⁰For brevity we are going to omit the hat sign over momentum and coordinate operators.

¹¹One should also use eq. (A.2) to introduce the integration over intermediate coordinates.

To show this let us go back to eq. (5.11). Using eq. (5.12) for the second term of the expansion and taking into account that $A_+ = 0$ we obtain

$$\begin{aligned}
 (x|\frac{1}{P^2+i\epsilon}|y) &= \left(-\frac{i}{2\pi}\theta(x^- - y^-) \int_0^\infty \frac{dp^-}{2p^-} + \frac{i}{2\pi}\theta(y^- - x^-) \int_{-\infty}^0 \frac{dp^-}{2p^-} \right) e^{-ip^-(x-y)^+} \\
 &\times (x|e^{-i\frac{p_\perp^2}{2p^-}x^-} \left\{ 1 + ig \int_{y^-}^{x^-} dz^- e^{i\frac{p_\perp^2}{2p^-}z^-} \left(A_-(z^-) + \frac{p^k}{2p^-} A_k(z^-) + A_k(z^-) \frac{p^k}{2p^-} \right. \right. \\
 &\left. \left. + \frac{g}{2p^-} A^k(z^-) A_k(z^-) \right) e^{-i\frac{p_\perp^2}{2p^-}z^-} + \dots \right\} e^{i\frac{p_\perp^2}{2p^-}y^-} |y),
 \end{aligned} \tag{5.15}$$

where the ellipsis stand for the higher-order terms of the expansion (5.11).

Now let us use the following identity for an arbitrary operator O :

$$e^{i\frac{p_\perp^2}{2p^-}z^-} O e^{-i\frac{p_\perp^2}{2p^-}z^-} = O + i\frac{z^-}{2p^-} [p_\perp^2, O] - \frac{1}{2} \left(\frac{z^-}{2p^-} \right)^2 [p_\perp^2, [p_\perp^2, O]] + \dots, \tag{5.16}$$

which, taking into account that

$$[p_\perp^2, O] = -i\{p^s, \partial_s O\}, \tag{5.17}$$

can be rewritten as

$$e^{i\frac{p_\perp^2}{2p^-}z^-} O e^{-i\frac{p_\perp^2}{2p^-}z^-} = O + \frac{z^-}{2p^-} \{p^s, \partial_s O\} + \frac{1}{2} \left(\frac{z^-}{2p^-} \right)^2 \{p^s, \{p^m, \partial_s \partial_m O\}\} + \dots \tag{5.18}$$

Note that p^s is an operator acting on everything to its right, while the partial derivatives in $\partial_s O$ and $\partial_s \partial_m O$ act only on O .

Employing this result in eq. (5.15) we obtain

$$\begin{aligned}
 (x|\frac{1}{P^2+i\epsilon}|y)^{ab} &= \left(-\frac{i}{2\pi}\theta(x^- - y^-) \int_0^\infty \frac{dp^-}{2p^-} + \frac{i}{2\pi}\theta(y^- - x^-) \int_{-\infty}^0 \frac{dp^-}{2p^-} \right) e^{-ip^-(x-y)^+} \\
 &\times (x|e^{-i\frac{p_\perp^2}{2p^-}x^-} \left\{ 1 + ig \int_{y^-}^{x^-} dz^- A_-(z^-) + \frac{ig}{2p^-} \int_{y^-}^{x^-} dz^- \left(\{p^k, A_k(z^-)\} + gA^k(z^-) A_k(z^-) \right) \right. \\
 &\left. + \frac{ig}{2p^-} \int_{y^-}^{x^-} dz^- z^- \{p^s, \partial_s A_-(z^-)\} + \dots \right\} e^{i\frac{p_\perp^2}{2p^-}y^-} |y),
 \end{aligned} \tag{5.19}$$

where we explicitly keep only the first two terms of (5.18).

A similar calculation can be done for the other terms in the expansion (5.11). Eventually, each insertion of $\{p^\mu, A_\mu\} + A^\mu A_\mu$ generates a structure similar to (5.19). As a result we see that each coupling to the background field brings an extra inverse power of p^- . The only exception is the eikonal coupling $\{p^\mu, A_\mu\} \rightarrow p^- A^+$ which does not change

the counting in inverse powers of p^- . However, these terms can be resummed into Wilson-line factors, which in the operator form are given by eq. (A.6) in appendix A. After this resummation the scalar propagator takes the form

$$\begin{aligned}
 (x|\frac{1}{P^2+i\epsilon}|y) &= \left(-\frac{i}{2\pi}\theta(x^- - y^-) \int_0^\infty \frac{dp^-}{2p^-} + \frac{i}{2\pi}\theta(y^- - x^-) \int_{-\infty}^0 \frac{dp^-}{2p^-} \right) e^{-ip^-(x-y)^+} \\
 &\times (\underline{x}|e^{-i\frac{p_1^2}{2p^-}x^-} \left\{ V[x^-, y^-] + \frac{ig}{2p^-} \int_{y^-}^{x^-} dz^- V[x^-, z^-] (\{p^k, A_k(z^-)\} + gA^k(z^-)A_k(z^-)) V[z^-, y^-] \right. \\
 &\left. + \frac{ig}{2p^-} \int_{y^-}^{x^-} dz^- z^- V[x^-, z^-] \{p^s, \partial_s A_-(z^-)\} V[z^-, y^-] + O\left(\frac{1}{(p^-)^2}\right) \right\} e^{i\frac{p_1^2}{2p^-}y^-} |\underline{y}).
 \end{aligned} \tag{5.20}$$

Here $V[x^-, y^-]$ are the light-cone Wilson-line operators akin to those in eq. (A.6), but defined with finite integration limits.

Now let us rewrite this result in a gauge-covariant form. Introducing $\frac{d}{dz^-}(z^-) = 1$ in the second term in the curly brackets of eq. (5.20) and integrating by parts we can recombine the resulting terms to get the following form of the propagator,

$$\begin{aligned}
 (x|\frac{1}{P^2+i\epsilon}|y) &= \left(-\frac{i}{2\pi}\theta(x^- - y^-) \int_0^\infty \frac{dp^-}{2p^-} + \frac{i}{2\pi}\theta(y^- - x^-) \int_{-\infty}^0 \frac{dp^-}{2p^-} \right) e^{-ip^-(x-y)^+} (\underline{x}|e^{-i\frac{p_1^2}{2p^-}x^-} \\
 &\times \left\{ V[x^-, y^-] + \frac{igx^-}{2p^-} (\{p^k, A_k\} + gA^k A_k)(x^-) V[x^-, y^-] - \frac{igy^-}{2p^-} V[x^-, y^-] (\{p^k, A_k\} + gA^k A_k)(y^-) \right. \\
 &\left. - \frac{ig}{2p^-} \int_{y^-}^{x^-} dz^- z^- V[x^-, z^-] \{P^k, F_{-k}\} V[z^-, y^-] + O\left(\frac{1}{(p^-)^2}\right) \right\} e^{i\frac{p_1^2}{2p^-}y^-} |\underline{y}),
 \end{aligned} \tag{5.21}$$

where the second and third terms in the curly brackets are the boundary terms which we obtained in the integration by parts.

Note that up to this point our calculation has been completely general. Now let us consider the scalar propagator in the shock-wave approximation with the shock wave localized near $x^- = 0$. Since there are no fields outside the shock-wave we can neglect the boundary terms and simplify the gauge factors $V[x^-, y^-] \rightarrow V$ for $x^- > 0 > y^-$ (with V the infinite light-cone Wilson line operator (A.6)), which yields

$$\begin{aligned}
 (x|\frac{1}{P^2+i\epsilon}|y) &= -\frac{i}{2\pi} \int_0^\infty \frac{dp^-}{2p^-} e^{-ip^-(x-y)^+} \\
 &\times (\underline{x}|e^{-i\frac{p_1^2}{2p^-}x^-} \left\{ V - \frac{ig}{2p^-} \int_{-\infty}^\infty dz^- z^- V[\infty, z^-] \{P^k, F_{-k}\} V[z^-, -\infty] + O\left(\frac{1}{(p^-)^2}\right) \right\} e^{i\frac{p_1^2}{2p^-}y^-} |\underline{y}),
 \end{aligned} \tag{5.22}$$

which agrees with ref. [66]. Here we assume that $x^- > 0 > y^-$.

We find that at the leading order of the $1/p^-$ expansion the interaction of the scalar particle with the background field is defined by the eikonal Wilson line V , while at the

next order the interaction is described by the sub-eikonal operator

$$\int_{-\infty}^{\infty} dz^- z^- V[\infty, z^-] \{P^k, F_{-k}\} V[z^-, -\infty]. \quad (5.23)$$

In the subsequent sections we will relate this operator to the polarized Wilson lines (2.7c) and (3.17).

Note that this type of sub-eikonal operators is neglected in the unpolarized evolution. Indeed the z^- factor under the integral in eq. (5.23) leads to the suppression of the operator in the shock-wave approximation by a factor of $1/P^+$, which, when combined with the $1/p^-$ prefactor of this operator in eq. (5.22) gives a suppression by a factor of $1/s \sim x$. Therefore, the unpolarized evolution is driven by the eikonal gauge factors (light-cone Wilson lines). However, as we will see, the interactions via eikonal factors do not contribute to helicity evolution, which starts with sub-eikonal operators like the one in eq. (5.23).

5.2.2 Gluon propagator in the shock-wave background

In this section we are going to derive the gluon propagator in the background field in the axial gauge. Using the approach developed in the previous section we will consider the expansion of the propagator in inverse powers of p^- and reconstruct the first several terms of this expansion by analyzing the first few orders of the perturbative expansion in the background field,

$$\begin{aligned} \text{T}[C_\mu^a(x)C_\nu^b(y)] &= (x| \frac{-id_{\mu\nu}(p)\delta^{ab}}{p^2+i\epsilon} |y) \\ &- ig(x| \frac{-id_{\mu\rho}(p)}{p^2+i\epsilon} \left[g^{\rho\sigma} \{p_\alpha, \mathcal{A}^\alpha\} + 2i(\partial^\rho \mathcal{A}^\sigma - \partial^\sigma \mathcal{A}^\rho) - p^\rho \mathcal{A}^\sigma - \mathcal{A}^\rho p^\sigma \right] \frac{-id_{\sigma\nu}(p)}{p^2+i\epsilon} |y)^{ab} \\ &- g^2(x| \frac{-id_{\mu\rho}(p)}{p^2} \bar{\psi} \gamma^\rho t^a \frac{i\cancel{p}}{p^2+i\epsilon} \gamma^\sigma t^b \psi \frac{-id_{\sigma\nu}(p)}{p^2} |y) - g^2(y| \frac{-id_{\nu\sigma}(p)}{p^2+i\epsilon} \bar{\psi} \gamma^\sigma t^b \frac{i\cancel{p}}{p^2+i\epsilon} \gamma^\rho t^a \psi \frac{-id_{\rho\mu}(p)}{p^2+i\epsilon} |x) + \dots, \end{aligned} \quad (5.24)$$

where $\psi, \bar{\psi}$ are background quark and anti-quark fields and the expression in the square brackets is the QCD three-gluon vertex in the background field. For the free gluon propagator in the axial gauge we have

$$d_{\mu\nu}(p) \equiv g_{\mu\nu} - \frac{n_\mu p_\nu + p_\mu n_\nu}{n \cdot p}, \quad (5.25)$$

where n is a light-like vector with $n^+ = 1$, $n^- = 0$, and $\underline{n} = 0$.

The first term in eq. (5.24) is the free gluon propagator. Integrating over p^+ we can rewrite it as

$$\begin{aligned} (x| \frac{-id_{\mu\nu}(p)}{p^2+i\epsilon} |y) &= \left(-\frac{1}{2\pi} \theta(x^- - y^-) \int_0^\infty \frac{dp^-}{2p^-} + \frac{1}{2\pi} \theta(y^- - x^-) \int_{-\infty}^0 \frac{dp^-}{2p^-} \right) e^{-ip^-(x-y)^+} \\ &\times (\underline{x}| (g_{\mu i} - \frac{n_\mu}{n \cdot p} p_i) e^{-i\frac{p^2}{2p^-} x^-} e^{i\frac{p^2}{2p^-} y^-} (\delta_\nu^i - p^i \frac{n_\nu}{n \cdot p}) |y) + i(x| \frac{n_\mu n_\nu}{(n \cdot p)^2} |y). \end{aligned} \quad (5.26)$$

The last term here is the instantaneous term in the LCPT terminology which we neglect in our calculation. Substituting the right-hand side of eq. (5.26) for each free propagator in the expansion (5.24) one finds the following general structure of the gluon propagator in the background field,

$$\begin{aligned} \text{T}[C_\mu^a(x)C_\nu^b(y)] &= \left(-\frac{1}{2\pi}\theta(x^- - y^-) \int_0^\infty \frac{dp^-}{2p^-} + \frac{1}{2\pi}\theta(y^- - x^-) \int_{-\infty}^0 \frac{dp^-}{2p^-} \right) e^{-ip^-(x-y)^+} \quad (5.27) \\ &\quad \times (\underline{x}|(g_{\mu i} - \frac{n_\mu}{n \cdot p} \mathcal{P}_i) e^{-i\frac{p_1^2}{2p^-}x^-} \mathcal{G}^{ij}(x^-, y^-) e^{i\frac{p_1^2}{2p^-}y^-} (g_{j\nu} - \mathcal{P}_j \frac{n_\nu}{n \cdot p}) | \underline{y})^{ab}, \end{aligned}$$

where $\mathcal{P}_\mu = p_\mu + g\mathcal{A}_\mu$ and the operator $\mathcal{G}(x^-, y^-)$ is constructed out of the background quark and gluon fields and describes the interaction of the “quantum” gluon with the background. Similarly to the scalar case, the operator \mathcal{G} can be expanded in the inverse powers of p^- ,

$$\mathcal{G}^{ij}(x^-, y^-) = \mathcal{G}_0^{ij}(x^-, y^-) + \frac{1}{p^-} \mathcal{G}_1^{ij}(x^-, y^-) + \frac{1}{(p^-)^2} \mathcal{G}_2^{ij}(x^-, y^-) + \dots \quad (5.28)$$

Following the approach developed for the scalar propagator we are going to construct the first few terms in the series (5.28) using the perturbative expansion (5.24). It is easy to observe that each intermediate propagator in (5.24) leads to suppression by an extra inverse power of p^- , see eq. (5.26). This suppression can only be compensated by the eikonal term $p^- A^+$ of the three-gluon vertex. However, such terms can be easily resummed to all orders in the perturbation theory into Wilson-line gauge factors.

As a result, substituting eq. (5.26) into eq. (5.24) and performing manipulations similar to those done in section 5.2.1 we find

$$\begin{aligned} \text{T}[C_\mu^a(x)C_\nu^b(y)] &= \left(-\frac{1}{2\pi}\theta(x^- - y^-) \int_0^\infty \frac{dp^-}{2p^-} + \frac{1}{2\pi}\theta(y^- - x^-) \int_{-\infty}^0 \frac{dp^-}{2p^-} \right) e^{-ip^-(x-y)^+} \quad (5.29) \\ &\quad \times (\underline{x}|(g_{\mu i} - \frac{n_\mu}{p^-} \mathcal{P}_i)^{ac} e^{-i\frac{p_1^2}{2p^-}x^-} \left[g^{ij} U^{cd}[x^-, y^-] \right. \\ &\quad - \frac{ig g^{ij}}{2p^-} \int_{y^-}^{x^-} dz^- z^- (U[x^-, z^-] \{ \mathcal{P}^k, \mathcal{F}_{-k} \} U[z^-, y^-])^{cd} - \frac{g\epsilon^{ij}}{p^-} \int_{y^-}^{x^-} dz^- (U[x^-, z^-] \mathcal{F}^{12}(z^-) U[z^-, y^-])^{cd} \\ &\quad - \frac{g^2 g^{ij}}{4p^-} \int_{y^-}^{x^-} dz^- \int_{y^-}^{z^-} dz'^- \left(U^{cc'}[x^-, z^-] \bar{\psi}(z^-) t^{c'} V[z^-, z'^-] \gamma^+ t^{d'} \psi(z'^-) U^{d'd}[z'^-, y^-] + \text{c.c.} \right) \\ &\quad \left. + \frac{ig^2 \epsilon^{ij}}{4p^-} \int_{y^-}^{x^-} dz^- \int_{y^-}^{z^-} dz'^- \left(U^{cc'}[x^-, z^-] \bar{\psi}(z^-) t^{c'} V[z^-, z'^-] \gamma^+ \gamma_5 t^{d'} \psi(z'^-) U^{d'd}[z'^-, y^-] + \text{c.c.} \right) + O\left(\frac{1}{(p^-)^2}\right) \right] \\ &\quad \times e^{i\frac{p_1^2}{2p^-}y^-} \left(g_{j\nu} - \mathcal{P}_j \frac{n_\nu}{p^-} \right)^{db} | \underline{y}) + \dots \end{aligned}$$

One can see that the structure of the operators in the gluon propagator in the background field, which is in agreement with refs. [33, 63, 66], is richer than the one in the scalar propagator. But what is more important is that now we explicitly see that the interaction

of the “quantum” gluon with the shock-wave background fields is described by the polarized Wilson lines (2.11). Indeed, taking into account that

$$\begin{aligned} \int_{y^-}^{x^-} dz^- z^- U[x^-, z^-] \{ \mathcal{P}^k, \mathcal{F}_{-k} \} U[z^-, y^-] &= \int_{y^-}^{x^-} dz^- z^- \mathcal{P}^k U[x^-, z^-] \mathcal{F}_{-k} U[z^-, y^-] \\ &+ \int_{y^-}^{x^-} dz^- z^- U[x^-, z^-] \mathcal{F}_{-k} U[z^-, y^-] \mathcal{P}^k - g \int_{y^-}^{x^-} dz_1^- \int_{y^-}^{z_1^-} dz_2^- (z_1^- - z_2^-) U[x^-, z_1^-] \mathcal{F}_{-k} U[z_1^-, z_2^-] \mathcal{F}_{-k} U[z_2^-, y^-] \end{aligned} \quad (5.30)$$

we can finally write the gluon propagator in the shock-wave background as

$$\begin{aligned} \mathbb{T}[C_\mu^a(x) C_\nu^b(y)] &= -\frac{1}{2\pi} \int_0^\infty \frac{dp^-}{2p^-} e^{-ip^-(x-y)^+} \\ &\times (\underline{x} | (g_{\mu i} - \frac{n_\mu}{p^-} p_i)^{ac} e^{-i \frac{p_1^2}{2p^-} x^-} \mathcal{G}^{ij}(\infty, -\infty) e^{i \frac{p_1^2}{2p^-} y^-} (g_{j\nu} - p_j \frac{n_\nu}{p^-})^{db} | \underline{y}) + \dots \end{aligned} \quad (5.31)$$

where we assume that $x^- > 0 > y^-$ and

$$\begin{aligned} \mathcal{G}^{ij}(\infty, -\infty) &= g^{ij} U + \frac{g^{ij} s}{2P^+ p^-} U^{\text{q[2]}} + \frac{i\epsilon^{ij} s}{2P^+ p^-} U^{\text{pol[1]}} \\ &- \frac{igg^{ij}}{2p^-} p^k \int_{-\infty}^\infty dz^- z^- U[\infty, z^-] \mathcal{F}_{-k} U[z^-, -\infty] - \frac{igg^{ij}}{2p^-} \int_{-\infty}^\infty dz^- z^- U[\infty, z^-] \mathcal{F}_{-k} U[z^-, -\infty] p^k \\ &+ \frac{ig^2 g^{ij}}{2p^-} \int_{-\infty}^\infty dz_1^- \int_{-\infty}^{z_1^-} dz_2^- (z_1^- - z_2^-) U[\infty, z_1^-] \mathcal{F}_{-k} U[z_1^-, z_2^-] \mathcal{F}_{-k} U[z_2^-, -\infty] + O\left(\frac{1}{(p^-)^2}\right). \end{aligned} \quad (5.32)$$

As we will show in the next section, see eqs. (5.42) and (5.52), the operator

$$\int_{-\infty}^\infty dz^- z^- U[\infty, z^-] \mathcal{F}_{-k} U[z^-, -\infty]$$

can be further related to the polarized Wilson line (2.12c) and the adjoint version of the operator (3.17) given in eq. (4.7).¹² We will also see that operators U , $U^{\text{q[2]}}$ and the operator in the last line of (5.32) do not contribute to the helicity evolution.

5.2.3 Quark propagator in the shock-wave background field

In this section we will consider quark propagator in the background of quark and gluon fields. To simplify the problem we will start the derivation taking into account only the background gluon field and later extend it to include the contribution of background quarks.

The most general form of the quark propagator, which can be obtained by resummation of an infinite number of couplings to background gluons, is

$$\mathbb{T}[\psi(x) \bar{\psi}(y)]_A = (x | \frac{i}{\not{P} + i\epsilon} | y) = (x | \not{P} \frac{i}{P^2 + \frac{g}{2} \sigma^{\mu\nu} F_{\mu\nu} + i\epsilon} | y), \quad (5.33)$$

¹²Note that the fundamental-representation version of this operator, given by eq. (3.17), appears in the dipole gluon helicity TMD and the Jaffe-Manohar (JM) gluon helicity PDF at small- x after the expansion of the exponential phases, as shown above in section 3.1.

where we use the identity

$$\not{p}^2 = P^2 + \frac{g}{2}\sigma^{\mu\nu}F_{\mu\nu}. \quad (5.34)$$

Here the subscript A denotes the gluon-only background field.

To construct the expansion in inverse powers of p^- we write the propagator as an infinite series

$$\begin{aligned} \text{T}[\psi(x)\bar{\psi}(y)]_A &= i(x|\not{P}\frac{1}{P^2+i\epsilon}|y) - ig(x|\not{P}\frac{1}{P^2+i\epsilon}\frac{1}{2}\sigma^{\mu\nu}F_{\mu\nu}\frac{1}{P^2+i\epsilon}|y) \\ &+ ig^2(x|\not{P}\frac{1}{P^2+i\epsilon}\frac{1}{2}\sigma^{\mu\nu}F_{\mu\nu}\frac{1}{P^2+i\epsilon}\frac{1}{2}\sigma^{\rho\sigma}F_{\rho\sigma}\frac{1}{P^2+i\epsilon}|y) + \dots \end{aligned} \quad (5.35)$$

and substitute eq. (5.23) for each scalar propagator. Since each scalar propagator is proportional to $1/p^-$, it is easy to see that to find the leading contribution at small x , it is sufficient to consider only the first few orders of the expansion (5.35).

For brevity, let us also simplify the problem and instead of calculating the full quark propagator consider only its contraction with $\gamma^+\gamma^5$. Indeed, as shown above in the LCOT approach, it is the only contraction we need in order to derive the helicity evolution equations (cf. eq. (2.7b)).¹³

Starting with eq. (5.35) we obtain¹⁴

$$\begin{aligned} &\text{T}[\psi_\beta(x)\bar{\psi}_\alpha(y)]_A[\gamma^+\gamma^5]_{\alpha\beta} \quad (5.36) \\ &= \left(-\frac{1}{2\pi}\theta(x^- - y^-)\int_0^\infty \frac{dp^-}{(2p^-)^2} + \frac{1}{2\pi}\theta(y^- - x^-)\int_{-\infty}^0 \frac{dp^-}{(2p^-)^2}\right) e^{-ip^-(x-y)^+} (x|\text{tr}\left\{\left(\left(\frac{p_\perp^2}{2p^-} + A^+\right)\gamma^- - P^i\gamma^i\right)\right. \\ &\times e^{-i\frac{p_\perp^2}{2p^-}x^-} \left[-\frac{ig}{2}\int_{y^-}^{x^-} dz^- \left(V[x^-, z^-] + \frac{igx^-}{2p^-}(\{p^k, A_k\} + gA^k A_k)(x^-)V[x^-, z^-] + \frac{iz^-}{2p^-}V[x^-, z^-]P_\perp^2\right.\right. \\ &- \frac{ig}{2p^-}\int_{z^-}^{x^-} dz_1^- z_1^- V[x^-, z_1^-]\{P^k, F_{-k}\}V[z_1^-, z^-]\left.\left.\right)\sigma^{\mu\nu}F_{\mu\nu}(z^-)\left(V[z^-, y^-] - \frac{iz^-}{2p^-}P_\perp^2V[z^-, y^-]\right.\right. \\ &- \left.\left.\frac{igy^-}{2p^-}V[z^-, y^-](\{p^k, A_k\} + gA^k A_k)(y^-) - \frac{ig}{2p^-}\int_{y^-}^{z^-} dz_2^- z_2^- V[z^-, z_2^-]\{P^k, F_{-k}\}V[z_2^-, y^-]\right)\right. \\ &\left. + \frac{g^2}{8p^-}\int_{y^-}^{x^-} dz_1^- \int_{y^-}^{z_1^-} dz_2^- V[x^-, z_1^-]\sigma^{\mu\nu}F_{\mu\nu}(z_1^-)V[z_1^-, z_2^-]\sigma^{\rho\sigma}F_{\rho\sigma}(z_2^-)V[z_2^-, y^-]\right] e^{i\frac{p_\perp^2}{2p^-}y^-} \gamma^+\gamma^5 \left.\right\}|y) + O\left(\frac{1}{(p^-)^4}\right). \end{aligned}$$

Now we calculate the trace of gamma matrices and simplify the structure of operators. To do the latter, we utilize the following relations:

$$[P^2, P_\mu] = i\{P^\alpha, F_{\alpha\mu}\} \quad (5.37)$$

and

$$g\int_{y^-}^{x^-} dz^- [x^-, z^-]F_{-m}[z^-, y^-] = P_m[x^-, y^-] - [x^-, y^-]P_m. \quad (5.38)$$

¹³For a more general derivation see refs. [63–65].

¹⁴Note that in the scalar propagators one should take care of the exponential factors which, after expansion, can be combined with boundary terms yielding contributions proportional to P_\perp^2 .

After a somewhat lengthy algebra we obtain

$$\begin{aligned}
 & \Gamma[\psi_\beta(x)\bar{\psi}_\alpha(y)]_A[\gamma^+\gamma_5]_{\alpha\beta} \tag{5.39} \\
 &= \left(-\frac{i}{2\pi}\theta(x^- - y^-) \int_0^\infty \frac{dp^-}{(2p^-)^2} + \frac{i}{2\pi}\theta(y^- - x^-) \int_{-\infty}^0 \frac{dp^-}{(2p^-)^2} \right) e^{-ip^-(x-y)^+} \\
 &\times \langle x | \left\{ 4\epsilon^{im} P^i e^{-i\frac{p_\perp^2}{2p^-}x^-} \left[P^m V[x^-, y^-] - V[x^-, y^-] P^m + \frac{ix^-}{2p^-} (p_\perp^2 P^m - P^m P_\perp^2) V[x^-, y^-] \right. \right. \\
 &+ \frac{ix^-}{2p^-} (P_\perp^2 - p_\perp^2) V[x^-, y^-] P^m + \frac{iy^-}{2p^-} V[x^-, y^-] (P^m p_\perp^2 - P_\perp^2 P^m) + \frac{iy^-}{2p^-} P^m V[x^-, y^-] (P_\perp^2 - p_\perp^2) \\
 &- \frac{ig}{2p^-} P^m \int_{y^-}^{x^-} dz^- z^- V[x^-, z^-] \{P^k, F_{-k}\} V[z^-, y^-] + \frac{ig}{2p^-} \int_{y^-}^{x^-} dz^- z^- V[x^-, z^-] \{P^k, F_{-k}\} V[z^-, y^-] P^m \Big] \\
 &+ g\epsilon^{mn} P^i e^{-i\frac{p_\perp^2}{2p^-}x^-} \frac{1}{p^-} \left[\int_{y^-}^{x^-} dz^- V[x^-, z^-] F_{mn}(z^-) V[z^-, y^-] P^i + P^i \int_{y^-}^{x^-} dz^- V[x^-, z^-] F_{mn}(z^-) V[z^-, y^-] \right] \\
 &\left. - 2g\epsilon^{mn} \left(\frac{p_\perp^2}{2p^-} + A^+ \right) e^{-i\frac{p_\perp^2}{2p^-}x^-} \int_{y^-}^{x^-} dz_1^- V[x^-, z_1^-] F_{mn}(z_1^-) V[z_1^-, y^-] \right\} e^{i\frac{p_\perp^2}{2p^-}y^-} |y\rangle + O\left(\frac{1}{(p^-)^4}\right).
 \end{aligned}$$

This result contains three types of operators. The first is the eikonal coupling of the quark to the background field via Wilson lines $V[x^-, y^-]$. As we will see in explicit calculation below, this operator does not contribute to helicity evolution. The helicity evolution is defined by the sub-eikonal coupling via operators

$$\int_{y^-}^{x^-} dz^- V[x^-, z^-] F_{mn}(z^-) V[z^-, y^-] \tag{5.40}$$

and

$$\int_{y^-}^{x^-} dz^- z^- V[x^-, z^-] \{P^k, F_{-k}\} V[z^-, y^-]. \tag{5.41}$$

While the former operator is obviously related to the small- x polarized Wilson line (2.7a), the relation of the latter to eqs. (2.7c) and (3.17) can be observed from the identity

$$\begin{aligned}
 & g \int_{y^-}^{x^-} dz^- z^- V[x^-, z^-] \{P^k, F_{-k}\} V[z^-, y^-] = i \int_{y^-}^{x^-} dz^- z^- V[x^-, z^-] [P_-, P_\perp^2] V[z^-, y^-] \\
 &= -x^- P_\perp^2 V[x^-, y^-] + y^- V[x^-, y^-] P_\perp^2 + \int_{y^-}^{x^-} dz^- V[x^-, z^-] P_\perp^2 V[z^-, y^-], \tag{5.42}
 \end{aligned}$$

where the last operator is nothing else but the polarized Wilson line (2.7c).

Alternatively, one can use

$$\begin{aligned}
 & g \int_{y^-}^{x^-} dz^- z^- [x^-, z^-] \{P^k, F_{-k}\} [z^-, y^-] = P^k g \int_{y^-}^{x^-} dz^- z^- [x^-, z^-] F_{-k} [z^-, y^-] + g \int_{y^-}^{x^-} dz^- z^- [x^-, z^-] F_{-k} [z^-, y^-] P^k \\
 & - g^2 \int_{y^-}^{x^-} dz_1^- \int_{y^-}^{z_1^-} dz_2^- (z_1^- - z_2^-) [x^-, z_1^-] F_{-k} [z_1^-, z_2^-] F_{-k} [z_2^-, y^-]
 \end{aligned} \tag{5.43}$$

and (5.52) at small- x to relate the operator (5.41) to the polarized Wilson line (3.17). Note that the helicity-independent operators like the one in the last line of eq. (5.43) or the eikonal Wilson lines never contribute to helicity evolution which we will explicitly show in our calculation below.

For now, let us keep the form of eq. (5.39) and calculate the coupling of the propagator to the background quark field. It is easy to see that each such coupling comes along with $1/p^-$, so that at the leading order of the expansion in the inverse powers of p^- it is sufficient to add just a single quark insertion. As a result, for the full quark propagator in the background field (contracted with $\gamma^+ \gamma_5$) we have

$$\begin{aligned}
 & \text{T}[\psi_\beta(x) \bar{\psi}_\alpha(y)] [\gamma^+ \gamma_5]_{\alpha\beta} = \text{T}[\psi_\beta(x) \bar{\psi}_\alpha(y)]_A [\gamma^+ \gamma_5]_{\alpha\beta} \\
 & - g^2 \int d^4 z_1 \int d^4 z_2 \text{tr} \left\{ (x | \frac{i \not{P}}{P^2 + i\epsilon} | z_1) \gamma^\rho t^a \psi(z_1) (z_1 | \frac{-i}{P^2 + i\epsilon} | z_2)^{ab} \bar{\psi}(z_2) \gamma_\rho t^b (z_2 | \frac{i \not{P}}{P^2 + i\epsilon} | y) \gamma^+ \gamma_5 \right\} \\
 & + O\left(\frac{1}{(p^-)^4}\right).
 \end{aligned} \tag{5.44}$$

Substituting the scalar propagators we obtain

$$\begin{aligned}
 & \text{T}[\psi_\beta(x) \bar{\psi}_\alpha(y)] [\gamma^+ \gamma_5]_{\alpha\beta} = \text{T}[\psi_\beta(x) \bar{\psi}_\alpha(y)]_A [\gamma^+ \gamma_5]_{\alpha\beta} \\
 & + \left(-\frac{i}{2\pi} \theta(x^- - y^-) \int_0^\infty \frac{dp^-}{(2p^-)^2} + \frac{i}{2\pi} \theta(y^- - x^-) \int_{-\infty}^0 \frac{dp^-}{(2p^-)^2} \right) e^{-ip^-(x-y)^+} \text{tr} \left\{ (x | P^i \gamma_i e^{-i \frac{p_\perp^2}{2p^-} x^-} \right. \\
 & \times \frac{ig^2}{2p^-} \int_{y^-}^{x^-} dz_1^- \int_{y^-}^{z_1^-} dz_2^- V[x^-, z_1^-] \gamma^\rho t^a \psi(z_1^-) U[z_1^-, z_2^-]^{ab} \bar{\psi}(z_2^-) \gamma_\rho t^b V[z_2^-, y^-] e^{i \frac{p_\perp^2}{2p^-} y^-} \gamma_j P^j | y) \gamma^+ \gamma_5 \left. \right\} \\
 & + O\left(\frac{1}{(p^-)^4}\right).
 \end{aligned} \tag{5.45}$$

Next we use the Fierz identity to decompose the product of background quark fields in terms of the Dirac matrices, i.e., we apply

$$\Gamma = \frac{1}{4} \text{tr}[\Gamma] \text{I} + \frac{1}{4} \text{tr}[\gamma_\mu \Gamma] \gamma^\mu + \frac{1}{8} \text{tr}[\sigma_{\mu\nu} \Gamma] \sigma^{\mu\nu} - \frac{1}{4} \text{tr}[\gamma_\mu \gamma^5 \Gamma] \gamma^\mu \gamma^5 + \frac{1}{4} \text{tr}[\gamma^5 \Gamma] \gamma^5, \tag{5.46}$$

which is valid for an arbitrary gamma-matrix Γ . Employing eq. (5.46) we can calculate the

trace in (5.45) getting

$$\begin{aligned}
& \text{T} [\psi_\beta(x) \bar{\psi}_\alpha(y)] [\gamma^+ \gamma_5]_{\alpha\beta} = \text{T} [\psi_\beta(x) \bar{\psi}_\alpha(y)]_A [\gamma^+ \gamma_5]_{\alpha\beta} \tag{5.47} \\
& + \left(-\frac{i}{2\pi} \theta(x^- - y^-) \int_0^\infty \frac{dp^-}{(2p^-)^2} + \frac{i}{2\pi} \theta(y^- - x^-) \int_{-\infty}^0 \frac{dp^-}{(2p^-)^2} \right) e^{-ip^-(x-y)^+} (\underline{x} | P_i e^{-i \frac{p_\perp^2}{2p^-} x^-} \\
& \times \frac{ig^2}{p^-} \int_{y^-}^{x^-} dz^- \int_{y^-}^{z^-} dz'^- V[x^-, z^-] t^a \left(-i \epsilon^{ij} \psi_\beta(z^-) \bar{\psi}_\alpha(z'^-) [\gamma^+]_{\alpha\beta} \right. \\
& \left. + g^{ij} \psi_\beta(z^-) \bar{\psi}_\alpha(z'^-) [\gamma^+ \gamma_5]_{\alpha\beta} \right) U[z^-, z'^-]^{ab} t^b V[z'^-, y^-] e^{i \frac{p_\perp^2}{2p^-} y^-} P_j | \underline{y} \rangle + O\left(\frac{1}{(p^-)^4}\right).
\end{aligned}$$

At this point we clearly see that the coupling of the propagator to the background quark field is defined by the polarized Wilson line (2.7b). We will also see that the coupling via (2.7d) does not survive in helicity evolution.

Though the equation (5.47) we obtained is quite lengthy, it can be significantly simplified in the case of the shock-wave background when there are no fields outside the shock-wave. The result (5.47) can be simplified even further if we integrate it over the longitudinal coordinates and consider a particular case of $\underline{x} = \underline{y} = \underline{x}_1$ which we will use later in the derivation of helicity evolution, see the diagram III in figure 3.

Indeed, after changing the sign of p^- and taking into account that

$$(\underline{x}_1 | \frac{p_i}{p_\perp^2} \mathcal{O} \frac{p_j}{p_\perp^2} | \underline{x}_1) = \int d^2 z (\underline{x}_1 | \frac{p_i}{p_\perp^2} | z) \mathcal{O}(z) (z | \frac{p_j}{p_\perp^2} | \underline{x}_1) = \int d^2 z (\underline{x}_1 | \frac{p_j}{p_\perp^2} | z) \mathcal{O}(z) (z | \frac{p_i}{p_\perp^2} | \underline{x}_1) = (\underline{x}_1 | \frac{p_j}{p_\perp^2} \mathcal{O} \frac{p_i}{p_\perp^2} | \underline{x}_1) \tag{5.48}$$

is symmetric under $i \leftrightarrow j$ for an arbitrary operator $\mathcal{O}(z)$, we obtain

$$\begin{aligned}
& \int_{-\infty}^0 dx^- \int_0^\infty dy^- \text{T} [\psi_\beta(x^-, \underline{x}_1) \bar{\psi}_\alpha(y^-, \underline{x}_1)] [\gamma^+ \gamma_5]_{\alpha\beta} \tag{5.49} \\
& = -\frac{1}{\pi} \int_0^\infty \frac{dp^-}{p^-} (\underline{x}_1 | \frac{\epsilon^{im} p^i}{p_\perp^2} g \int_{-\infty}^\infty dz^- z^- V[-\infty, z^-] \{P^k, F_{-k}\} V[z^-, \infty] \frac{p_m}{p_\perp^2} | \underline{x}_1) \\
& - \frac{1}{2\pi} \int_0^\infty \frac{dp^-}{p^-} (\underline{x}_1 | \frac{p_i}{p_\perp^2} \left(\epsilon^{mn} ig \int_{-\infty}^\infty dz^- V[-\infty, z^-] F_{mn} V[z^-, \infty] \right. \\
& \left. - g^2 \int_{-\infty}^\infty dz_1^- \int_{-\infty}^{z_1^-} dz_2^- V[-\infty, z_2^-] t^a \psi_\beta(z_2^-) U[z_2^-, z_1^-]^{ab} \bar{\psi}_\alpha(z_1^-) [\gamma^+ \gamma_5]_{\alpha\beta} t^b V[z_1^-, \infty] \right) \frac{p_i}{p_\perp^2} | \underline{x}_1) + O\left(\frac{1}{(p^-)^2}\right).
\end{aligned}$$

Note that the higher-order terms of the expansion in inverse powers of p^- do not contain a logarithm $\int \frac{dp^-}{p^-}$ which dominates at small x . The reader should also note that the large logarithm arises in the terms with sub-eikonal operators (5.40) and (5.41), while the eikonal Wilson lines do not contribute.

Now we use the identity (5.43), introduce the integration over the intermediate transverse coordinate \underline{x}_2 and perform the Fourier transformations over transverse momenta

using¹⁵

$$(\underline{x}_1 | \frac{p^i}{p_\perp^2} | \underline{x}_2) = \frac{i}{2\pi} \frac{\underline{x}_{12}^i}{\underline{x}_{12}^2}, \quad (\underline{x}_1 | \frac{p^i p^k}{p_\perp^2} | \underline{x}_2) = \frac{1}{2\pi} \frac{\delta^{ik} \underline{x}_{12}^2 - 2\underline{x}_{12}^i \underline{x}_{12}^k}{\underline{x}_{12}^4}. \quad (5.50)$$

We obtain

$$\begin{aligned} & \int_{-\infty}^0 dx^- \int_0^\infty dy^- \text{T}[\psi_\beta(x^-, \underline{x}_1) \bar{\psi}_\alpha(y^-, \underline{x}_1)] [\gamma^+ \gamma_5]_{\alpha\beta} \\ &= \frac{ig}{2\pi^3} \int_0^\infty \frac{dp^-}{p^-} \int d^2 \underline{x}_2 \frac{\epsilon^{mk} \underline{x}_{12}^m}{\underline{x}_{12}^4} \left[\int_{-\infty}^\infty dz^- z^- V_{\underline{x}_2}[-\infty, z^-] F_{-k}(z^-, \underline{x}_2) V_{\underline{x}_2}[z^-, \infty] \right. \\ & \quad - \frac{i}{8\pi^3} \int_0^\infty \frac{dp^-}{p^-} \int d^2 \underline{x}_2 \frac{1}{\underline{x}_{12}^2} \left[2g \int_{-\infty}^\infty dz^- V_{\underline{x}_2}[-\infty, z^-] F_{12}(z^-, \underline{x}_2) V_{\underline{x}_2}[z^-, \infty] \right. \\ & \quad \left. \left. + ig^2 \int_{-\infty}^\infty dz_1^- \int_{-\infty}^{z_1^-} dz_2^- V_{\underline{x}_2}[-\infty, z_2^-] t^a \psi_\beta(z_2^-, \underline{x}_2) U_{\underline{x}_2}[z_2^-, z_1^-]^{ab} \bar{\psi}_\alpha(z_1^-, \underline{x}_2) [\gamma^+ \gamma_5]_{\alpha\beta} t^b V_{\underline{x}_2}[z_1^-, \infty] \right] \right]. \end{aligned} \quad (5.51)$$

We can finally relate the operator in the first term of (5.51) to the polarized Wilson line (3.17),

$$\begin{aligned} ig \int_{-\infty}^\infty dz^- z^- V_{\underline{x}_2}[\infty, z^-] F_{-k} V_{\underline{x}_2}[z^-, -\infty] &= -ig \int_{-\infty}^\infty dz^- V_{\underline{x}_2}[\infty, z^-] (z^- \partial_k A_- + A_k) V_{\underline{x}_2}[z^-, -\infty] \\ &= -\frac{ig}{2} \lim_{L^- \rightarrow \infty} \left[\int_{-\infty}^\infty dz^- V_{\underline{x}_2}[\infty, z^-] \left(\int_{-L^-}^{z^-} d\xi^- \partial_k A_- + A_k \right) V_{\underline{x}_2}[z^-, -\infty] \right. \\ & \quad \left. + \int_{-\infty}^\infty dz^- V_{\underline{x}_2}[\infty, z^-] \left(- \int_{z^-}^{L^-} d\xi^- \partial_k A_- + A_k \right) V_{\underline{x}_2}[z^-, -\infty] \right] = \frac{1}{2} \int_{-\infty}^\infty dz^- V_{\underline{x}_2}[\infty, z^-] [D_k - \overleftarrow{D}_k] V_{\underline{x}_2}[z^-, -\infty], \end{aligned} \quad (5.52)$$

and rewrite our result in a compact form

$$\frac{P^+}{2s} \int_{-\infty}^0 dx^- \int_0^\infty dy^- \text{T}[\psi_\beta(x^-, \underline{x}_1) \bar{\psi}_\alpha(y^-, \underline{x}_1)] [\gamma^+ \gamma_5]_{\alpha\beta} = \frac{1}{8\pi^3} \int_0^\infty \frac{dp^-}{p^-} \int \frac{d^2 \underline{x}_2}{\underline{x}_{21}^2} \left[2 \frac{\epsilon^{km} \underline{x}_{21}^m}{\underline{x}_{21}^2} V_{\underline{x}_2}^{kG[2]\dagger} + V_{\underline{x}_2}^{\text{pol}[1]\dagger} \right]. \quad (5.53)$$

This is our final result for the quark propagator in the background field which we will use in the calculation of the helicity evolution equations. While we consider a particular projection of the propagator, we should mention that our method of derivation is completely general and can be used beyond the problem of helicity evolution.

5.3 Evolution equation for Q_{10} in the background field method

In this section we will use the results we obtained in the previous section for the gluon and quark propagators in the background field to derive the evolution equation for the

¹⁵Note that in the last equation we neglect the instantaneous term, see the discussion after eq. (4.3) above.

polarized dipole amplitude Q_{10} . Following the logic of the background field method and the rapidity factorization approach we define the amplitude as

$$Q_{10}(\sigma) \equiv \frac{1}{2N_c} \left\langle \left\langle \text{T tr} \left[V_{\underline{0}} V_{\underline{1}}^{\text{pol}[1]\dagger} \right] + \text{T tr} \left[V_{\underline{1}}^{\text{pol}[1]} V_{\underline{0}}^\dagger \right] \right\rangle \right\rangle(\sigma), \quad (5.54)$$

where the operators are constructed from fields with longitudinal momentum fraction p^- restricted from above by a cutoff scale σ . As we discussed in section 5.1, to construct the evolution equation for the amplitude we shift the scale to a lower value σ' and integrate the matrix element in (5.54) over the fields with $\sigma > p^- > \sigma'$, see eq. (5.8), while keeping the fields with momenta $p^- < \sigma'$ fixed. We will perform this integration at the one-loop level which is represented by the diagrams in figure 3.

Let us start with the calculation of the diagram I. Expanding Wilson lines of the operators in eq. (5.54) one can readily obtain

$$\begin{aligned} \left(\text{T tr} \left[V_{\underline{0}} V_{\underline{1}}^{\text{pol}[1]\dagger} \right] + \text{c.c.} \right)_I &= \frac{g^2 P^+}{s} \int_0^\infty dx_0^- \int_{-\infty}^0 dx_1^- \text{tr} \left[V_{\underline{0}}[\infty, x_0^-] t^a V_{\underline{0}}[x_0^-, -\infty] \right. \\ &\quad \times V_{\underline{1}}[-\infty, x_1^-] t^b V_{\underline{1}}[x_1^-, \infty] \left. \right] \text{T} \left[A^{a+}(x_0^-, \underline{x}_0) F^{b12}(x_1^-, \underline{x}_1) \right] + \text{c.c.} \\ &= \frac{g^2 P^+ \epsilon^{ij}}{s} \text{tr} \left[t^a V_{\underline{0}} t^b V_{\underline{1}}^\dagger \right] \int_0^\infty dx_0^- \int_{-\infty}^0 dx_1^- \text{T} \left[A^{a+}(x_0^-, \underline{x}_0) \partial_i A_j^b(x_1^-, \underline{x}_1) \right] + \text{c.c.}, \end{aligned} \quad (5.55)$$

where in the last line we use the shock-wave approximation to simplify the gauge factors as $V_{\underline{0}}[\infty, x_0^-] \rightarrow 1$, $V_{\underline{0}}[x_0^-, -\infty] \rightarrow V_{\underline{0}}$, both for $x_0^- > 0$, etc.

The subsequent steps of the calculation are straightforward. Substituting the gluon propagator in the shock-wave background field (5.31)

$$\text{T} \left[A^{a+}(x_0^-, \underline{x}_0) \partial^i A^{bj}(x_1^-, \underline{x}_1) \right] \Big|_{x_0^- > x_1^-} = \frac{i}{2\pi} \int_0^\infty \frac{dp^-}{2p^-} (\underline{x}_0 | e^{-i \frac{p_1^2}{2p^-} x_0^-} \frac{p_m}{p^-} \mathcal{G}^{mn}(\infty, -\infty) p^i \delta_n^j e^{i \frac{p_1^2}{2p^-} x_1^-} | \underline{x}_1)^{ab}, \quad (5.56)$$

where operator \mathcal{G}^{mn} describes the interaction of the “quantum” gluon with the shock-wave background, and integrating over the longitudinal coordinates we obtain

$$\left(\text{T tr} \left[V_{\underline{0}} V_{\underline{1}}^{\text{pol}[1]\dagger} \right] + \text{c.c.} \right)_I = -\frac{ig^2 P^+ \epsilon^{ij}}{\pi s} \text{tr} \left[t^a V_{\underline{0}} t^b V_{\underline{1}}^\dagger \right] \int_0^\infty dp^- (\underline{x}_0 | \frac{p_m}{p_1^2} \mathcal{G}^{mn}(\infty, -\infty) \frac{p^i \delta_n^j}{p_1^2} | \underline{x}_1)^{ab} + \text{c.c.} \quad (5.57)$$

Note that until this point we have not explicitly restricted the integration over the longitudinal momentum p^- . However, one should take into account that the matrix element 5.54 is integrated over the fields with $\sigma > p^- > \sigma'$. As a result, the integration over p^- in eq. (5.57) should be restricted to

$$\int_0^\infty dp^- \rightarrow \int_{\sigma'}^\sigma dp^-. \quad (5.58)$$

For brevity, we will perform this substitution at the very end of our calculation.

In an analogous way one can perform the calculation of diagrams II, I' and II' in figure 3. Adding all terms together we obtain

$$\begin{aligned}
 & \left(\text{Tr} \left[V_{\underline{0}} V_{\underline{1}}^{\text{pol}[1]\dagger} \right] + \text{c.c.} \right)_{\text{I+II+I'+II'}} = -\frac{ig^2 P^+ \epsilon^{ij}}{\pi s} \text{tr} \left[t^a V_{\underline{0}} t^b V_{\underline{1}}^\dagger \right] \int_0^\infty dp^- \quad (5.59) \\
 & \times \left[(\underline{x}_0 | \frac{p_m}{p_\perp^2} \mathcal{G}^{mn}(\infty, -\infty) \frac{p^i \delta_n^j}{p_\perp^2} | \underline{x}_1) - (\underline{x}_1 | \frac{p^i \delta_m^j}{p_\perp^2} \mathcal{G}^{mn}(\infty, -\infty) \frac{p_n}{p_\perp^2} | \underline{x}_0) - (\underline{x}_0 \rightarrow \underline{x}_1) \right]^{ab} + \text{c.c.},
 \end{aligned}$$

where the second term in the last line corresponds to the diagram II, and the last two terms are the sum of the diagrams I' and II'.

Now we need to substitute the explicit form of the operator \mathcal{G}^{mn} from eq. (5.32). Let us show that the first term of the operator, i.e., the interaction described by the Wilson line U does not provide any contribution to the evolution equation. Indeed, substituting this term into eq. (5.59) we obtain a trivial combination

$$\begin{aligned}
 & (\underline{x}_0 | \frac{p_m}{p_\perp^2} \mathcal{G}^{mn}(\infty, -\infty) \frac{p^i \delta_n^j}{p_\perp^2} | \underline{x}_1)^{ab} - (\underline{x}_1 | \frac{p^i \delta_m^j}{p_\perp^2} \mathcal{G}^{mn}(\infty, -\infty) \frac{p_n}{p_\perp^2} | \underline{x}_0)^{ab} \quad (5.60) \\
 & \rightarrow (\underline{x}_0 | \frac{p^j}{p_\perp^2} U^{ab} \frac{p^i}{p_\perp^2} | \underline{x}_1) - (\underline{x}_1 | \frac{p^i}{p_\perp^2} U^{ab} \frac{p^j}{p_\perp^2} | \underline{x}_0) = (\underline{x}_1 | \frac{p^i}{p_\perp^2} U^{ab} \frac{p^j}{p_\perp^2} | \underline{x}_0) - (\underline{x}_1 | \frac{p^i}{p_\perp^2} U^{ab} \frac{p^j}{p_\perp^2} | \underline{x}_0) = 0.
 \end{aligned}$$

Moreover, for the same reason, the interaction of the gluon with the shock wave via operators $U^{\text{pol}[1]}$ and

$$\int_{-\infty}^\infty dz_1^- \int_{-\infty}^{z_1^-} dz_2^- (z_1^- - z_2^-) U[\infty, z_1^-] \mathcal{F}_{-k} U[z_1^-, z_2^-] \mathcal{F}_{-k} U[z_2^-, -\infty] \quad (5.61)$$

does not contribute to helicity evolution as well.

Substituting the remaining three terms of eq. (5.32) into eq. (5.59) and introducing the integration over the intermediate coordinate \underline{x}_2 (see eq. (A.2)), after some straightforward algebra we obtain

$$\begin{aligned}
 & \left(\text{Tr} \left[V_{\underline{0}} V_{\underline{1}}^{\text{pol}[1]\dagger} \right] + \text{c.c.} \right)_{\text{I+II+I'+II'}} = \frac{g^2 \epsilon^{ij}}{\pi} \text{tr} \left[t^a V_{\underline{0}} t^b V_{\underline{1}}^\dagger \right] \int_0^\infty \frac{dp^-}{p^-} \int d^2 \underline{x}_2 \quad (5.62) \\
 & \times \left[\left((\underline{x}_1 | \frac{p^i}{p_\perp^2} | \underline{x}_2) (\underline{x}_2 | \frac{p^j p^k}{p_\perp^2} | \underline{x}_0) + (\underline{x}_1 | \frac{p^i p^k}{p_\perp^2} | \underline{x}_2) (\underline{x}_2 | \frac{p^j}{p_\perp^2} | \underline{x}_0) \right) \frac{g P^+}{s} \int_{-\infty}^\infty dz^- z^- U_2[\infty, z^-] \mathcal{F}_{-k}(z^-, \underline{x}_2) U_2[z^-, -\infty] \right. \\
 & \left. - \epsilon^{jn} (\underline{x}_1 | \frac{p^i}{p_\perp^2} | \underline{x}_2) (\underline{x}_2 | \frac{p_n}{p_\perp^2} | \underline{x}_0) U_2^{\text{pol}[1]} - (\underline{x}_0 \rightarrow \underline{x}_1) \right]^{ab} + \text{c.c.}
 \end{aligned}$$

Finally, we need to substitute the Fourier transformations¹⁶

$$(\underline{x}_1 | \frac{p^i}{p_\perp^2} | \underline{x}_2) = \frac{i}{2\pi} \frac{\underline{x}_{12}^i}{\underline{x}_{12}^2}, \quad (\underline{x}_1 | \frac{p^i p^k}{p_\perp^2} | \underline{x}_2) = \frac{1}{2\pi} \frac{\delta^{ik} \underline{x}_{12}^2 - 2 \underline{x}_{12}^i \underline{x}_{12}^k}{\underline{x}_{12}^4} \quad (5.63)$$

¹⁶Note again that in the last equation we neglect the instantaneous contribution, see the discussion after eq. (4.3).

into eq. (5.62), which yields

$$\begin{aligned}
& \left(\text{Tr} \left[V_0 V_1^{\text{pol}[1]\dagger} \right] + \text{c.c.} \right)_{\text{I+II+I'+II'}} = -\frac{g^2}{4\pi^3} \text{tr} \left[t^a V_0 t^b V_1^\dagger \right] \int_0^\infty \frac{dp^-}{p^-} \int d^2 \underline{x}_2 \quad (5.64) \\
& \times \left\{ \left[2\epsilon^{kj} \frac{\underline{x}_{21}^j}{\underline{x}_{21}^4} - \frac{\epsilon^{kj} (\underline{x}_{21}^j + \underline{x}_{20}^j)}{\underline{x}_{21}^2 \underline{x}_{20}^2} - \frac{2\underline{x}_{20} \times \underline{x}_{21}}{\underline{x}_{21}^2 \underline{x}_{20}^2} \left(\frac{\underline{x}_{21}^k}{\underline{x}_{21}^2} - \frac{\underline{x}_{20}^k}{\underline{x}_{20}^2} \right) \right] \frac{igP^+}{s} \int_{-\infty}^\infty dz^- z^- U_2[\infty, z^-] \mathcal{F}_{-k}(z^-, \underline{x}_2) U_2[z^-, -\infty] \right. \\
& \left. - \left[\frac{1}{\underline{x}_{21}^2} - \frac{\underline{x}_{21} \cdot \underline{x}_{20}}{\underline{x}_{21}^2 \underline{x}_{20}^2} \right] U_2^{\text{pol}[1]} \right\}^{ab} + \text{c.c.}
\end{aligned}$$

Now let us discuss the operator in the second line of eq. (5.64). It is easy to see that this operator is nothing else but a small- x version of the operator in the dipole gluon helicity TMD and the Jaffe-Manohar (JM) gluon helicity PDF (see also the discussion in section 3.1). This operator can be obtained by expanding the exponential factor and keeping only the term linear in x , cf. eq. (3.6),

$$\begin{aligned}
& \int_{-\infty}^\infty dz^- e^{ixP^+ z^-} U_2[\infty, z^-] \mathcal{F}^{+k}(z^-, \underline{x}_2) U_2[z^-, -\infty] \quad (5.65) \\
& = \int_{-\infty}^\infty dz^- U_2[\infty, z^-] \mathcal{F}^{+k} U_2[z^-, -\infty] + ixP^+ \int_{-\infty}^\infty dz^- z^- U_2[\infty, z^-] \mathcal{F}^{+k} U_2[z^-, -\infty] + \dots \\
& = - \int_{-\infty}^\infty dz^- U_2[\infty, z^-] \partial^k \mathcal{A}^+ U_2[z^-, -\infty] + ixP^+ \int_{-\infty}^\infty dz^- z^- U_2[\infty, z^-] \mathcal{F}^{+k} U_2[z^-, -\infty] + \dots
\end{aligned}$$

Here the first term of the last line can be rewritten as a derivative of the Wilson line and for this reason describes the eikonal helicity-independent coupling of the ‘‘quantum’’ gluon to the shock-wave background. The helicity-dependent coupling in the small- x limit is described by the second term which explicitly appears in eqs. (5.65) and (5.31) for the gluon propagator.

Using eq. (5.52) one can rewrite this operator in terms of the adjoint polarized Wilson line of the second kind defined in eq. (4.7). We obtain

$$\begin{aligned}
& \left(\text{Tr} \left[V_0 V_1^{\text{pol}[1]\dagger} \right] + \text{c.c.} \right)_{\text{I+II+I'+II'}} = \frac{g^2}{4\pi^3} \text{tr} \left[t^b V_0 t^a V_1^\dagger \right] \int_0^\infty \frac{dp^-}{p^-} \int d^2 \underline{x}_2 \quad (5.66) \\
& \times \left\{ \left[2\epsilon^{kj} \frac{\underline{x}_{21}^j}{\underline{x}_{21}^4} - \frac{\epsilon^{kj} (\underline{x}_{21}^j + \underline{x}_{20}^j)}{\underline{x}_{21}^2 \underline{x}_{20}^2} - \frac{2\underline{x}_{20} \times \underline{x}_{21}}{\underline{x}_{21}^2 \underline{x}_{20}^2} \left(\frac{\underline{x}_{21}^k}{\underline{x}_{21}^2} - \frac{\underline{x}_{20}^k}{\underline{x}_{20}^2} \right) \right] U_2^{kG[2]} + \left[\frac{1}{\underline{x}_{21}^2} - \frac{\underline{x}_{21} \cdot \underline{x}_{20}}{\underline{x}_{21}^2 \underline{x}_{20}^2} \right] U_2^{\text{pol}[1]} \right\}^{ba} + \text{c.c.}
\end{aligned}$$

Let us now calculate the contribution of the diagram III. Using the shock-wave approximation we can write the following expression for this diagram

$$\begin{aligned}
& \left(\text{Tr} \left[V_0 V_1^{\text{pol}[1]\dagger} \right] + \text{c.c.} \right)_{\text{III}} \quad (5.67) \\
& = \frac{g^2 P^+}{2s} \int_{-\infty}^0 dx_1^- \int_0^\infty dx_2^- \text{tr} \left(V_0 t^a \text{T}[\psi_\beta(x_1^-, \underline{x}_1) \bar{\psi}_\alpha(x_2^-, \underline{x}_1)] [\gamma^+ \gamma^5]_{\alpha\beta} t^b \right) U_1^{ba} + \text{c.c.}
\end{aligned}$$

Substituting the expression for the quark propagator in the background field (5.53) and integrating over longitudinal coordinates we obtain

$$\begin{aligned} & \left(\text{T tr} \left[V_{\underline{0}} V_{\underline{1}}^{\text{pol}[1]\dagger} \right] + \text{c.c.} \right)_{\text{III}} \tag{5.68} \\ &= \frac{\alpha_s}{2\pi^2} \int_0^\infty \frac{dp^-}{p^-} \int d^2 \underline{x}_2 \left(2 \frac{\epsilon^{ij} \underline{x}_{21}^j}{\underline{x}_{21}^4} \text{tr} [t^b V_{\underline{0}} t^a V_{\underline{2}}^{iG[2]\dagger}] U_{\underline{1}}^{ba} + \frac{1}{\underline{x}_{21}^2} \text{tr} [V_{\underline{0}} t^a V_{\underline{2}}^{\text{pol}[1]\dagger} t^b] U_{\underline{1}}^{ba} \right) + \text{c.c.} . \end{aligned}$$

Finally, one needs to calculate the eikonal diagrams. Since this calculation is similar to the derivation of the Balitsky-Kovchegov (BK) evolution equation [44–47] with the well-known kernel $\frac{x_{10}^2}{x_{21}^2 x_{20}^2}$, we will not present the details of the calculation here. Let us just mention that this calculation can be done similar to the calculation presented above. However, for the eikonal diagrams, the dominant contribution with the logarithmic integral $\int \frac{dp^-}{p^-}$ comes from the interaction through the eikonal Wilson line of the gluon propagator in the background field, see the first term in eq. (5.32).

Let us now assemble all the terms together. We have

$$\begin{aligned} & \frac{1}{2N_c} \left\langle \left\langle \text{T tr} \left[V_{\underline{0}} V_{\underline{1}}^{\text{pol}[1]\dagger} \right] + \text{c.c.} \right\rangle \right\rangle (\sigma) = \frac{1}{2N_c} \left\langle \left\langle \text{T tr} \left[V_{\underline{0}} V_{\underline{1}}^{\text{pol}[1]\dagger} \right] + \text{c.c.} \right\rangle \right\rangle_0 (\sigma) \tag{5.69} \\ &+ \frac{\alpha_s N_c}{2\pi^2} \int_{\sigma'}^\sigma \frac{dp^-}{p^-} \int d^2 \underline{x}_2 \left\{ \left[\frac{1}{\underline{x}_{21}^2} - \frac{\underline{x}_{21} \cdot \underline{x}_{20}}{\underline{x}_{21}^2 \underline{x}_{20}^2} \right] \frac{1}{N_c^2} \left\langle \left\langle \text{tr} \left[t^b V_{\underline{0}} t^a V_{\underline{1}}^\dagger \right] (U_{\underline{2}}^{\text{pol}[1]})^{ba} + \text{c.c.} \right\rangle \right\rangle (\sigma') \right. \\ &+ \left. \left[2\epsilon^{ij} \frac{\underline{x}_{21}^j}{\underline{x}_{21}^4} - \frac{\epsilon^{ij} (\underline{x}_{21}^j + \underline{x}_{20}^j)}{\underline{x}_{21}^2 \underline{x}_{20}^2} - \frac{2\underline{x}_{20} \times \underline{x}_{21}}{\underline{x}_{21}^2 \underline{x}_{20}^2} \left(\frac{\underline{x}_{21}^i}{\underline{x}_{21}^2} - \frac{\underline{x}_{20}^i}{\underline{x}_{20}^2} \right) \right] \frac{1}{N_c^2} \left\langle \left\langle \text{tr} \left[t^b V_{\underline{0}} t^a V_{\underline{1}}^\dagger \right] (U_{\underline{2}}^{iG[2]})^{ba} + \text{c.c.} \right\rangle \right\rangle (\sigma') \right\} \\ &+ \frac{\alpha_s N_c}{4\pi^2} \int_{\sigma'}^\sigma \frac{dp^-}{p^-} \int \frac{d^2 \underline{x}_2}{\underline{x}_{21}^2} \left\{ \frac{1}{N_c^2} \left\langle \left\langle \text{tr} [V_{\underline{0}} t^a V_{\underline{2}}^{\text{pol}[1]\dagger} t^b] U_{\underline{1}}^{ba} \right\rangle \right\rangle (\sigma') + 2 \frac{\epsilon^{ij} \underline{x}_{21}^j}{\underline{x}_{21}^2} \frac{1}{N_c^2} \left\langle \left\langle \text{tr} [t^b V_{\underline{0}} t^a V_{\underline{2}}^{iG[2]\dagger}] U_{\underline{1}}^{ba} \right\rangle \right\rangle (\sigma') + \text{c.c.} \right\} \\ &+ \frac{\alpha_s N_c}{2\pi^2} \int_{\sigma'}^\sigma \frac{dp^-}{p^-} \int d^2 \underline{x}_2 \frac{x_{10}^2}{x_{21}^2 x_{20}^2} \left\{ \frac{1}{N_c^2} \left\langle \left\langle \text{tr} \left[t^b V_{\underline{0}} t^a V_{\underline{1}}^{\text{pol}[1]\dagger} \right] U_{\underline{2}}^{ba} \right\rangle \right\rangle (\sigma') - \frac{C_F}{N_c^2} \left\langle \left\langle \text{tr} \left[V_{\underline{0}} V_{\underline{1}}^{\text{pol}[1]\dagger} \right] \right\rangle \right\rangle (\sigma') + \text{c.c.} \right\}, \end{aligned}$$

where, following the logic of the background field method, we insert the limits of the integral over p^- and identify the Wilson lines as constructed out of the background fields with $p^- < \sigma'$. Now we can see that up to a trivial change of variables we are in a full agreement with the result obtained in the LCOT approach above, given in eq. (4.15). The result of a similar calculation employing the background field method in the adjoint representation, which is not shown here, is also in agreement with eq. (4.19).

5.4 Evolution equation for G_{10}^i in the background field method

The operator definition of the polarized dipole amplitude G_{10}^i is given by eq. (4.2). Of course, to derive the evolution equation for the amplitude one can directly start with that definition. However, we would like to remind the reader that the corresponding operator (3.17) is a small- x version of the operator in the definition of the dipole gluon helicity TMD and the Jaffe-Manohar (JM) gluon helicity PDF in eqs. (3.1) and (3.2). To emphasise this relation let us start with an alternative definition of the amplitude G_{10}^i which is more obviously related to the aforementioned distributions.

Indeed, using eq. (5.52) one can rewrite the definition (4.2) as

$$G_{10}^i(\sigma) \equiv \frac{igP^+}{2sN_c} \left\langle \left\langle \text{T tr} \left[V_0^\dagger \int_{-\infty}^{\infty} dz^- z^- V_1[\infty, z^-] F^{+i} V_1[z^-, -\infty] \right] + \text{c.c.} \right\rangle \right\rangle(\sigma). \quad (5.70)$$

Following the background field method, to derive the evolution equation for G_{10}^i let us start with the operator definition (5.70) and integrate the matrix element over fields with $\sigma > p^- > \sigma'$ while keeping the background fields with $p^- < \sigma'$ fixed. At the one-loop level this corresponds to the calculation of diagrams in figure 5.

Let us start with the calculation of the diagram IV. Rewriting the initial operator as

$$\begin{aligned} & \text{T tr} \left[V_0^\dagger \int_{-\infty}^{\infty} dz^- z^- V_1[\infty, z^-] F^{+i} V_1[z^-, -\infty] \right] + \text{c.c.} \\ &= -\text{T tr} \left[V_0^\dagger \int_{-\infty}^{\infty} dz^- V_1[\infty, z^-] (z^- \partial^i A^+ + A^i) V_1[z^-, -\infty] \right] + \text{c.c.}, \end{aligned} \quad (5.71)$$

expanding the Wilson lines and simplifying the gauge factors using the shock-wave approximation we obtain

$$\begin{aligned} & \left(\text{T tr} \left[V_0^\dagger \int_{-\infty}^{\infty} dz^- z^- V_1[\infty, z^-] F^{+i} V_1[z^-, -\infty] \right] + \text{c.c.} \right)_{\text{IV}} \\ &= \text{tr} [V_0^\dagger t^a V_1 t^b] ig \int_0^\infty dx^- \int_{-\infty}^0 dz^- (z^- \text{T}[A^{a+}(x^-, \underline{x}_0) \partial^i A^{b+}(z^-, \underline{x}_1)] + \text{T}[A^{a+}(x^-, \underline{x}_0) A^{bi}(z^-, \underline{x}_1)]) + \text{c.c.} \end{aligned} \quad (5.72)$$

Now we need to substitute the gluon propagators in the shock-wave background. Using eq. (5.31) we find

$$\text{T}[A^{a+}(x^-, \underline{x}_0) \partial^i A^{b+}(z^-, \underline{x}_1)] \Big|_{x^- > z^-} = -\frac{i}{2\pi} \int_0^\infty \frac{dp^-}{2p^-} (\underline{x}_0 | e^{-i \frac{p_1^2}{2p^-} x^-} \frac{p_m}{p^-} \mathcal{G}^{mn}(\infty, -\infty) \frac{p^i p_n}{p^-} e^{i \frac{p_1^2}{2p^-} z^-} | \underline{x}_1)^{ab} \quad (5.73)$$

and

$$\text{T}[A^{a+}(x^-, \underline{x}_0) A^{bi}(z^-, \underline{x}_1)] \Big|_{x^- > z^-} = \frac{1}{2\pi} \int_0^\infty \frac{dp^-}{2p^-} (\underline{x}_0 | e^{-i \frac{p_1^2}{2p^-} x^-} \frac{p_m}{p^-} \mathcal{G}^{mn}(\infty, -\infty) \delta_n^i e^{i \frac{p_1^2}{2p^-} z^-} | \underline{x}_1)^{ab}. \quad (5.74)$$

With this result it is straightforward to integrate over the longitudinal coordinates x^- and z^- , obtaining

$$\begin{aligned} & \left(\text{T tr} \left[V_0^\dagger \int_{-\infty}^{\infty} dz^- z^- V_1[\infty, z^-] F^{+i} V_1[z^-, -\infty] \right] + \text{c.c.} \right)_{\text{IV}} \\ &= -\text{tr} [V_0^\dagger t^a V_1 t^b] \frac{ig}{\pi} \int_0^\infty dp^- \left\{ 2(\underline{x}_0 | \frac{p_m}{p_1^2} \mathcal{G}^{mn}(\infty, -\infty) \frac{p^i p_n}{p_1^4} | \underline{x}_1)^{ab} + (\underline{x}_0 | \frac{p_m}{p_1^2} \mathcal{G}^{mi}(\infty, -\infty) \frac{1}{p_1^2} | \underline{x}_1)^{ab} \right\}. \end{aligned} \quad (5.75)$$

Employing a similar technique one can calculate the diagrams V, IV' and V' in figure 5. For the sum of the diagrams we have

$$\begin{aligned}
 & \left(\text{Tr tr} \left[V_0^\dagger \int_{-\infty}^{\infty} dz^- z^- V_1[\infty, z^-] F^{+i} V_1[z^-, -\infty] \right] + \text{c.c.} \right)_{\text{IV}+\text{V}+\text{IV}'+\text{V}'} \quad (5.76) \\
 &= -\text{tr} \left[V_0^\dagger t^a V_1 t^b \right] \frac{ig}{\pi} \int_0^{\infty} dp^- \left\{ 2(\underline{x}_0 | \frac{p^m}{p_1^2} \mathcal{G}^{mn}(\infty, -\infty) \frac{p^i p_n}{p_1^4} | \underline{x}_1) + 2(\underline{x}_1 | \frac{p^i p^m}{p_1^4} \mathcal{G}^{mn}(\infty, -\infty) \frac{p_n}{p_1^2} | \underline{x}_0) \right. \\
 & \quad \left. + (\underline{x}_0 | \frac{p^m}{p_1^2} \mathcal{G}^{mi}(\infty, -\infty) \frac{1}{p_1^2} | \underline{x}_1) + (\underline{x}_1 | \frac{1}{p_1^2} \mathcal{G}^{in}(\infty, -\infty) \frac{p_n}{p_1^2} | \underline{x}_0) - (\underline{x}_0 \rightarrow \underline{x}_1) \right\}^{ab}.
 \end{aligned}$$

After this we need to substitute the operator \mathcal{G}^{mn} which describes the interaction of the “quantum” gluon in figure 5 with the shock-wave background field. Similar to the case of the dipole amplitude Q_{10} , the operators U , $U^{\text{pol}[1]}$, and (5.61) do not contribute to the evolution of the dipole amplitude G_{10}^i . For example, substituting

$$\mathcal{G}^{mn}(\infty, -\infty) \rightarrow g^{mn} U \quad (5.77)$$

we obtain

$$\begin{aligned}
 & 2(\underline{x}_0 | \frac{p^m}{p_1^2} U \frac{p^i p^m}{p_1^4} | \underline{x}_1) + 2(\underline{x}_1 | \frac{p^i p^m}{p_1^4} U \frac{p^m}{p_1^2} | \underline{x}_0) + (\underline{x}_0 | \frac{p^i}{p_1^2} U \frac{1}{p_1^2} | \underline{x}_1) + (\underline{x}_1 | \frac{1}{p_1^2} U \frac{p^i}{p_1^2} | \underline{x}_0) - (\underline{x}_0 \rightarrow \underline{x}_1) \quad (5.78) \\
 &= -2(\underline{x}_1 | \frac{p^i p^m}{p_1^4} U \frac{p^m}{p_1^2} | \underline{x}_0) + 2(\underline{x}_1 | \frac{p^i p^m}{p_1^4} U \frac{p^m}{p_1^2} | \underline{x}_0) - (\underline{x}_1 | \frac{1}{p_1^2} U \frac{p^i}{p_1^2} | \underline{x}_0) + (\underline{x}_1 | \frac{1}{p_1^2} U \frac{p^i}{p_1^2} | \underline{x}_0) - (\underline{x}_0 \rightarrow \underline{x}_1) = 0.
 \end{aligned}$$

Substituting the remaining terms of \mathcal{G}^{mn} and introducing the integration over the intermediate variable \underline{x}_2 we rewrite eq. (5.76) as

$$\begin{aligned}
 & \left(\text{Tr tr} \left[V_0^\dagger \int_{-\infty}^{\infty} dz^- z^- V_1[\infty, z^-] F^{+i} V_1[z^-, -\infty] \right] + \text{c.c.} \right)_{\text{IV}+\text{V}+\text{IV}'+\text{V}'} \quad (5.79) \\
 &= -\text{tr} \left[V_0^\dagger t^a V_1 t^b \right] \frac{g}{\pi} \int_0^{\infty} \frac{dp^-}{p^-} \int d^2 \underline{x}_2 \left\{ \left[(\underline{x}_1 | \frac{1}{p_1^2} \left(\delta^{im} - \frac{2p^i p^m}{p_1^2} \right) | \underline{x}_2) (\underline{x}_2 | \frac{p^m p^k}{p_1^2} | \underline{x}_0) \right. \right. \\
 & \quad \left. \left. + 2(\underline{x}_1 | \frac{p^i p^m p^k}{p_1^4} | \underline{x}_2) (\underline{x}_2 | \frac{p^m}{p_1^2} | \underline{x}_0) + (\underline{x}_1 | \frac{p^k}{p_1^2} | \underline{x}_2) (\underline{x}_2 | \frac{p^i}{p_1^2} | \underline{x}_0) \right] g \int_{-\infty}^{\infty} dz^- z^- U_2[\infty, z^-]_z \mathcal{F}_{-k} U_2[z^-, -\infty]_z \right. \\
 & \quad \left. - \epsilon^{mn} (\underline{x}_1 | \frac{1}{p_1^2} \left(\delta^{im} - \frac{2p^i p^m}{p_1^2} \right) | \underline{x}_2) (\underline{x}_2 | \frac{p_n}{p_1^2} | \underline{x}_0) \frac{s}{P^+} U_2^{\text{pol}[1]} - (\underline{x}_0 \rightarrow \underline{x}_1) \right\}^{ab}.
 \end{aligned}$$

The Fourier transformations in this equation can be calculated using eqs. (4.22), (5.50), and

$$(\underline{x}_1 | \frac{p^i p^m p^k}{p_1^4} | \underline{x}_2) = \frac{i}{4\pi} \left[\frac{\delta^{im} x_{12}^k}{x_{12}^2} + \frac{\delta^{ik} x_{12}^m}{x_{12}^2} + \frac{\delta^{mk} x_{12}^i}{x_{12}^2} - 2 \frac{x_{12}^i x_{12}^m x_{12}^k}{x_{12}^4} \right], \quad (5.80)$$

which gives

$$\begin{aligned}
 & \left(\text{Tr} \left[V_0^\dagger \int_{-\infty}^{\infty} dz^- z^- V_1[\infty, z^-] F^{+i} V_1[z^-, -\infty] \right] + \text{c.c.} \right)_{\text{IV}+\text{V}+\text{IV}'+\text{V}'} = \text{tr} [V_0^\dagger t^a V_1 t^b] \frac{g}{8\pi^3} \int_0^\infty \frac{dp^-}{p^-} \int d^2 \underline{x}_2 \\
 & \times \left\{ \left[\delta^{ik} \left(-2 \frac{\underline{x}_{12} \cdot \underline{x}_{20}}{\underline{x}_{12}^2 \underline{x}_{20}^2} + \frac{1}{\underline{x}_{20}^2} \right) + 2 \frac{\underline{x}_{12}^i \underline{x}_{20}^k}{\underline{x}_{12}^2 \underline{x}_{20}^2} \left(2 \frac{\underline{x}_{12} \cdot \underline{x}_{20}}{\underline{x}_{20}^2} - 1 \right) + 2 \frac{\underline{x}_{12}^i \underline{x}_{12}^k}{\underline{x}_{12}^2 \underline{x}_{20}^2} \left(2 \frac{\underline{x}_{12} \cdot \underline{x}_{20}}{\underline{x}_{12}^2} - 1 \right) \right. \right. \\
 & \left. \left. - 2 \frac{\underline{x}_{20}^i \underline{x}_{20}^k}{\underline{x}_{20}^4} \right] g \int_{-\infty}^{\infty} dz^- z^- U_2[\infty, z^-] \mathcal{F}_{-k} U_2[z^-, -\infty] + \left[\epsilon^{in} \frac{\underline{x}_{20}^n}{\underline{x}_{20}^2} - 2 \underline{x}_{12}^i \frac{\underline{x}_{12} \times \underline{x}_{20}}{\underline{x}_{12}^2 \underline{x}_{20}^2} \right] \frac{is}{P^+} U_2^{\text{Pol}[1]} - (\underline{x}_0 \rightarrow \underline{x}_1) \right\}^{ab}. \tag{5.81}
 \end{aligned}$$

From this result we see that at small x the helicity evolution operator

$$\int_{-\infty}^{\infty} dz^- z^- V_{\underline{x}}[\infty, z^-] F_{-k} V_{\underline{x}}[z^-, -\infty]$$

mixes with the adjoint version of the same operator and with $U_2^{\text{Pol}[1]}$. We can finally use eq. (5.52) and write the sum of all the diagrams in figure 5 as a single evolution equation¹⁷

$$\begin{aligned}
 & \frac{1}{2N_c} \left\langle \left\langle \text{tr} \left[V_0^\dagger V_1^{iG[2]} \right] + \text{c.c.} \right\rangle \right\rangle (\sigma) = \frac{1}{2N_c} \left\langle \left\langle \text{tr} \left[V_0^\dagger V_1^{iG[2]} \right] + \text{c.c.} \right\rangle \right\rangle_0 (\sigma) \\
 & + \frac{\alpha_s N_c}{4\pi^2} \int_{\sigma'} \frac{dp^-}{p^-} \int d^2 \underline{x}_2 \left\{ \left[\epsilon^{ij} \frac{\underline{x}_{21}^j}{\underline{x}_{21}^2} - \epsilon^{ij} \frac{\underline{x}_{20}^j}{\underline{x}_{20}^2} + 2 \underline{x}_{21}^i \frac{\underline{x}_{21} \times \underline{x}_{20}}{\underline{x}_{12}^2 \underline{x}_{20}^2} \right] \frac{1}{N_c^2} \left\langle \left\langle \text{tr} \left[t^b V_0^\dagger t^a V_1 \right] (U_2^{\text{Pol}[1]})^{ab} + \text{c.c.} \right\rangle \right\rangle (\sigma') \right. \\
 & + \left[\delta^{ij} \left(3 \frac{1}{\underline{x}_{21}^2} - 2 \frac{\underline{x}_{21} \cdot \underline{x}_{20}}{\underline{x}_{12}^2 \underline{x}_{20}^2} - \frac{1}{\underline{x}_{20}^2} \right) - 2 \frac{\underline{x}_{21}^i \underline{x}_{20}^j}{\underline{x}_{12}^2 \underline{x}_{20}^2} \left(2 \frac{\underline{x}_{21} \cdot \underline{x}_{20}}{\underline{x}_{20}^2} + 1 \right) + 2 \frac{\underline{x}_{21}^i \underline{x}_{21}^j}{\underline{x}_{21}^2 \underline{x}_{20}^2} \left(2 \frac{\underline{x}_{21} \cdot \underline{x}_{20}}{\underline{x}_{21}^2} + 1 \right) \right. \\
 & \left. + 2 \frac{\underline{x}_{20}^i \underline{x}_{20}^j}{\underline{x}_{20}^4} - 2 \frac{\underline{x}_{21}^i \underline{x}_{21}^j}{\underline{x}_{21}^4} \right] \frac{1}{N_c^2} \left\langle \left\langle \text{tr} \left[t^b V_0^\dagger t^a V_1 \right] (U_2^{jG[2]})^{ab} + \text{c.c.} \right\rangle \right\rangle (\sigma') - (\underline{x}_0 \rightarrow \underline{x}_1) \left. \right\} \\
 & + \frac{\alpha_s N_c}{2\pi^2} \int_{\sigma'} \frac{dp^-}{p^-} \int d^2 \underline{x}_2 \frac{\underline{x}_{10}^2}{\underline{x}_{21}^2 \underline{x}_{20}^2} \left\{ \frac{1}{N_c^2} \left\langle \left\langle \text{tr} \left[t^b V_0^\dagger t^a V_1^{iG[2]} \right] (U_2)^{ab} \right\rangle \right\rangle (\sigma') - \frac{C_F}{N_c^2} \left\langle \left\langle \text{tr} \left[V_0^\dagger V_1^{iG[2]} \right] \right\rangle \right\rangle (\sigma') + \text{c.c.} \right\}, \tag{5.82}
 \end{aligned}$$

where the last line is the sum of the eikonal diagrams, see the discussion after eq. (5.68). After a trivial change of variables we find a complete agreement with eq. (4.26) above. A similar calculation employing the background field method in the adjoint representation yields the helicity evolution equation (4.27).

6 Small- x asymptotics of the quark and gluon helicity distributions and g_1 structure function in the large- N_c limit

As can be seen in eqs. (3.25), (3.26), (3.50), (3.52) and (3.61), gluon and quark helicity TMD and PDF, together with the g_1 structure function, can be determined for small x using the polarized dipole amplitudes. In particular, the small- x asymptotics of the former will have the same intercepts as the large- zs asymptotics of the latter. In the large- N_c limit considered in this section, the polarized dipole amplitudes, $G(x_{10}^2, zs)$ and $G_2(x_{10}^2, zs)$, can be specified by solving eqs. (4.53). Since, at large N_c , $Q(x_{10}^2, zs) \approx G(x_{10}^2, zs)$, knowing G

¹⁷Here we also explicitly introduce the limits for the integral over p^- .

and G_2 gives us all the flavor-singlet helicity PDFs and TMDs, along with the g_1 structure function. Owing to the complicated form of eqs. (4.53), we solve the system numerically.

As mentioned above, we begin by examining the asymptotic forms of $G(x_{10}^2, zs)$ and $G_2(x_{10}^2, zs)$ as zs grows large. As discussed in [31, 37], it is more convenient to express eqs. (4.53) in terms of

$$\begin{aligned} \eta &= \sqrt{\frac{\alpha_s N_c}{2\pi}} \ln \frac{zs}{\Lambda^2}, & \eta' &= \sqrt{\frac{\alpha_s N_c}{2\pi}} \ln \frac{z's}{\Lambda^2} & \text{and} & & \eta'' &= \sqrt{\frac{\alpha_s N_c}{2\pi}} \ln \frac{z''s}{\Lambda^2}, \\ s_{10} &= \sqrt{\frac{\alpha_s N_c}{2\pi}} \ln \frac{1}{x_{10}^2 \Lambda^2}, & s_{21} &= \sqrt{\frac{\alpha_s N_c}{2\pi}} \ln \frac{1}{x_{21}^2 \Lambda^2} & \text{and} & & s_{32} &= \sqrt{\frac{\alpha_s N_c}{2\pi}} \ln \frac{1}{x_{32}^2 \Lambda^2}. \end{aligned} \quad (6.1)$$

In terms of these parameters, eqs. (4.53), with the help of eq. (4.81), can be written as

$$G(s_{10}, \eta) = G^{(0)}(s_{10}, \eta) + \int_{s_{10}}^{\eta} d\eta' \int_{s_{10}}^{\eta'} ds_{21} \left[\Gamma(s_{10}, s_{21}, \eta') + 3G(s_{21}, \eta') \right. \\ \left. + 2G_2(s_{21}, \eta') + 2\Gamma_2(s_{10}, s_{21}, \eta') \right], \quad (6.2a)$$

$$\Gamma(s_{10}, s_{21}, \eta') = G^{(0)}(s_{10}, \eta') + \int_{s_{10}}^{\eta'} d\eta'' \int_{\max[s_{10}, s_{21} + \eta'' - \eta']}^{\eta''} ds_{32} \left[\Gamma(s_{10}, s_{32}, \eta'') + 3G(s_{32}, \eta'') \right. \\ \left. + 2G_2(s_{32}, \eta'') + 2\Gamma_2(s_{10}, s_{32}, \eta'') \right], \quad (6.2b)$$

$$G_2(s_{10}, \eta) = G_2^{(0)}(s_{10}, \eta) + 2 \int_0^{s_{10}} ds_{21} \int_{s_{21}}^{\eta - s_{10} + s_{21}} d\eta' [G(s_{21}, \eta') + 2G_2(s_{21}, \eta')], \quad (6.2c)$$

$$\Gamma_2(s_{10}, s_{21}, \eta') = G_2^{(0)}(s_{10}, \eta') + 2 \int_0^{s_{10}} ds_{32} \int_{s_{32}}^{\eta' - s_{21} + s_{32}} d\eta'' [G(s_{32}, \eta'') + 2G_2(s_{32}, \eta'')], \quad (6.2d)$$

where the ordering $0 \leq s_{10} \leq s_{21} \leq \eta'$ is assumed in eqs. (6.2b) and (6.2d). This is the only region where Γ and Γ_2 appear in any large- N_c evolution kernel.

Now, we discretize the integrals in eqs. (6.2) with step size δ both in η and s_{10} directions. We express the discretized version of the dipole amplitudes such that

$$\begin{aligned} G_{ij} &= G(i\delta, j\delta), & \Gamma_{ikj} &= \Gamma(i\delta, k\delta, j\delta), \\ G_{2,ij} &= G_2(i\delta, j\delta), & \Gamma_{2,ikj} &= \Gamma_2(i\delta, k\delta, j\delta). \end{aligned} \quad (6.3)$$

With all the definitions outlined above, we obtain the following discretized evolution equa-

tions.

$$G_{ij} = G_{ij}^{(0)} + \delta^2 \sum_{j'=i}^{j-1} \sum_{i'=i}^{j'} [\Gamma_{ii'j'} + 3G_{i'j'} + 2G_{2,i'j'} + 2\Gamma_{2,ii'j'}], \quad (6.4a)$$

$$\Gamma_{ikj} = G_{ij}^{(0)} + \delta^2 \sum_{j'=i}^{j-1} \sum_{i'=\max[i, k+j'-j]}^{j'} [\Gamma_{ii'j'} + 3G_{i'j'} + 2G_{2,i'j'} + 2\Gamma_{2,ii'j'}], \quad (6.4b)$$

$$G_{2,ij} = G_{2,ij}^{(0)} + 2\delta^2 \sum_{i'=0}^{i-1} \sum_{j'=i'}^{j-i+i'} [G_{i'j'} + 2G_{2,i'j'}], \quad (6.4c)$$

$$\Gamma_{2,ikj} = G_{2,ij}^{(0)} + 2\delta^2 \sum_{i'=0}^{i-1} \sum_{j'=i'}^{j-k+i'} [G_{i'j'} + 2G_{2,i'j'}]. \quad (6.4d)$$

To obtain the values of G_{ij} and $G_{2,ij}$ for $0 \leq i \leq i_{\max}$ and $0 \leq j \leq j_{\max}$, we only need to know the following dipole amplitudes:

- G_{ij} and $G_{2,ij}$ such that $0 \leq i < j$, with $i \leq i_{\max}$ and $j \leq j_{\max}$. Note that if $i \geq j$, then we have $G_{ij} = G_{ij}^{(0)}$ and $G_{2,ij} = G_{2,ij}^{(0)}$, as can be seen from eq. (6.4a) and eq. (6.4c).
- Γ_{ikj} and $\Gamma_{2,ikj}$ such that $0 \leq i \leq k \leq j$, with $k \leq i_{\max}$ and $j \leq j_{\max}$. This is because the neighbor dipole amplitudes only appear in eqs. (6.4a) and (6.4b).

In a fashion similar to [37], the numerical computation becomes more efficient once we realize the following recursive relations that follow directly from eqs. (6.4) for $j > 0$:

$$G_{ij} = \begin{cases} G_{ij}^{(0)} - G_{i(j-1)}^{(0)} + G_{i(j-1)} + \delta^2 \sum_{i'=i}^{j-1} [\Gamma_{ii'(j-1)} + 3G_{i'(j-1)} + 2G_{2,i'(j-1)} + 2\Gamma_{2,ii'(j-1)}] & , i < j \\ G_{ij}^{(0)} & , i = j \end{cases}, \quad (6.5a)$$

$$\Gamma_{ikj} = \begin{cases} G_{ij}^{(0)} - G_{i(j-1)}^{(0)} + \Gamma_{i(k-1)(j-1)} + \delta^2 \sum_{i'=k-1}^{j-1} [\Gamma_{ii'(j-1)} + 3G_{i'(j-1)} + 2G_{2,i'(j-1)} + 2\Gamma_{2,ii'(j-1)}] & , i < k \\ G_{ij} & , i = k \end{cases}, \quad (6.5b)$$

$$G_{2,ij} = \begin{cases} G_{2,ij}^{(0)} - G_{2,i(j-1)}^{(0)} + G_{2,i(j-1)} + 2\delta^2 \sum_{i'=0}^{i-1} [G_{i'(i'+j-i)} + 2G_{2,i'(i'+j-i)}] & , i < j \\ G_{2,ij}^{(0)} & , i = j \end{cases}, \quad (6.5c)$$

$$\Gamma_{2,ikj} = \begin{cases} G_{2,ij}^{(0)} - G_{2,i(j-1)}^{(0)} + \Gamma_{2,i(k-1)(j-1)} & , i < k \\ G_{2,ij} & , i = k \end{cases}. \quad (6.5d)$$

In the case where $j = 0$, each of the dipole amplitudes simply equals its corresponding inhomogeneous term, as can be seen from eqs. (6.4).

In order to perform the numerical computation, we also need to rewrite the non-homogeneous terms, eq. (4.54), in terms of the new variables, s_{10} and η . This gives

$$G^{(0)}(s_{10}, \eta) = \frac{\alpha_s^2 C_F}{2N_c} \pi \sqrt{\frac{2\pi}{\alpha_s N_c}} [C_F \eta - 2(\eta - s_{10})] \Rightarrow G_{ij}^{(0)} = \frac{\alpha_s^2 C_F}{2N_c} \pi \sqrt{\frac{2\pi}{\alpha_s N_c}} [(C_F - 2)j + 2i] \delta, \quad (6.6a)$$

$$G_2^{(0)}(s_{10}, \eta) = \frac{\alpha_s^2 C_F}{2N_c} \pi \sqrt{\frac{2\pi}{\alpha_s N_c}} s_{10} \Rightarrow G_{2,ij}^{(0)} = \frac{\alpha_s^2 C_F}{2N_c} \pi \sqrt{\frac{2\pi}{\alpha_s N_c}} i \delta. \quad (6.6b)$$

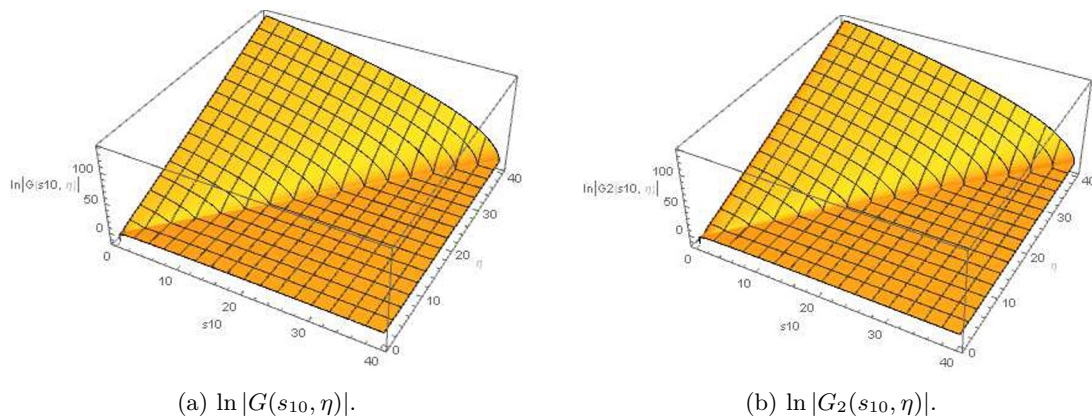


Figure 6. The plots of logarithms of the absolute values of the two polarized dipole amplitudes G and G_2 versus s_{10} and η , for the $0 \leq s_{10}, \eta \leq \eta_{\max} = 40$ range. The amplitudes are computed numerically using step size $\delta = 0.05$. The inhomogeneities near the $\eta = s_{10}$ line result from the Born initial conditions and the discretization error.

In particular, in terms of the discrete variables, i and j , the one-step differences of the non-homogeneous terms are

$$G_{ij}^{(0)} - G_{i(j-1)}^{(0)} = \frac{\alpha_s^2 C_F}{2N_c} \pi \sqrt{\frac{2\pi}{\alpha_s N_c}} (C_F - 2) \delta, \quad G_{2,ij}^{(0)} - G_{2,i(j-1)}^{(0)} = 0. \quad (6.7)$$

Now, we numerically compute all the dipole amplitudes in eqs. (6.5) with the help of eq. (6.7), using the step size of $\delta = 0.05$. In the range where $0 \leq \eta, s_{10} \leq \eta_{\max} = 40$, the logarithms of $G(x_{10}^2, zs)$ and $G_2(x_{10}^2, zs)$ are plotted in figure 6. From the plots, we see that both amplitudes grow roughly linearly with $\eta - s_{10}$, which corresponds to an exponential growth in zsx_{10}^2 . Mild deviations from the aforementioned pattern, including the inhomogeneities along $\eta = s_{10}$ line, likely result from discretization errors. However, their actual cause must be determined with certainty through an analytic solution.

As mentioned previously, for the purpose of this section, it is sufficient for us to determine the asymptotic form of $G(s_{10} = 0, \eta)$ and $G_2(s_{10} = 0, \eta)$ as $\eta \rightarrow \infty$. To do so, we plot the logarithm of each amplitude at $s_{10} = 0$ against η . These plots are shown in figure 7. As expected, both functions increase linearly once we get sufficiently far away from $\eta = 0$, where the non-homogeneous term and the discretization error remain relatively significant. This justifies the following *ansatze* as $\eta \rightarrow \infty$,

$$G(s_{10} = 0, \eta) \sim e^{\alpha_h \eta \sqrt{\frac{2\pi}{\alpha_s N_c}}}, \quad G_2(s_{10} = 0, \eta) \sim e^{\alpha_{h,2} \eta \sqrt{\frac{2\pi}{\alpha_s N_c}}}, \quad (6.8)$$

where α_h and $\alpha_{h,2}$ are given by the slopes of the functions in figures 7a and 7b, respectively. Since the exponential growth is more dominant at larger η 's, we deduce the approximation of α_h and $\alpha_{h,2}$ for this step size, δ , and maximum rapidity, η_{\max} , by regressing $\ln [G(0, \eta)]$ and $\ln [G_2(0, \eta)]$, respectively, on η over the range where $0.75 \eta_{\max} \leq \eta \leq \eta_{\max}$. For example, at $\delta = 0.05$ and $\eta_{\max} = 40$, corresponding to figure 7, we obtain $\alpha_h = (3.6825 \pm 0.0002) \sqrt{\frac{\alpha_s N_c}{2\pi}}$ and $\alpha_{h,2} = (3.6821 \pm 0.0002) \sqrt{\frac{\alpha_s N_c}{2\pi}}$. The uncertainty is estimated from the residual of linear regression performed on $\ln [G(0, \eta)]$ or $\ln [G_2(0, \eta)]$ at 95% confidence level.

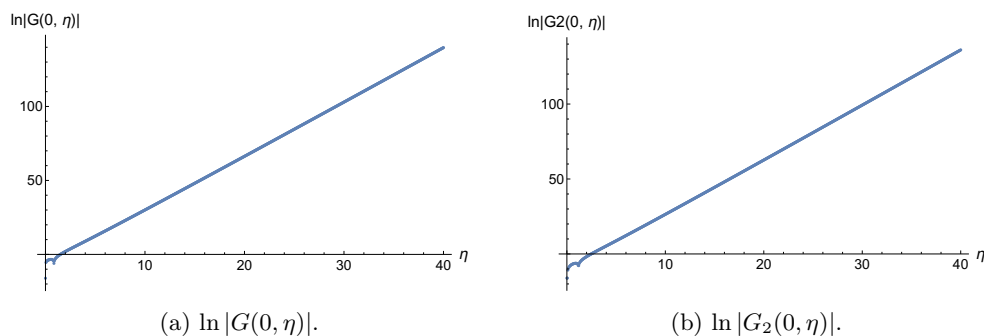


Figure 7. The plots of logarithms of the absolute values of the two polarized dipole amplitudes at $s_{10} = 0$ versus η , for the $0 \leq \eta \leq \eta_{\max} = 40$ range. The amplitudes are computed numerically using step size $\delta = 0.05$. The kinks near $\eta = 0$ occur due to sign flips in $G(0, \eta)$ and $G_2(0, \eta)$. By eqs. (6.6), the Born initial condition leads to $G_{0j}^{(0)} < 0$ for $G(0, \eta)$ at any $j > 0$.

| δ | 0.0125 | 0.016 | 0.025 | 0.032 | 0.0375 | 0.05 | 0.0625 | 0.075 | 0.08 | 0.1 |
|-------------|--------|-------|-------|-------|--------|------|--------|-------|------|-----|
| $M(\delta)$ | 10 | 10 | 20 | 20 | 30 | 40 | 50 | 60 | 60 | 70 |

Table 1. The maximum, $M(\delta)$, of η_{\max} computed for each step size, δ .

Having estimated the intercepts, α_h and $\alpha_{h,2}$, at $\delta = 0.05$ and $\eta_{\max} = 40$, we then repeat the steps for other choices of δ and η_{\max} . In particular, for each step size, δ , we numerically compute the intercepts for $\eta_{\max} \in \{10, 20, \dots, M(\delta)\}$, where $M(\delta)$ is given in table 1 for each δ employed in this work.

Now, we obtain the estimated intercepts and their uncertainties for all 37 combinations of δ and η_{\max} . Since the continuum limit corresponds to $\delta \rightarrow 0$ and $\eta_{\max} \rightarrow \infty$, we attempt to model the intercepts using δ and $1/\eta_{\max}$ as independent variables. Afterward, with the correct model at hand, we will be able to predict the intercepts at $\delta = 1/\eta_{\max} = 0$ and use them as our best estimate for the actual intercepts in the continuum limit.

In what follows, we will detail our process to determine the intercept, α_h , in the continuum limit. The process for $\alpha_{h,2}$ will be similar. Inspired by the success of [31] in numerically estimating the correct intercept as verified by the analytic solution [32], we employ polynomial regression models of various degrees, with interaction terms included, weighted by the uncertainties of the estimated intercepts. In particular, we consider four following nested models with increasing maximum polynomial degrees:

- Model 1: $\alpha_h = a_1$,
- Model 2: $\alpha_h = a_1 + a_2\delta + \frac{a_3}{\eta_{\max}}$,
- Model 3: $\alpha_h = a_1 + a_2\delta + \frac{a_3}{\eta_{\max}} + a_4\delta^2 + \frac{a_5\delta}{\eta_{\max}} + \frac{a_6}{\eta_{\max}^2}$,
- Model 4: $\alpha_h = a_1 + a_2\delta + \frac{a_3}{\eta_{\max}} + a_4\delta^2 + \frac{a_5\delta}{\eta_{\max}} + \frac{a_6}{\eta_{\max}^2} + a_7\delta^3 + \frac{a_8\delta^2}{\eta_{\max}} + \frac{a_9\delta}{\eta_{\max}^2} + \frac{a_{10}}{\eta_{\max}^3}$.

Once we fit and evaluate all four models to our numerical estimates for α_h , the Akaike information criterion (AIC) [125] decreases significantly from model 1 to model 2 and from model 2 to model 3. However, the AIC is roughly equal for models 3 and 4. Furthermore,

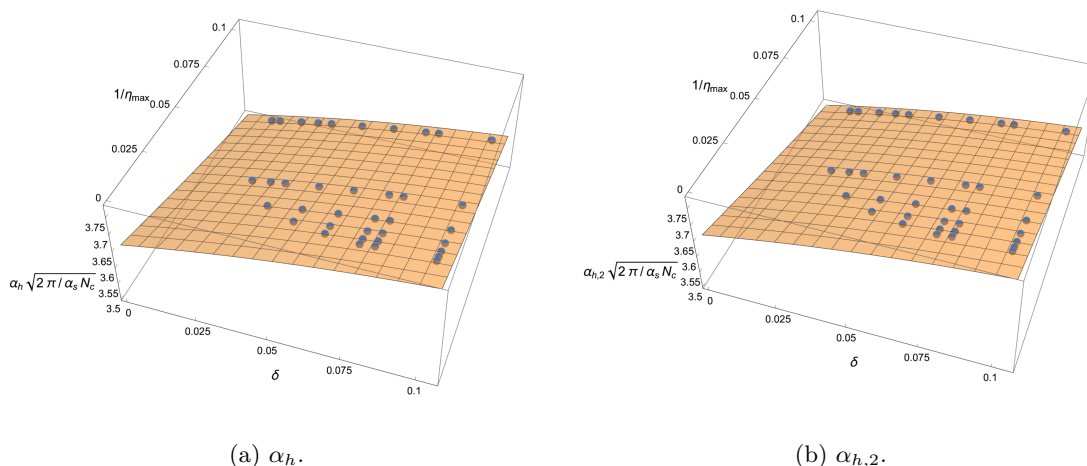


Figure 8. The plots of estimated intercepts, α_h and $\alpha_{h,2}$, at each δ and $1/\eta_{\max}$ (blue dots), together with the best-fitted quadratic surface given by eq. (6.9) (yellow surfaces). The continuum limit, $\delta = 1/\eta_{\max} = 0$, corresponds to the lower-left corner of each plot.

the parameters a_7 , a_8 , a_9 and a_{10} are all insignificant when the t -test is performed at 10% significance level for each of them. This implies that all degree-3 terms in model 4 are not significantly different from zero, that is, model 4 would not account for our intercept results any better than model 3. Together with the fact that all parameters for model 3 are significant, we decide to use model 3, the quadratic model, to fit the values of α_h . The process and, more importantly, the conclusion about the final model choice are exactly the same for $\alpha_{h,2}$, although the resulting parameter values are slightly different.

With model 3, the estimated relation between each intercept and δ and $1/\eta_{\max}$ are given by

$$\alpha_h = \left[3.661 + 1.503\delta - 1.740(1/\eta_{\max}) - 4.414\delta^2 + 0.116\delta(1/\eta_{\max}) + 1.429(1/\eta_{\max})^2 \right] \sqrt{\frac{\alpha_s N_c}{2\pi}}, \quad (6.9a)$$

$$\alpha_{h,2} = \left[3.660 + 1.509\delta - 1.734(1/\eta_{\max}) - 4.438\delta^2 - 0.034\delta(1/\eta_{\max}) + 0.873(1/\eta_{\max})^2 \right] \sqrt{\frac{\alpha_s N_c}{2\pi}}. \quad (6.9b)$$

The estimated quadratic surfaces are plotted together with the intercepts we computed previously for various combinations of δ and $1/\eta_{\max}$ in figure 8.

Next, we compute the continuum-limit intercepts, whose estimated values are the first terms in the right-hand sides of eq. (6.9). The uncertainties are estimated while taking into account both the residuals of the quadratic model and the uncertainties of each data point, i.e., intercept estimated at each δ and $1/\eta_{\max}$. This gives

$$\alpha_h = (3.661 \pm 0.006) \sqrt{\frac{\alpha_s N_c}{2\pi}}, \quad \alpha_{h,2} = (3.660 \pm 0.009) \sqrt{\frac{\alpha_s N_c}{2\pi}}. \quad (6.10)$$

Recall that the uncertainties in eq. (6.10) come from (i) the residual of linear regression performed on $\ln |G(0, \eta)|$ and $\ln |G_2(0, \eta)|$ at each δ and η_{\max} , and (ii) the residual of polynomial regression performed on α_h and $\alpha_{h,2}$.

Now, the pure-gluon BER intercept can be shown to be

$$\alpha_h = \sqrt{\frac{17 + \sqrt{97}}{2}} \sqrt{\frac{\alpha_s N_c}{2\pi}} \approx 3.664 \sqrt{\frac{\alpha_s N_c}{2\pi}} \quad (6.11)$$

by solving the corresponding IREE from [5] analytically [2]. Eq. (6.11) agrees with both α_h and $\alpha_{h,2}$ from eq. (6.10), within the uncertainties. While the construction of an analytic solution for eqs. (4.53) is left for future work, eq. (6.11) already provides us with the analytic expression for the intercept.

Finally, employing eqs. (6.8) and (6.10) in eqs. (3.26), (3.50) and (3.62), we obtain the following small- x asymptotics for the quark and gluon helicity PDF, together with the g_1 structure function:

$$\Delta\Sigma(x, Q^2) \sim \Delta G(x, Q^2) \sim g_1(x, Q^2) \sim \left(\frac{1}{x}\right)^{3.66 \sqrt{\frac{\alpha_s N_c}{2\pi}}}. \quad (6.12)$$

7 Conclusions and outlook

Let us summarize what we have accomplished here. We have extended the helicity evolution formalism of [1–3, 31–33, 36, 37, 40] to include the sub-eikonal operator $\overleftarrow{D} D^i$ (or, equivalently, $D^i - \overleftarrow{D}$). This generalized the small- x evolution equations for the relevant sub-eikonal operators $D^i - \overleftarrow{D}$, F^{12} , and $\bar{\psi}\gamma^+\gamma^5\psi$ to those in eqs. (4.15), (4.19), (4.26), and (4.27). The corresponding DLA evolution equations are given by eqs. (4.53) and (4.75) in the large- N_c and large- $N_c\&N_f$ limits, respectively. We demonstrated that the large- N_c equations agree with the spin-dependent DGLAP evolution at small x including up to three loops in the splitting function. We solved these equations numerically showing that the resulting asymptotics of the gluon and flavor-singlet quark helicity distributions, along with the g_1 structure function, are given by eq. (6.12) and agree with that found by BER [5] in the pure-gluon case. We have thus completed the construction of the DLA helicity evolution equations at small- x in the s -channel/shock wave formalism, which we also refer to as the light-cone operator treatment (LCOT). We have also cross-checked the LCOT calculation using the background field method and found a full agreement between the two.

The future steps of working with this now-complete LCOT formalism include solving the large- $N_c\&N_f$ equations (4.75) and comparing the solution to those found in [5] and in [37]. The two solutions in [5] and [37] have a qualitatively different dependence on x : the latter exhibits sign-changing oscillations with $\ln(1/x)$, while the former changes sign only once with decreasing x . It would be important to identify which, if any, of those behaviours are exhibited by the solution of eqs. (4.75).

In the effort to go beyond the large- N_c and large- $N_c\&N_f$ limits, a helicity version of the Jalilian-Marian-Iancu-McLerran-Weigert-Leonidov-Kovner (JIMWLK) [48–53] evolution was constructed in [36], also without taking the operator $\overleftarrow{D} D^i$ into account. The helicity JIMWLK kernel from [36] also needs to be extended to include the effects of this operator. The initial conditions for the helicity JIMWLK evolution are given by the

helicity-dependent version of the McLerran-Venugopalan (MV) model [100–102] derived in [38], which may also have to be extended to include the terms into the weight functional needed for the calculations of the expectation value of the $D^i - \overleftarrow{D}^i$ operator.

To further improve the precision of helicity evolution one should go beyond the DLA limit. This was attempted in [40] using the earlier s -channel helicity formalism of [1–3, 31–33, 36, 37]. In addition to resumming all the DLA and SLA_L terms, the evolution equations constructed in [40] sum up all the single logarithmic corrections coming from the UV transverse integrals. These corrections were labeled SLA_T in [40]. It remains to be seen whether the results of [40] can simply be added to the equations obtained in this work for a complete DLA+SLA helicity evolution at small x . It appears likely that the IR transverse logarithms need to be resummed as well, such that an interfacing of our evolution found above with the full spin-dependent DGLAP equation may also be needed for the DLA+SLA helicity evolution.

Last but not least, the helicity formalism of [1–3, 31] has recently been used to successfully describe the world data on the proton and neutron g_1 structure functions at small x [22]. This was the first-ever helicity phenomenology work based on small- x evolution only, not taken as an improvement of the DGLAP anomalous dimension [28, 29]. It would be interesting and important to see how much the conclusions of [22] would be affected by the corrections included in this work. At the very least, the formalism presented here would allow for a natural inclusion of the gluon helicity PDF (3.26) into the calculation. The fact that the intercept/power of x in eq. (6.12) is larger than that given by the evolution in [1–3, 31–33, 36, 37] may generate more quark and gluon spin at small x , while simultaneously challenging the convergence of the integrals in eqs. (1.2) at small x . The latter problem may be addressed by including saturation corrections (non-trivial unpolarized dipole S -matrices) and/or running of the coupling constant in the kernels of our helicity evolution.

Acknowledgments

One of the authors (Y.K.) would like to thank Bob Jaffe and Cedric Lorcé for discussions of the Jaffe-Manohar distribution and its role in small- x evolution. A.T. would like to thank Ian Balitsky and Raju Venugopalan for useful and inspiring conversations. Y.T. would like to thank Daniel Adamiak for discussions leading to important corrections to the results and great insights to the next steps.

This material is based upon work supported by the U.S. Department of Energy, Office of Science, Office of Nuclear Physics under Award Number DE-SC0004286.

The work is performed within the framework of the TMD Topical Collaboration.

The work of F.C. has been supported by the Academy of Finland, by the Centre of Excellence in Quark Matter and project 321840, and under the European Union’s Horizon 2020 research and innovation programme by the STRONG-2020 project (grant agreement No 824093) and by the European Research Council, grant agreement ERC-2015-CoG-681707. The content of this article does not reflect the official opinion of the European Union and responsibility for the information and views expressed therein lies entirely with the authors.

A Schwinger's notation

In this appendix, we introduce the Schwinger's notation that we use for the quark and gluon propagators in section 5. Following Schwinger [126], we consider the coherent states $|x\rangle$ and $|p\rangle$ which are eigenvectors of the position and momentum operators,

$$\hat{x}_\mu|x\rangle = x_\mu|x\rangle, \quad \hat{p}_\mu|p\rangle = p_\mu|p\rangle. \quad (\text{A.1})$$

The states define a particle with position x and momentum p , respectively, and satisfy the completeness

$$\int d^4x|x\rangle\langle x| = 1, \quad \int \frac{d^4p}{(2\pi)^4}|p\rangle\langle p| = 1, \quad (\text{A.2})$$

and orthogonality

$$\langle x|p\rangle = e^{-ipx}, \quad \langle p|x\rangle = e^{ipx}, \quad \langle x|y\rangle = \delta^4(x-y), \quad \langle p|q\rangle = (2\pi)^4\delta^4(p-q) \quad (\text{A.3})$$

relations.

For an arbitrary function of the momentum operator, we have

$$\langle x|f(\hat{p})|y\rangle = \int \frac{d^4q}{(2\pi)^4} \langle x|f(\hat{p})|q\rangle \langle q|y\rangle = \int \frac{d^4q}{(2\pi)^4} f(q) e^{-iq(x-y)}. \quad (\text{A.4})$$

In particular, this motivates the following representation for the scalar propagator:

$$\langle x|\frac{1}{\hat{p}^2 + i\epsilon}|y\rangle = \int \frac{d^4p}{(2\pi)^4} \frac{1}{p^2 + i\epsilon} e^{-ip(x-y)}. \quad (\text{A.5})$$

Similarly, for an arbitrary function of the position operator $f(\hat{x})|x\rangle = f(x)|x\rangle$. As a result, for the Wilson line operator

$$\hat{V} \equiv \mathcal{P} \exp \left[ig \int_{-\infty}^{\infty} dx^- A^+(x^-, \hat{x}) \right], \quad (\text{A.6})$$

we write

$$\hat{V}|\underline{x}\rangle = V_{\underline{x}}|\underline{x}\rangle. \quad (\text{A.7})$$

Note that, for brevity, in the main text of the paper we omit the hat symbol over the position and momentum operators.

Open Access. This article is distributed under the terms of the Creative Commons Attribution License ([CC-BY 4.0](https://creativecommons.org/licenses/by/4.0/)), which permits any use, distribution and reproduction in any medium, provided the original author(s) and source are credited. SCOAP³ supports the goals of the International Year of Basic Sciences for Sustainable Development.

References

- [1] Y.V. Kovchegov, D. Pitonyak and M.D. Sievert, *Helicity evolution at small- x* , *JHEP* **01** (2016) 072 [Erratum *ibid.* **10** (2016) 148] [[arXiv:1511.06737](#)] [[INSPIRE](#)].
- [2] Y.V. Kovchegov, D. Pitonyak and M.D. Sievert, *Helicity evolution at small- x : flavor singlet and non-singlet observables*, *Phys. Rev. D* **95** (2017) 014033 [[arXiv:1610.06197](#)] [[INSPIRE](#)].
- [3] Y.V. Kovchegov and M.D. Sievert, *Small- x helicity evolution: an operator treatment*, *Phys. Rev. D* **99** (2019) 054032 [[arXiv:1808.09010](#)] [[INSPIRE](#)].
- [4] R.L. Jaffe and A. Manohar, *The g_1 problem: fact and fantasy on the spin of the proton*, *Nucl. Phys. B* **337** (1990) 509 [[INSPIRE](#)].
- [5] J. Bartels, B.I. Ermolaev and M.G. Ryskin, *Flavor singlet contribution to the structure function g_1 at small x* , *Z. Phys. C* **72** (1996) 627 [[hep-ph/9603204](#)] [[INSPIRE](#)].
- [6] C.A. Aidala, S.D. Bass, D. Hasch and G.K. Mallot, *The spin structure of the nucleon*, *Rev. Mod. Phys.* **85** (2013) 655 [[arXiv:1209.2803](#)] [[INSPIRE](#)].
- [7] A. Accardi et al., *Electron ion collider: the next QCD frontier. Understanding the glue that binds us all*, *Eur. Phys. J. A* **52** (2016) 268 [[arXiv:1212.1701](#)] [[INSPIRE](#)].
- [8] E. Leader and C. Lorcé, *The angular momentum controversy: what's it all about and does it matter?*, *Phys. Rept.* **541** (2014) 163 [[arXiv:1309.4235](#)] [[INSPIRE](#)].
- [9] E.C. Aschenauer et al., *The RHIC spin program: achievements and future opportunities*, [arXiv:1304.0079](#) [[INSPIRE](#)].
- [10] E.-C. Aschenauer et al., *The RHIC SPIN program: achievements and future opportunities*, [arXiv:1501.01220](#) [[INSPIRE](#)].
- [11] D. Boer et al., *Gluons and the quark sea at high energies: distributions, polarization, tomography*, [arXiv:1108.1713](#) [[INSPIRE](#)].
- [12] A. Prokudin, Y. Hatta, Y. Kovchegov and C. Marquet eds., *Proceedings, probing nucleons and nuclei in high energy collisions: dedicated to the physics of the electron ion collider: Seattle, WA, U.S.A., 1 October–26 November 2018*, *World Scientific*, Singapore (2020) [[INSPIRE](#)].
- [13] X. Ji, F. Yuan and Y. Zhao, *What we know and what we don't know about the proton spin after 30 years*, *Nature Rev. Phys.* **3** (2021) 27 [[arXiv:2009.01291](#)] [[INSPIRE](#)].
- [14] R. Abdul Khalek et al., *Science requirements and detector concepts for the electron-ion collider: EIC yellow report*, [arXiv:2103.05419](#) [[INSPIRE](#)].
- [15] X.-D. Ji, *Gauge-invariant decomposition of nucleon spin*, *Phys. Rev. Lett.* **78** (1997) 610 [[hep-ph/9603249](#)] [[INSPIRE](#)].
- [16] S. Bashinsky and R.L. Jaffe, *Quark and gluon orbital angular momentum and spin in hard processes*, *Nucl. Phys. B* **536** (1998) 303 [[hep-ph/9804397](#)] [[INSPIRE](#)].
- [17] P. Hagler and A. Schafer, *Evolution equations for higher moments of angular momentum distributions*, *Phys. Lett. B* **430** (1998) 179 [[hep-ph/9802362](#)] [[INSPIRE](#)].
- [18] A. Harindranath and R. Kundu, *On orbital angular momentum in deep inelastic scattering*, *Phys. Rev. D* **59** (1999) 116013 [[hep-ph/9802406](#)] [[INSPIRE](#)].
- [19] Y. Hatta and S. Yoshida, *Twist analysis of the nucleon spin in QCD*, *JHEP* **10** (2012) 080 [[arXiv:1207.5332](#)] [[INSPIRE](#)].

- [20] X. Ji, X. Xiong and F. Yuan, *Probing parton orbital angular momentum in longitudinally polarized nucleon*, *Phys. Rev. D* **88** (2013) 014041 [[arXiv:1207.5221](#)] [[INSPIRE](#)].
- [21] J.J. Ethier, N. Sato and W. Melnitchouk, *First simultaneous extraction of spin-dependent parton distributions and fragmentation functions from a global QCD analysis*, *Phys. Rev. Lett.* **119** (2017) 132001 [[arXiv:1705.05889](#)] [[INSPIRE](#)].
- [22] JEFFERSON LAB ANGULAR MOMENTUM collaboration, *First analysis of world polarized DIS data with small- x helicity evolution*, *Phys. Rev. D* **104** (2021) L031501 [[arXiv:2102.06159](#)] [[INSPIRE](#)].
- [23] J. Bartels, B.I. Ermolaev and M.G. Ryskin, *Nonsinglet contributions to the structure function g_1 at small x* , *Z. Phys. C* **70** (1996) 273 [[hep-ph/9507271](#)] [[INSPIRE](#)].
- [24] R. Kirschner and L.N. Lipatov, *Double logarithmic asymptotics and Regge singularities of quark amplitudes with flavor exchange*, *Nucl. Phys. B* **213** (1983) 122 [[INSPIRE](#)].
- [25] R. Kirschner, *Reggeon interactions in perturbative QCD*, *Z. Phys. C* **65** (1995) 505 [[hep-th/9407085](#)] [[INSPIRE](#)].
- [26] R. Kirschner, *Regge asymptotics of scattering with flavor exchange in QCD*, *Z. Phys. C* **67** (1995) 459 [[hep-th/9404158](#)] [[INSPIRE](#)].
- [27] S. Griffiths and D.A. Ross, *Studying the perturbative Reggeon*, *Eur. Phys. J. C* **12** (2000) 277 [[hep-ph/9906550](#)] [[INSPIRE](#)].
- [28] J. Blumlein and A. Vogt, *On the behavior of nonsinglet structure functions at small x* , *Phys. Lett. B* **370** (1996) 149 [[hep-ph/9510410](#)] [[INSPIRE](#)].
- [29] J. Blümlein and A. Vogt, *The singlet contribution to the structure function $g_1(x, Q^2)$ at small x* , *Phys. Lett. B* **386** (1996) 350 [[hep-ph/9606254](#)] [[INSPIRE](#)].
- [30] Y. Hatta, Y. Nakagawa, F. Yuan, Y. Zhao and B. Xiao, *Gluon orbital angular momentum at small- x* , *Phys. Rev. D* **95** (2017) 114032 [[arXiv:1612.02445](#)] [[INSPIRE](#)].
- [31] Y.V. Kovchegov, D. Pitonyak and M.D. Sievert, *Small- x asymptotics of the quark helicity distribution*, *Phys. Rev. Lett.* **118** (2017) 052001 [[arXiv:1610.06188](#)] [[INSPIRE](#)].
- [32] Y.V. Kovchegov, D. Pitonyak and M.D. Sievert, *Small- x asymptotics of the quark helicity distribution: analytic results*, *Phys. Lett. B* **772** (2017) 136 [[arXiv:1703.05809](#)] [[INSPIRE](#)].
- [33] Y.V. Kovchegov, D. Pitonyak and M.D. Sievert, *Small- x asymptotics of the gluon helicity distribution*, *JHEP* **10** (2017) 198 [[arXiv:1706.04236](#)] [[INSPIRE](#)].
- [34] Y.V. Kovchegov, *Orbital angular momentum at small x* , *JHEP* **03** (2019) 174 [[arXiv:1901.07453](#)] [[INSPIRE](#)].
- [35] R. Boussarie, Y. Hatta and F. Yuan, *Proton spin structure at small- x* , *Phys. Lett. B* **797** (2019) 134817 [[arXiv:1904.02693](#)] [[INSPIRE](#)].
- [36] F. Cougoulic and Y.V. Kovchegov, *Helicity-dependent generalization of the JIMWLK evolution*, *Phys. Rev. D* **100** (2019) 114020 [[arXiv:1910.04268](#)] [[INSPIRE](#)].
- [37] Y.V. Kovchegov and Y. Tawabutr, *Helicity at small x : oscillations generated by bringing back the quarks*, *JHEP* **08** (2020) 014 [[arXiv:2005.07285](#)] [[INSPIRE](#)].
- [38] F. Cougoulic and Y.V. Kovchegov, *Helicity-dependent extension of the McLerran-Venugopalan model*, *Nucl. Phys. A* **1004** (2020) 122051 [[arXiv:2005.14688](#)] [[INSPIRE](#)].

- [39] G.A. Chirilli, *High-energy operator product expansion at sub-eikonal level*, *JHEP* **06** (2021) 096 [[arXiv:2101.12744](#)] [[INSPIRE](#)].
- [40] Y.V. Kovchegov, A. Tarasov and Y. Tawabutr, *Helicity evolution at small- x : the single-logarithmic contribution*, *JHEP* **03** (2022) 184 [[arXiv:2104.11765](#)] [[INSPIRE](#)].
- [41] A.H. Mueller, *Soft gluons in the infinite momentum wave function and the BFKL Pomeron*, *Nucl. Phys. B* **415** (1994) 373 [[INSPIRE](#)].
- [42] A.H. Mueller and B. Patel, *Single and double BFKL Pomeron exchange and a dipole picture of high-energy hard processes*, *Nucl. Phys. B* **425** (1994) 471 [[hep-ph/9403256](#)] [[INSPIRE](#)].
- [43] A.H. Mueller, *Unitarity and the BFKL Pomeron*, *Nucl. Phys. B* **437** (1995) 107 [[hep-ph/9408245](#)] [[INSPIRE](#)].
- [44] I. Balitsky, *Operator expansion for high-energy scattering*, *Nucl. Phys. B* **463** (1996) 99 [[hep-ph/9509348](#)] [[INSPIRE](#)].
- [45] I. Balitsky, *Factorization and high-energy effective action*, *Phys. Rev. D* **60** (1999) 014020 [[hep-ph/9812311](#)] [[INSPIRE](#)].
- [46] Y.V. Kovchegov, *Small- x F_2 structure function of a nucleus including multiple Pomeron exchanges*, *Phys. Rev. D* **60** (1999) 034008 [[hep-ph/9901281](#)] [[INSPIRE](#)].
- [47] Y.V. Kovchegov, *Unitarization of the BFKL Pomeron on a nucleus*, *Phys. Rev. D* **61** (2000) 074018 [[hep-ph/9905214](#)] [[INSPIRE](#)].
- [48] J. Jalilian-Marian, A. Kovner and H. Weigert, *The Wilson renormalization group for low x physics: gluon evolution at finite parton density*, *Phys. Rev. D* **59** (1998) 014015 [[hep-ph/9709432](#)] [[INSPIRE](#)].
- [49] J. Jalilian-Marian, A. Kovner, A. Leonidov and H. Weigert, *The Wilson renormalization group for low x physics: towards the high density regime*, *Phys. Rev. D* **59** (1998) 014014 [[hep-ph/9706377](#)] [[INSPIRE](#)].
- [50] H. Weigert, *Unitarity at small Bjorken x* , *Nucl. Phys. A* **703** (2002) 823 [[hep-ph/0004044](#)] [[INSPIRE](#)].
- [51] E. Iancu, A. Leonidov and L.D. McLerran, *The renormalization group equation for the color glass condensate*, *Phys. Lett. B* **510** (2001) 133 [[hep-ph/0102009](#)] [[INSPIRE](#)].
- [52] E. Iancu, A. Leonidov and L.D. McLerran, *Nonlinear gluon evolution in the color glass condensate. 1*, *Nucl. Phys. A* **692** (2001) 583 [[hep-ph/0011241](#)] [[INSPIRE](#)].
- [53] E. Ferreiro, E. Iancu, A. Leonidov and L. McLerran, *Nonlinear gluon evolution in the color glass condensate. 2*, *Nucl. Phys. A* **703** (2002) 489 [[hep-ph/0109115](#)] [[INSPIRE](#)].
- [54] L.V. Gribov, E.M. Levin and M.G. Ryskin, *Semihard processes in QCD*, *Phys. Rept.* **100** (1983) 1 [[INSPIRE](#)].
- [55] E. Iancu and R. Venugopalan, *The color glass condensate and high-energy scattering in QCD*, in *Quark-gluon plasma 4*, R.C. Hwa and X.-N. Wang eds., [World Scientific](#), Singapore (2003), p. 249 [[hep-ph/0303204](#)] [[INSPIRE](#)].
- [56] H. Weigert, *Evolution at small x_{bj} : the color glass condensate*, *Prog. Part. Nucl. Phys.* **55** (2005) 461 [[hep-ph/0501087](#)] [[INSPIRE](#)].
- [57] J. Jalilian-Marian and Y.V. Kovchegov, *Saturation physics and deuteron-gold collisions at RHIC*, *Prog. Part. Nucl. Phys.* **56** (2006) 104 [[hep-ph/0505052](#)] [[INSPIRE](#)].

- [58] F. Gelis, E. Iancu, J. Jalilian-Marian and R. Venugopalan, *The color glass condensate*, *Ann. Rev. Nucl. Part. Sci.* **60** (2010) 463 [[arXiv:1002.0333](#)] [[INSPIRE](#)].
- [59] J.L. Albacete and C. Marquet, *Gluon saturation and initial conditions for relativistic heavy ion collisions*, *Prog. Part. Nucl. Phys.* **76** (2014) 1 [[arXiv:1401.4866](#)] [[INSPIRE](#)].
- [60] Y.V. Kovchegov and E. Levin, *Quantum chromodynamics at high energy*, Cambridge University Press, Cambridge, U.K. (2012).
- [61] A. Morreale and F. Salazar, *Mining for gluon saturation at colliders*, *Universe* **7** (2021) 312 [[arXiv:2108.08254](#)] [[INSPIRE](#)].
- [62] T. Altinoluk, N. Armesto, G. Beuf, M. Martínez and C.A. Salgado, *Next-to-eikonal corrections in the CGC: gluon production and spin asymmetries in pA collisions*, *JHEP* **07** (2014) 068 [[arXiv:1404.2219](#)] [[INSPIRE](#)].
- [63] G.A. Chirilli, *Sub-eikonal corrections to scattering amplitudes at high energy*, *JHEP* **01** (2019) 118 [[arXiv:1807.11435](#)] [[INSPIRE](#)].
- [64] T. Altinoluk, G. Beuf, A. Czajka and A. Tymowska, *Quarks at next-to-eikonal accuracy in the CGC: forward quark-nucleus scattering*, *Phys. Rev. D* **104** (2021) 014019 [[arXiv:2012.03886](#)] [[INSPIRE](#)].
- [65] T. Altinoluk and G. Beuf, *Quark and scalar propagators at next-to-eikonal accuracy in the CGC through a dynamical background gluon field*, *Phys. Rev. D* **105** (2022) 074026 [[arXiv:2109.01620](#)] [[INSPIRE](#)].
- [66] I. Balitsky and A. Tarasov, *Rapidity evolution of gluon TMD from low to moderate x* , *JHEP* **10** (2015) 017 [[arXiv:1505.02151](#)] [[INSPIRE](#)].
- [67] I. Balitsky and A. Tarasov, *Gluon TMD in particle production from low to moderate x* , *JHEP* **06** (2016) 164 [[arXiv:1603.06548](#)] [[INSPIRE](#)].
- [68] J. Jalilian-Marian, *Quark jets scattering from a gluon field: from saturation to high p_t* , *Phys. Rev. D* **99** (2019) 014043 [[arXiv:1809.04625](#)] [[INSPIRE](#)].
- [69] J. Jalilian-Marian, *Rapidity loss, spin, and angular asymmetries in the scattering of a quark from the color field of a proton or nucleus*, *Phys. Rev. D* **102** (2020) 014008 [[arXiv:1912.08878](#)] [[INSPIRE](#)].
- [70] Y.V. Kovchegov and M.G. Santiago, *Quark sivers function at small x : spin-dependent odderon and the sub-eikonal evolution*, *JHEP* **11** (2021) 200 [[arXiv:2108.03667](#)] [[INSPIRE](#)].
- [71] G.P. Lepage and S.J. Brodsky, *Exclusive processes in perturbative quantum chromodynamics*, *Phys. Rev. D* **22** (1980) 2157 [[INSPIRE](#)].
- [72] S.J. Brodsky, H.-C. Pauli and S.S. Pinsky, *Quantum chromodynamics and other field theories on the light cone*, *Phys. Rept.* **301** (1998) 299 [[hep-ph/9705477](#)] [[INSPIRE](#)].
- [73] V.N. Gribov and L.N. Lipatov, *Deep inelastic ep scattering in perturbation theory*, *Sov. J. Nucl. Phys.* **15** (1972) 438 [*Yad. Fiz.* **15** (1972) 781] [[INSPIRE](#)].
- [74] G. Altarelli and G. Parisi, *Asymptotic freedom in parton language*, *Nucl. Phys. B* **126** (1977) 298 [[INSPIRE](#)].
- [75] Y.L. Dokshitzer, *Calculation of the structure functions for deep inelastic scattering and e^+e^- annihilation by perturbation theory in quantum chromodynamics*, *Sov. Phys. JETP* **46** (1977) 641 [*Zh. Eksp. Teor. Fiz.* **73** (1977) 1216] [[INSPIRE](#)].

- [76] L.F. Abbott, *The background field method beyond one loop*, *Nucl. Phys. B* **185** (1981) 189 [INSPIRE].
- [77] L.F. Abbott, *Introduction to the background field method*, *Acta Phys. Polon. B* **13** (1982) 33 [INSPIRE].
- [78] G. 't Hooft, *A planar diagram theory for strong interactions*, *Nucl. Phys. B* **72** (1974) 461 [INSPIRE].
- [79] G. Veneziano, *Some aspects of a unified approach to gauge, dual and Gribov theories*, *Nucl. Phys. B* **117** (1976) 519 [INSPIRE].
- [80] G. Altarelli and G.G. Ross, *The anomalous gluon contribution to polarized lepton production*, *Phys. Lett. B* **212** (1988) 391 [INSPIRE].
- [81] R.D. Carlitz, J.C. Collins and A.H. Mueller, *The role of the axial anomaly in measuring spin dependent parton distributions*, *Phys. Lett. B* **214** (1988) 229 [INSPIRE].
- [82] G.M. Shore and G. Veneziano, *The U(1) Goldberger-Treiman relation and the two components of the proton 'spin'*, *Phys. Lett. B* **244** (1990) 75 [INSPIRE].
- [83] G.M. Shore and G. Veneziano, *The U(1) Goldberger-Treiman relation and the proton 'spin': a renormalization group analysis*, *Nucl. Phys. B* **381** (1992) 23 [INSPIRE].
- [84] A. Tarasov and R. Venugopalan, *Role of the chiral anomaly in polarized deeply inelastic scattering: finding the triangle graph inside the box diagram in Bjorken and Regge asymptotics*, *Phys. Rev. D* **102** (2020) 114022 [arXiv:2008.08104] [INSPIRE].
- [85] A. Tarasov and R. Venugopalan, *Role of the chiral anomaly in polarized deeply inelastic scattering. II. Topological screening and transitions from emergent axionlike dynamics*, *Phys. Rev. D* **105** (2022) 014020 [arXiv:2109.10370] [INSPIRE].
- [86] Y. Hatta, *CP-odd gluonic operators in QCD spin physics*, *Phys. Rev. D* **102** (2020) 094004 [arXiv:2009.03657] [INSPIRE].
- [87] A. Radyushkin and S. Zhao, *Parton distribution function for topological charge at one loop*, *JHEP* **02** (2022) 163 [arXiv:2201.02181] [INSPIRE].
- [88] E.A. Kuraev, L.N. Lipatov and V.S. Fadin, *The Pomeron singularity in non-Abelian gauge theories*, *Sov. Phys. JETP* **45** (1977) 199 [*Zh. Eksp. Teor. Fiz.* **72** (1977) 377] [INSPIRE].
- [89] I.I. Balitsky and L.N. Lipatov, *The Pomeron singularity in quantum chromodynamics*, *Sov. J. Nucl. Phys.* **28** (1978) 822 [*Yad. Fiz.* **28** (1978) 1597] [INSPIRE].
- [90] R. Mertig and W.L. van Neerven, *The calculation of the two loop spin splitting functions $P_{ij}^{(1)}(x)$* , *Z. Phys. C* **70** (1996) 637 [hep-ph/9506451] [INSPIRE].
- [91] S. Moch, J.A.M. Vermaseren and A. Vogt, *The three-loop splitting functions in QCD: the helicity-dependent case*, *Nucl. Phys. B* **889** (2014) 351 [arXiv:1409.5131] [INSPIRE].
- [92] Y.V. Kovchegov and M.D. Sievert, *Valence quark transversity at small- x* , *Phys. Rev. D* **99** (2019) 054033 [arXiv:1808.10354] [INSPIRE].
- [93] C.J. Bomhof, P.J. Mulders and F. Pijlman, *The construction of gauge-links in arbitrary hard processes*, *Eur. Phys. J. C* **47** (2006) 147 [hep-ph/0601171] [INSPIRE].
- [94] C. Lorce, *Wilson lines and orbital angular momentum*, *Phys. Lett. B* **719** (2013) 185 [arXiv:1210.2581] [INSPIRE].

- [95] A.H. Mueller and S. Munier, p_{\perp} -broadening and production processes versus dipole/quadrupole amplitudes at next-to-leading order, *Nucl. Phys. A* **893** (2012) 43 [[arXiv:1206.1333](#)] [[INSPIRE](#)].
- [96] PARTICLE DATA GROUP collaboration, *Review of particle physics*, *PTEP* **2020** (2020) 083C01 [[INSPIRE](#)].
- [97] B. Lampe and E. Reya, *Spin physics and polarized structure functions*, *Phys. Rept.* **332** (2000) 1 [[hep-ph/9810270](#)] [[INSPIRE](#)].
- [98] J. Bjorken and S. Drell, *Relativistic quantum fields*, McGraw-Hill, U.S.A. (1965).
- [99] A.H. Mueller, *Small- x behavior and parton saturation: a QCD model*, *Nucl. Phys. B* **335** (1990) 115 [[INSPIRE](#)].
- [100] L.D. McLerran and R. Venugopalan, *Computing quark and gluon distribution functions for very large nuclei*, *Phys. Rev. D* **49** (1994) 2233 [[hep-ph/9309289](#)] [[INSPIRE](#)].
- [101] L.D. McLerran and R. Venugopalan, *Gluon distribution functions for very large nuclei at small transverse momentum*, *Phys. Rev. D* **49** (1994) 3352 [[hep-ph/9311205](#)] [[INSPIRE](#)].
- [102] L.D. McLerran and R. Venugopalan, *Green's functions in the color field of a large nucleus*, *Phys. Rev. D* **50** (1994) 2225 [[hep-ph/9402335](#)] [[INSPIRE](#)].
- [103] J. Bartels, *High-energy behavior in a non-Abelian gauge theory (II): first corrections to $T_{n \rightarrow m}$ beyond the leading $\ln s$ approximation*, *Nucl. Phys. B* **175** (1980) 365 [[INSPIRE](#)].
- [104] J. Kwiecinski and M. Praszalowicz, *Three gluon integral equation and odd c singlet Regge singularities in QCD*, *Phys. Lett. B* **94** (1980) 413 [[INSPIRE](#)].
- [105] B. Nicolescu, *The odderon today*, presented at the *Moriond 1990 conference*, Les Arcs, France (1990) [[INSPIRE](#)].
- [106] R.A. Janik and J. Wosiek, *Solution of the odderon problem*, *Phys. Rev. Lett.* **82** (1999) 1092 [[hep-th/9802100](#)] [[INSPIRE](#)].
- [107] J. Bartels, L.N. Lipatov and G.P. Vacca, *A new odderon solution in perturbative QCD*, *Phys. Lett. B* **477** (2000) 178 [[hep-ph/9912423](#)] [[INSPIRE](#)].
- [108] G.P. Korchemsky, J. Kotanski and A.N. Manashov, *Solution of the multi-Reggeon compound state problem in multicolor QCD*, *Phys. Rev. Lett.* **88** (2002) 122002 [[hep-ph/0111185](#)] [[INSPIRE](#)].
- [109] Y.V. Kovchegov, L. Szymanowski and S. Wallon, *Perturbative odderon in the dipole model*, *Phys. Lett. B* **586** (2004) 267 [[hep-ph/0309281](#)] [[INSPIRE](#)].
- [110] C. Ewerz, *The odderon in quantum chromodynamics*, [hep-ph/0306137](#) [[INSPIRE](#)].
- [111] Y. Hatta, E. Iancu, K. Itakura and L. McLerran, *Odderon in the color glass condensate*, *Nucl. Phys. A* **760** (2005) 172 [[hep-ph/0501171](#)] [[INSPIRE](#)].
- [112] A. Kovner and M. Lublinsky, *Odderon and seven pomerons: QCD Reggeon field theory from JIMWLK evolution*, *JHEP* **02** (2007) 058 [[hep-ph/0512316](#)] [[INSPIRE](#)].
- [113] S. Jeon and R. Venugopalan, *A classical odderon in QCD at high energies*, *Phys. Rev. D* **71** (2005) 125003 [[hep-ph/0503219](#)] [[INSPIRE](#)].
- [114] Y. Hagiwara, Y. Hatta, R. Pasechnik and J. Zhou, *Spin-dependent pomeron and odderon in elastic proton-proton scattering*, *Eur. Phys. J. C* **80** (2020) 427 [[arXiv:2003.03680](#)] [[INSPIRE](#)].

- [115] K. Itakura, Y.V. Kovchegov, L. McLerran and D. Teaney, *Baryon stopping and valence quark distribution at small x* , *Nucl. Phys. A* **730** (2004) 160 [[hep-ph/0305332](#)] [[INSPIRE](#)].
- [116] J. Blümlein, P. Marquard, C. Schneider and K. Schönwald, *The three-loop polarized singlet anomalous dimensions from off-shell operator matrix elements*, *JHEP* **01** (2022) 193 [[arXiv:2111.12401](#)] [[INSPIRE](#)].
- [117] I.I. Balitsky and V.M. Braun, *Evolution equations for QCD string operators*, *Nucl. Phys. B* **311** (1989) 541 [[INSPIRE](#)].
- [118] I.I. Balitsky and V.M. Braun, *The nonlocal operator expansion for inclusive particle production in e^+e^- annihilation*, *Nucl. Phys. B* **361** (1991) 93 [[INSPIRE](#)].
- [119] M. Beneke, A.P. Chapovsky, M. Diehl and T. Feldmann, *Soft collinear effective theory and heavy to light currents beyond leading power*, *Nucl. Phys. B* **643** (2002) 431 [[hep-ph/0206152](#)] [[INSPIRE](#)].
- [120] C.W. Bauer, S. Fleming, D. Pirjol and I.W. Stewart, *An effective field theory for collinear and soft gluons: heavy to light decays*, *Phys. Rev. D* **63** (2001) 114020 [[hep-ph/0011336](#)] [[INSPIRE](#)].
- [121] C.W. Bauer, D. Pirjol and I.W. Stewart, *Soft collinear factorization in effective field theory*, *Phys. Rev. D* **65** (2002) 054022 [[hep-ph/0109045](#)] [[INSPIRE](#)].
- [122] T. Altinoluk, N. Armesto, G. Beuf and A. Moscoso, *Next-to-next-to-eikonal corrections in the CGC*, *JHEP* **01** (2016) 114 [[arXiv:1505.01400](#)] [[INSPIRE](#)].
- [123] I. Balitsky and A. Tarasov, *Higher-twist corrections to gluon TMD factorization*, *JHEP* **07** (2017) 095 [[arXiv:1706.01415](#)] [[INSPIRE](#)].
- [124] I. Balitsky and A. Tarasov, *Power corrections to TMD factorization for Z-boson production*, *JHEP* **05** (2018) 150 [[arXiv:1712.09389](#)] [[INSPIRE](#)].
- [125] H. Akaike, *A new look at the statistical model identification*, *IEEE Trans. Automat. Contr.* **19** (1974) 716.
- [126] J.S. Schwinger, *On gauge invariance and vacuum polarization*, *Phys. Rev.* **82** (1951) 664 [[INSPIRE](#)].